The Dissertation Committee for Heather McSharry Lander Certifies that this is the approved version of the following dissertation:

Investigations into endothelial cell permeability and adherens junction disruption induced by Junín virus infection.

Committee:

Clarence J. Peters, M.D., Mentor

Alan Barrett, Ph.D.

Joan Nichols, Ph.D.

Shinji Makino, D.V.M., Ph.D.

Francis William Luscinskas, Ph.D.

Dean, Graduate School

Investigations into endothelial cell permeability and adherens junction disruption induced by Junín virus infection.

by

Heather McSharry Lander, B.S.

Dissertation

Presented to the Faculty of the Graduate School of

The University of Texas Medical Branch

in Partial Fulfillment

of the Requirements

for the Degree of

Doctor of Philosophy

The University of Texas Medical Branch

December, 2013

Dedication

"If you are going through hell, keep going." Winston Churchill

This dissertation is dedicated to my husband Todd and my son Colten, whose love, support and patience could never be articulated accurately with mere words. I love you with all of my heart and because of you I never gave up. Thank you.

Acknowledgements

This dissertation is the culmination of extensive hard work, dedication and patience on the part of many extraordinary people. My sincere gratitude goes out to Dr. C.J. Peters, my Ph.D. Advisor. His career inspired me; his insatiable curiosity taught me what science really means and his willingness to listen to and encourage the tentative ideas of a new scientist made an extraordinary impact on my graduate school experience. His willingness to persevere along with me made this possible. I also owe an immense amount of gratitude to my committee members, who were in it for the long haul. Dr. Joan Nichols, Dr. Alan Barrett, Dr. Shinji Makino, and Dr. Bill Luscinskas: I thank each and every one of you, and am honored to have had the opportunity to work with you.

In addition to those exceptional scientists, I would also like to acknowledge those who helped me with my research: Dr. John Morrill, for training me in the BSL4; Dr. Thomas Albrecht for the amazing technical help with the confocal microscope; Dr. Eric Mossel for valuable virology technical help, and Dr. David Cheresh and Dr. Sara Weis at the UCSD Moores Cancer Center, for sharing with me their invaluable endothelial and adherens junction expertise. This would not have been possible without any of you.

I would also like to take this opportunity to thank a few others who, through their personal efforts on my behalf, made the difference between the success and failure of this dissertation. Thank you, Dr. Slobodan Paessler, for caring enough to steer me in the right direction when I couldn't see through my windshield. Thank you, Dr. Gracie Vargas, for caring enough to force my hand and advocate on my behalf. Thank you, Dr. David Niesel, for tirelessly going to bat for a struggling graduate student whom you'd never even met. Finally, I'd like to thank Dr. Dorian Coppenhaver for making this possible.

Investigations into endothelial cell permeability and adherens junction disruption induced by Junín virus infection.

Publication No._____

Heather McSharry Lander, Ph.D.

The University of Texas Medical Branch, 2013

Supervisor: Clarence J. Peters

Junín virus is found in the fertile Pampas of Argentina and is maintained in nature by the rodent host, *Calomys musculinus*. Junín is the causative agent of Argentine hemorrhagic fever (AHF) characterized by vascular dysfunction and fluid distribution abnormalities. Clinical, as well as experimental studies, have implicated involvement of the endothelium in pathogenesis of AHF, although the role it may play is poorly understood. Junín virus has been shown to produce productive infection of endothelial cells *in vitro* with no visible cytopathic effects which provides a unique opportunity to study the cells while they are infected. Here, we show that direct Junín virus infection of primary human endothelial cells (EC) corresponds to increased vascular permeability as measured by electric cell-substrate impedance sensing (ECIS) and transwell assays. We also show that EC adherens junctions are disrupted during infection which may provide insight into the role of the endothelium in the pathogenesis of AHF and possibly other viral hemorrhagic fevers (VHFs).

Contents

List of Tables

List of Figures

Chapter 1: Introduction

Viral Hemorrhagic Fevers

Overview of Viral Hemorrhagic Fevers

"Viral hemorrhagic fevers" (VHF) include severe diseases characterized by the involvement of multiple physiological systems in which vascular damage and dysfunction occur with subsequent fluid distribution problems, possible hemorrhaging and shock (1-5). The onset of VHFs is often generic, resembling other diseases that are regularly seen in the endemic areas. For this reason, delayed diagnosis can often lead to unchecked disease progression and adverse outcomes in the patients and health care workers (2, 3).

Four known virus families have been identified as responsible for causing VHF. These include arenaviruses, bunyaviruses, flaviviruses and filoviruses. Although these virus families exhibit unique features, they share some common traits (6). They each have natural animal reservoirs or arthropod vectors, which allow the viruses to survive, replicate and persist. The most common reservoirs and vectors for these virus families are rodents and arthropods. Some examples include the multimmate mouse (*Mastomys natalensis*) which harbors Lassa virus (7); the drylands vesper mouse (*Calomys musculinus)* which carries Junin virus (8); Aedes mosquitoes transmit Rift Valley or yellow fever (9, 10), and ticks which are responsible for the transmission of Crimean-Congo HF. The reservoirs for filoviruses have not yet been indisputably identified (11).

The four VHF virus families are distributed throughout the world. However, because of the nature of the specificity of the reservoirs to the virus, each virus is generally only found in areas in which its specific reservoir is naturally occurring (2). While this can limit the risk of becoming

infected to the local population, increased frequency of travel, as well as the encroachment of populations into host habitats can increase the at risk population. Additionally, if an infected individual travels to another part of the world, the virus can spread in the absence of its reservoir if person-to-person or person-to-vector transmission occurs (2).

Another way in which these deadly viruses could be disseminated in non-endemic areas, potentially infecting populations that are usually not at risk, would be through deliberate dispersal of infectious particles, as in the case of bioweapon use (12). Because the viruses that cause VHFs have high mortality rates and could potentially be weaponized, they have been categorized by the CDC as category A agents. Research into the pathogenesis of these agents and identification of potential therapeutic targets are the primary objectives of scientists studying these viruses.

Initial symptoms of the VHF syndrome include fatigue, fever, aches, and dizziness. Once the hemorrhagic phase occurs, patients often exhibit bleeding under the skin or from gums, eyes, ears, or internal organs, although blood loss itself is usually not the cause of death. Fluid distribution problems can lead to shock and some experience a neurological syndrome with seizures, while others experience kidney failure (13-16).

In the United States there are no FDA approved treatments specifically for VHFs, and patients receive supportive care which can improve the outcome if administered early enough. The antiviral drug Ribavirin has been used with some efficacy to treat CCHF, Lassa, or HFRS in endemic areas, and phase 2 clinical studies are currently underway to determine if Ribavirin is, in fact effective against all three (17-21). Plasma from patients that recovered from Argentine hemorrhagic fever has been used successfully to treat patients in the endemic area (22). However, the success of an attenuated vaccine to AHF (23) means that there is less immune plasma around for treatment purposes, and while this is good for those in the endemic area, if Junín virus ever

spread accidentally or through malicious means, there would only be supportive care to offer those infected.

To date, there are only two VHFs for which there are vaccines. AHF, as was mentioned earlier, and yellow fever (24). For this reason, it's critical that prevention focuses on avoiding contact with the host species as well as isolating patients to prevent person-to-person transmission, if that type of transmission might be possible. Efforts to control VHFs spread via rodents include rodent population control measures, efforts at keeping rodents out of people's homes and educating the people at risk about safe clean up practices for rodent nests and excrement as well as the importance of actually implementing the practices described (25).

In the case of VHFs transmitted by arthropod vectors, the focus is on arthropod population control. This can be accomplished by such measures as addressing standing water issues and employing pesticides. Further steps taken that are effective when employed include bite prevention techniques such as the use of mosquito nets, screens, chemical repellents and protective clothing.

Person-to-person transmission of some VHFs has been documented (26-28), and for those it is critical that medical workers, family members and those who handle the deceased are educated and prepared to protect themselves. This means using barrier nursing practices, isolating patients and using personal protective equipment when possible, as well as properly disposing of medical items used during treatments.

Researchers are challenged with learning how these viruses survive in nature; emerge, spread and cause disease. Knowledge gained through VHF research will lead to more effective efforts at containment, diagnostics, treatments and vaccines that will not only benefit those in endemic areas, but will also help protect other populations, including military personnel who

venture into endemic areas as well as any population that might be the target of a bioterrorist attack.

Overview of the four virus families

The four virus families that encompass the etiologic agents causing viral hemorrhagic fevers are Filoviridae, Bunyaviridae, Flaviviridae and Arenaviridae. Collectively they occur in natural virus-reservoir cycles involving rodents, arthropods, humans, domestic ruminants and bats.

Bunyaviruses include the hantaviruses, Crimean-Congo hemorrhagic fever (CCHF) virus, and Rift Valley fever (RVF) virus. Hantaviruses are rodent-borne, while CCHFV and RVFV are transmitted by arthropods, although RVF is often transmitted via infected blood or tissue during livestock slaughter or medical intervention (29, 30). CCHFV is carried by ticks and can be transmitted through a tick bite, crushing an infected tick against the skin, contact with infected animal tissues, blood or products, and human-to-human transmission is also possible (30). Hantaviruses are found globally and categorized into New World which cause hantavirus pulmonary syndrome (HPS) or Old World, which cause hemorrhagic fever with renal syndrome (HFRS) (31).

One of the most infamous and highly recognizable viruses in the world belongs to the family Filoviridae. Ebola outbreaks were first described in the 1970's, with patients experiencing severe and dramatically fatal hemorrhagic disease that was easily transmitted to health care workers and family members (32). Ebola has 4 subtypes: Zaire, Sudan, Ivory Coast, Bundibugyo, and Reston, which is the only known aerosol infectious form and only causes disease in non-human primates, but was found in pigs in 2009 (32, 33).

Also within the family *Filoviridae* is Marburg, actually the first filovirus found to cause disease. Marburg was initially discovered in Marburg, Germany, but was traced back to central Africa, where in Angola in 2004-2005, it was the agent responsible for a VHF outbreak with 90% case-fatality rate in 252 confirmed cases.

The flaviviruses are most well-known for the mosquito-borne HFs, yellow fever and dengue HF (34). They are found in many areas on several continents (Tropical Africa and Americas; Africa, Asia and Americas) and in addition to affecting local populations, are often encountered by military personnel. Dengue has become nearly as significant a tropical disease threat as malaria.

Of the Arenaviridae, Lassa is the most clinically relevant, with significant morbidity and mortality in its endemic region. However, there are several South American arenaviruses that cause severe HF in their respective countries (35). Arenaviruses are maintained, in nature, in rodent reservoirs which generally transmit the virus through infected excreta. The Arenaviridae will be discussed in more detail in the following section.

A more detailed breakdown of the virus families and the HF associated with them is shown in Table 1.1

Virus Family	Disease (Virus)	Endemic Regions	Source of Human Infection	Incubation Period (days)
Filoviridae				
Filovirus	Marburg	Africa	Unknown	2-14
	Ebola	Africa	Bats	2-12
Flaviviridae				
Flavivirus	Yellow Fever	Tropical Americas Tropical Africa	Mosquitoes	3-6
	Dengue HF Dengue	Asia, Africa, Americas	Mosquitoes	3-14
Arenaviridae				
Arenavirus Old World	Lassa Fever Lassa	Africa	Rodents	5-16
	Lujo	Africa	Rodents	2-7
New World	Bolivian HF (Machupo, Chapare)	S. America	Rodents	9-15; 7-14
	Venezuelan HF (Guanarito)	S. America	Rodents	7-14
	Brazilian HF (sabia)	S. America	Rodents	7-14
	Argentine HF (Junín)	S. America	Rodents	7-14
Bunyaviridae				
Nairovirus	Crimean-Congo HF	Africa, Europe, Central Asia, Middle East	Ticks	3-12
Phlebovirus	Rift Valley Fever	Africa, Saudi Arabia, Yemen	Direct contact w/infected blood or tissue; sandflies; mosquitoes	2-6
Hantavirus	HFRS Hantaan Dobrava Saaremaa Seoul Puumala	Eastern Asia, Scandinavia, Western Europe	Rodents	9-35

Table 1.1: The Four Virus Families that cause VHFs. This table depicts the virus families, and the viruses within them, that cause VHFs around the world, including the endemic areas, source of infection and incubation period.

Overview of the Arenaviridae

The Arenaviridae

In 1933 the first arenavirus was isolated from samples obtained during an epidemic of St. Louis encephalitis and named lymphocytic choriomeningitis virus (LCMV) (36). The agent was found to be the same as one that had been observed to chronically infect mouse colonies (37).

Within about 30 years, more viruses were identified that shared characteristics with LCMV, including morphology, serology and the fact that they all chronically infected rodents. This led to the inauguration of the Arenaviridae, the name taken from the Latin word for sandy, (*arenosus*) came from the fact that ribosomes incorporated into virions gave the viruses a sandy appearance (38). Over the next few decades, more arenaviruses were discovered. Some were serious health threats, causing hemorrhagic fevers in endemic areas, such as Guanarito, Sabia, Machupo, Junín, Lujo and Chapare (39-41); while others did not cause significant disease, such as Oliveros, Latino and Pinhal. See table 1.2 for details of the known arenaviruses.

List of Arenavirus species and newly discovered arenavirus not yet classified, and respective characteristics

Virus	Acronym	Lineage	Country	(Possible) host	BSL	S RNA	L RNA
						Number of complete (partial) sequences[b]	Number of complete (partial) sequences
Allpahuayo	ALLV	NW-A	Peru	*Oecomys bicolor, Oecomys paricola*	2	2(0)	1(0)
Amapari	AMAV	NW-B	Brazil	*Oryzomys goeldi, Neacomys guianae*	2	1(0)	1(0)
Bear Canyon	BCNV	NW-Rec	USA	*Peromyscus californicus, Neotoma macrotis*	2	3(4)	2(0)
Catarina	na	NW-Rec	USA	*Neotoma micropus*	2	2(0)	0(0)
Chapare	na	NW-B	Bolivia	Unknown	NC	1(0)	1(0)
Cupixi	CPXV	NW-B	Brazil	*Oryzomys capito*	2	1(0)	1(0)
Dandenong	na	OW	Australia	Unknown	NC	1(0)	1(0)
Flexal	FLEV	NW-A	Brazil	*Oryzomys* spp.	3	2(0)	1(0)
Guanarito	GTOV	NW-B	Venezuela	*Zygodontomys brevicauda, Sigmodon alstoni*	4	2(33)	1(12)
Ippy	IPPYV	OW	Central African Republic	*Arvicanthus* spp.	2	1(0)	1(0)
Junin	JUNV	NW-B	Argentina	*Callomys musculinus*	4	5(83)	5(1)
Kodoko	na	OW	Guinea	*Mus Nannomys minutoides*	NC	0(2)	0(2)
Lassa	LASV	OW	West Africa	*Mastomys natalensis*	4	11(95)	6(11)
Latino	LATV	NW-C	Bolivia	*Callomys callosus*	2	1(0)	1(0)
LCM[a]	LCMV	OW	ubiquitous	*Mus musculus, M. domesticus*	2/3	9(25)	8(5)
Machupo	MACV	NW-B	Bolivia	*Callomys callosus*	4	9(20)	3(8)
Mobala	MOBV	OW	Central African Republic	*Praomys* spp.	2	1(3)	1(2)
Mopeia	MOPV	OW	Mozambique, Zimbabwe	*Mastomys natalensis*	2	3(0)	2(1)
Morogoro	na	OW	Tanzania	*Mastomys* sp.	NC	0(0)	0(0)
Oliveros	OLVV	NW-C	Argentina	*Bolomys* spp.	2	1(0)	1(0)
Pampa	na	NW-C	Argentina	*Bolomys* spp.	2	0(1)	0(0)
Parana	PARV	NW-A	Paraguay	*Oryzomys buccinatus*	2	1(0)	1(0)
Pichinde	PICV	NW-A	Colombia	*Oryzomys albigularis*	2	3(2)	3(0)
Pinhal	na	NW-C	Brazil	*Calomys tener*	NC	0(5)	0(0)
Pirital	PIRV	NW-A	Venezuela	*Sigmodon alstoni*	2	1(28)	1(4)
Sabia	SABV	NW-B	Brazil	Unknown	4	1(0)	1(0)
Skinner Tank	na	NW-Rec	USA	*Neotoma mexicana*	NC	1(0)	0(0)
Tonto Creek	na	NW-Rec		*Neotoma* spp.	NC	0(0)	0(0)
Tacaribe	TCRV	NW-B	Trinidad	*Artibeus* bat	2	1(0)	1(0)
Tamiami	TAMV	NW-Rec	USA	*Sigmodon hispidus*	3	1(0)	1(0)
Whitewater Arroyo	WWAV	NW-Rec	USA	*Neotoma* spp.	2	5(11)	1(0)

Table 1.2 List of Arenaviruses:

a. Lymphocytic choriomeningitis virus.

b. Available in Genbank in December 2008.

With permission from Charrel *et al*. (2010) (34)

Arenavirus phylogenetics

There is only 1 genus within the Arenaviridae: arenavirus. This genus includes 24 species currently recognized and divided into the Old World and the New World (Tacaribe complex) classifications (42). Monoclonal antibodies, directed against epitopes on the viral NP and GP2 proteins, indicate that there are some shared epitopes between the two groups. Close antigenic relationships exist among Amapari, Junin, Latino, Machupo, and Tacaribe viruses while Flexal,

Pichinde, Parana, and Tamiami viruses are more closely related antigenically (42-44). LCMV related viruses are antigenically distinct from the African viruses, Lassa, Ippy, Mopeia and Mobala (45, 46).

Genetic analyses has offered an opportunity to group the arenavirus species according to phylogenetic relationships and provided valuable insight into their evolution. Figure 1.1 is a phylogenetic tree that clearly depicts the evolutionary relationships among the species within this virus family.

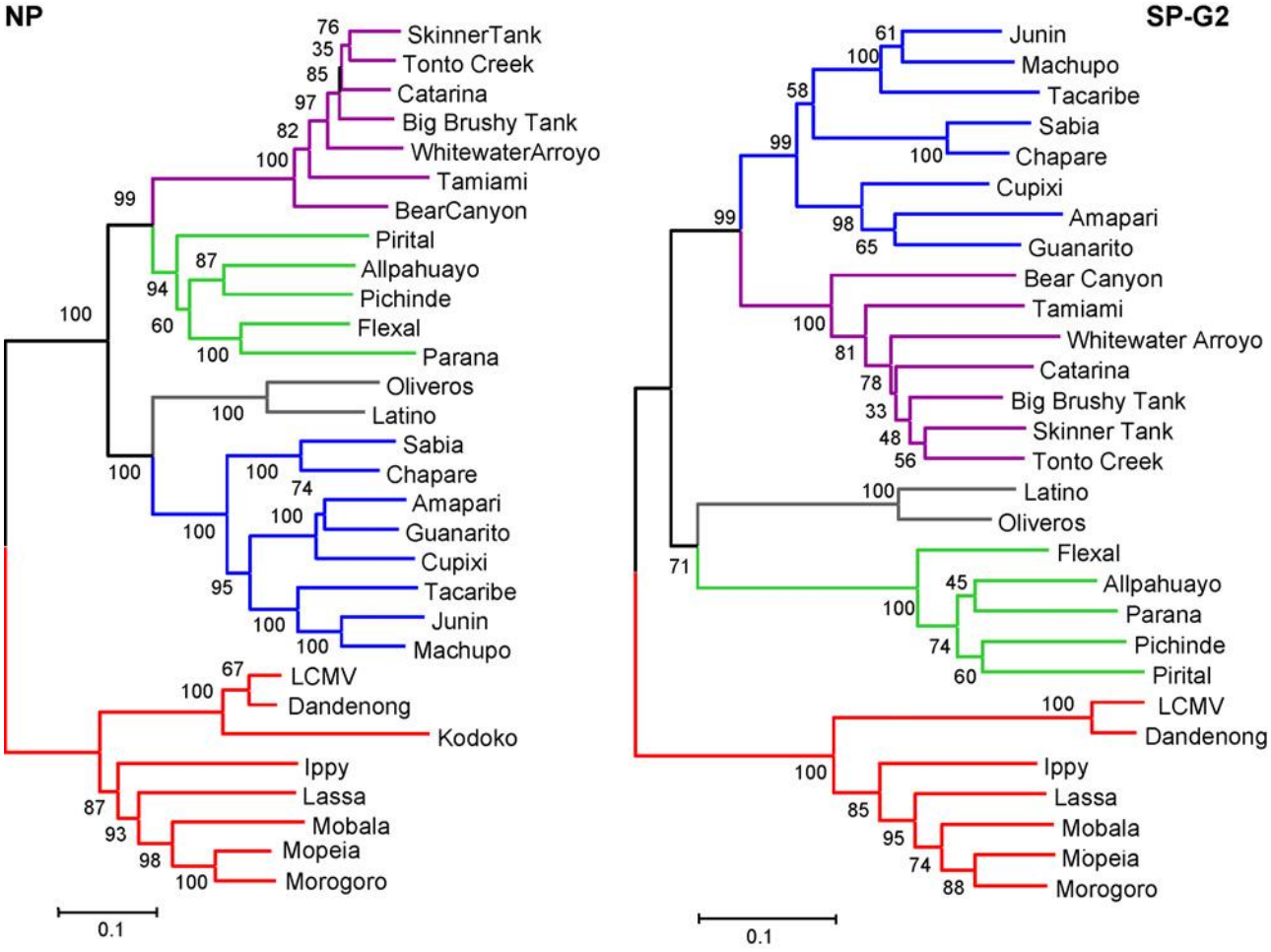

Figure 1.1 Arenavirus phylogenetic relationships:
Old world viruses; **lineage A new world viruses**; **lineage B new world viruses**; **lineage C new world viruses; recombinant new world viruses.**
Left phylogram is based on nucleoprotein amino acid sequences
Right phylogram is based on concatenated signal peptide and glycoprotein two amino acid sequences. The neighbor-joining, poisson and bootstrapping (200 pseudoreplications) algorithms were computed using MEGA 2 software. Used with permission from Charrel and de Lamballerie (2010) (47)

Virion morphology and genomic organization

All arenaviruses are enveloped, single-stranded, bisegemented, RNA viruses with an ambisense genome (48, 49). RNA segments are designated small (S) and large (L) that each code for two proteins that are encoded in opposite directions with a non-coding, stable hairpin intergenic region (IGR) between the two. (50). Several viruses have had their complete S segments sequenced, indicating a size range of approximately 3500 nucleotides. Fewer L segments have been sequenced thus far, but they range in size from 7102 to 7279 nucleotides (48, 51).

The S and L RNA segements have identical terminal sequences at 17 nucleotides. (for S it is 58...GCCUAGGAUCCACUGUGCG$_{OH}$38, and for L it is 58...GCCUAGGAUCCUCGGUGCG$_{OH}$38), and they are conserved among the arenaviruses (51-55). The 58 terminus of each segment contains a tri- or diphosphate group without a cap. The 58-end nucleotides near the start of each RNA are "imperfectly complementary" with the 38 end. It is believed, that the 38 and 58 termini base-pair to form panhandles, making the nucleotides appear circular. Some S RNAs contain an extra G residue on their 58 end which would remain unpaired, generating a panhandle lacking flushed ends (56-58).

The S RNA segment codes for three gene products on two genes: the nucleoprotein (NP or N), and the envelope glycoproteins GP1 and GP2, which arise from GPC, the glycoprotein precursor that is cleaved after translation (50, 59, 60). The L RNA segment consists of two genes that code for two gene products: the viral polymerase (L protein) and the Z protein (61). On both RNA segments, the genes are in an ambisense orientation (49, 50). The genes for the NP and polymerase proteins are located on the 38 end of their respective RNA segments, and are transcribed from genome-complementary mRNAs (50). The GPC and Z proteins are transcribed from antigenomes which are intermediates that facilitate the replication of the genes. Between the two genes on each segment is an intergenic region which are thought to form stable hairpin structures in the RNA

(50). Figure 1.2 depicts the arenavirus virion and genomic organization.

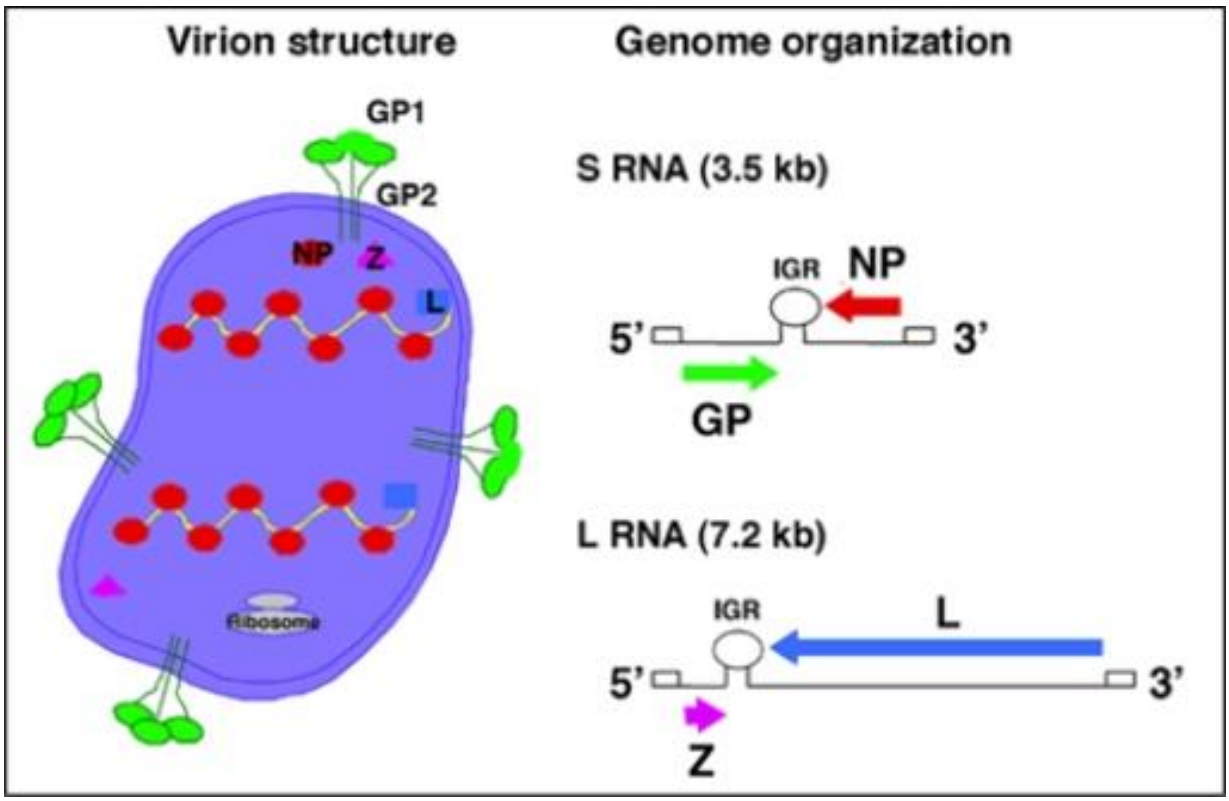

Figure 1.2 Diagramatic representation of arenavirus virion and genome organization and coding strategy. Arenavirus virions are pleomorphic and contain many electron-dense structures which are believed to be incorporated host cell ribosomes, giving the particle a "sandy" appearance. Both L and S RNA segments use an ambisense coding strategy. S encodes GP and NP; L encodes L polymerase and Z. Image: f2-viruses-02-02443 from Openi, the Open Access Subset of PubMed Central at http://openi.nlm.nih.gov

Viral Proteins

Arenavirus virions are pleomorphic, and can be over 200 nM in diameter. The envelope protein precursor, GPC, is a polyprotein that is cleaved after translation to form the envelope proteins, GP1 and GP2 which are incorporated as projections onto the surface of the virus particles (62). These glycoproteins mediate viral recognition of host cell receptors and viral entry, and in doing so, determine virus tissue tropism and range of viral hosts. The nucleoprotein (NP) is the major structural protein in arenaviruses, and the most prevalent viral protein in infected host cells

and virus particles. It encapsidates the viral RNA (NP-RNA complex) and associates with the polymerase to generate the ribonucleoprotein (RNP), and is important in viral RNA synthesis (63). It is a major component of the nucleocapsids, provides anti-interferon function and inhibits the activation of nuclear factor kappa B (64). It also interacts with the Z protein to mediate the incorporation of viral RNPs into matured infectious virions, and as part of the RNP, directs replication and transcription of arenavirus genomes (63).

The L protein is generally 180 to 250 kd. and provides the enzymatic activity necessary for viral RNA synthesis, including the RNA-dependent RNA polymerase. In addition it functions as an RNA endonuclease, stealing capped primers from host cell mRNAs; these capped primers are then utilized to initiate its own transcription (65). This protein also contains a central ring domain and projections that might play a role in the formation of the 5' cap (65).

The matrix (Z) protein is the smallest virus protein and contains a small RING-domain. Z has been shown to be critical for virus replication and also important in viral budding, and viral nucleocapsid incorporation (66). It is also important in viral RNA regulation; it binds with L, keeping the polymerase in an inactive state, thereby diminishing L's enzymatic activity and subsequent initiation of RNA synthesis (66).

Viral Entry, Transcription, and Replication

For host cell entry, the arenavirus GP1 binds to either the cellular receptor alpha-dystroglycan (Old World) or the transferrin1 receptor (New World) (67, 68). Infection is pH dependent and might involve dissociation of GP1 and GP2, which facilitates entry into the cell by revealing the fusion protein (69-71). Virus particles are taken into the host cell through an endocytic pathway; either clathrin-dependent (New World) or Clathrin-independent (Old World) (72, 73). Entry of Lassa and LCMV does not require actin, caveolin or dynamin, but they do require cholesterol (74).

Arenaviruses replicate solely within the cell cytoplasm and within hours of infection, mRNAs for NP and L proteins can be detected (75). The arenavirus ambisense coding strategy provides temporal separation between synthesis of NP and GPC proteins, with NPs being synthesized first. For expression of GPC and Z proteins, full length complimentary S and L antigenomes must be generated. The RNA-dependent RNA polymerase (L) and the nucleoprotein (N) are found in the infecting viral particle and are critical for replication (76). Inside the infected cell, L and N are produced from the transcription of mRNAs from viral genomic-sense RNAs. Once antigenomic-sense RNAs are generated, replication of progeny genomes begins. The antigenomes also function as templates for synthesis of mRNAs that encode the Z and GPC proteins. Full length RNA molecules (antigenomic-, and genomic-sense) are replicated through a "prime and align" strategy, while transcription of mRNAs commences via host cell-derived m7G-capped oligonucleotides (77). The viral RNA ambisense coding sequences are separated by non-polyadenylated intergenic hairpin regions (IGRs) within which the viral mRNAs terminate (78). It has recently been shown that arenavirus replication and transcription take place within cytosolic structures known as replication-transcription complexes (RTCs), in which full length and messenger RNAs are synthesized by the viral polymerase, after which the mRNAs are quickly translocated for translation on host cell ribosomes (79).

Although the actual process of arenavirus assembly is not well understood, it is thought that RNAs, NPs and Ls are assembled into nucleocapsids. Recent evidence indicates that Z likely functions to either mediate virion assembly, or inhibit RNA synthesis, based on the intracellular levels of the N and GP proteins (80). For an as yet unknown reason, arenavirus particles incorporate host cell ribosomes into their virions. Finally, the Z protein, GP complex and RNP work together to interact with the host cell plasma membrane where the virion buds off of the lipid bilayer to release newly generated infectious virus particles from the cell (80-82).

Overview of Pathogenesis

The current paradigm of arenavirus pathogenesis is that infectious aerosols are deposited in the lungs followed by viral replication and subsequent dissemination within the host. Additional important sites of virus growth include the hilar lymph nodes and other parenchymal organs. Animal models of Lassa and Junin have shown dissemination of the virus to the brain, but there are no reported human cases of brain infection (83). Macrophages are infected early, as has been shown by immunofluorescence in fatal AHF cases (84, 85). As the infection spreads, other cell types become infected as well. The cell types that can be infected in cell culture include endothelial cells, hepatocytes, macrophages, and megakaryocytes (86-88). Although many cell types become infected throughout the organism, there is little overt cell destruction reported. It appears that more "luxury" cellular functions are disrupted rather than the overall health of infected cells being compromised. For example, LCMV impairs production of pancreatic and thyroid cell insulin and can disrupt growth hormone release in rat pituitary cells (89, 90).

There is no data suggesting the direct replication of arenaviruses in lymphocytes, however, lymphopenia is common during systemic human and animal infections (86, 91). T cell activation has also been shown in Lassa infections and together with lymphopenia, the virus is able to more easily disseminate and replicate (92). While T cell response has been associated with survival in Lassa fever, and antibody appears to be insignificant in clearing acute LCMV, passive immune therapy, with neutralizing antibodies to LCMV, protects mice from death by reducing both the viral load in the tissues and the CD8+ response (93). There is also evidence indicating that in S. American arenaviruses neutralizing antibodies are important as well (22, 94, 95). Complement, through the classical pathway, is also important for virus neutralization (96).

Clinical Presentations

LCMV patients usually do not succumb to disease. It presents as aseptic meningitis, encephalitis or meningoencephalitis (97, 98). The first phase of disease generally includes fever, and headache with lymphadenopathy and a morbilliform rash, that lasts only a few days. Often, the headache returns, with more severe pain, which can be indicative of viral meningoencephalitis. However, it is also common for the disease to be asymptomatic or exhibit only mild febrile illnesses. Fetal infections result in worse outcomes such as congenital hydrocephalus, chorioretinitis, and mental retardation (97-100).

Lassa presents non-specifically with fever, headache, muscle aches and chest and abdominal pain. Vomiting and diarrhea with coughing and sore throat are common (101). Throat and eye inflammation is often seen. Hypotension or shock can occur, as well as fluid in the pleura or hemorrhages, and facial edema. Encephalopathy can be observed as well (101). In pregnant women, fetal loss is 80%. Recovery from disease during the convalescent stage includes additional temporary health problems such as hearing loss, hair loss or loss of coordination (102).

In the hemorrhagic fevers caused by New World arenaviruses, the similarity of symptoms makes it difficult to distinguish the etiologic agents, although the most well-studied is AHF. Locations of patient and travel history are helpful in a diagnosis. After approximately one week incubation, S. American HFs usually begin with headaches, fever, body aches and fatigue (35). Facial edema and periorbital edema are common. Some patients move into a hemorrhagic phase in which bleeding can occur, most often from the mucosa, or internal organs (94). Neurological problems can occur as well including tremors, seizures and loss of muscle control (94). Upon inspection of tissues, disseminated intravascular coagulation is not usually seen, and low platelet counts contribute to hemorrhaging, but studies of arenavirus infection of the endothelium are relatively few and offer only limited data on the nature of the vascular syndrome (87, 103, 104).

Argentine Hemorrhagic Fever

Overview of AHF

Of all the South American HF viruses, the most clinically relevant is Junín, with an esitmated 5 million individuals at risk in endemic regions(94, 105). The rodent hosts, including the drylands vesper mouse (*calomys musculinus*), are found in the Pampas of Argentina, which is the agricultural center of the country. Farm workers are at greatest risk of exposure, and are critical to the economy, but agricultural practices and machinery can cause aerosolization of mice and their nests, exposing workers to infectious aerosols (16). It is believed that alterations in the reservoir habitat in relation to agricultural practices, is what made AHF emerge in the 1950s (106, 107).

Clinical Presentation

AHF has a fatality rate of between 15-30% in untreated individuals, with hemorrhagic and neurologic manifestations (35). 80% of infected individuals develop clinical disease which begins slowly and can be misdiagnosed until symptoms reach advanced stages, making it even more critical to initially make a correct diagnosis (35, 94). Physicians rely on clinical and clinical laboratory findings to diagnose AHF (platelet count < 100,000/mm^3; white blood cell count < 2500/mm^3) but diagnostic tests have been developed including an RT-PCR-based assay which can improve the accuracy of diagnostics and improve patient outcome (108). There are three phases of AHF: prodromal, neurological-hemorrhagic and convalescence (94). The first week is the prodromal phase which includes fever, chills, anorexia, myalgia (lower back) headache and general malaise. Also common are retroorbital pain, photophobia, dizziness mild intestinal upset or epigastric pain. Patients often present with a flushed upper body (face, neck chest), periorbital edema and congestion of the conjuctiva. Oral surfaces are usually affected. Gentle pressure can

cause the gums to bleed and physicians often find small vesicle or petechiae on the soft palate. The lungs and pulmonary function are generally normal while orthostatic hypotension and relative brachycardia are common. Females usually exhibit inappropriate uterine bleeding but jaundice, splenomegaly and hepatomegaly are rarely seen. Patients nearing the end of this phase are often lethargic and irritable with fine tremors of the tongue or hands (16, 35, 94).

At this point, 20-30% of cases of AHF move into the neurologic-hemorrhagic phase, usually from 8 to 12 days after the symptoms first begin (16, 94). The hemorrhagic manifestations of this stage include: epistaxis, melena, hemoptysis, hematemesis, metrorrhagia, hematomas, and hematuria. Neurologic symptoms are ataxia, dysarthria and intention tremor. Over 90% of the cases that go into this phase are fatal. Convalescent patients develop an antibody response and clear the virus. Usually all neurological manifestations resolve, given enough time to recover (94).

Clinical lab data indicate that patients develop increased production of circulating interferons and TNF-alpha. Immunosuppression is seen as are lymphopenia and neutropenia (16, 94). Hemorrhage is thought to be due to thrombocytopenia and hemostatic dysfunction rather than DIC (16, 39, 94).

Endothelial cells express the New World arenavirus receptor, transferring receptor 1, at high levels, and have been productively infected in lab settings with no overt cytopathology (87, 109, 110). It has been reported that JUNV infected HUVECs produce increased levels of ICAM-1, VCAM-1, and nitric oxide with reduced levels of von willebrand factor (87, 104).

Treatment of AHF includes supportive care, with possible sedation and pain management drugs (94). Precautions for bleeding possibilities are taken including avoiding intramuscular injections and strict maintenance of hydration (94). Handling shock is more difficult. Small increases in hematocrit are indicative of vascular permeability problems, but are not as severe as is seen in HPS. Fluid administration must be cautious and cardiac monitoring critical (35, 94).

Convalescent plasma administration (3000U/kg body weight) is quite effective in humans and in animal studies, reducing mortality to 1-2%, if it is received early in disease (within the first 8 days) (22, 94, 111). Patients receiving immune plasma often develop a later neurologic syndrome that clears on its own. So far, antiviral drugs, although promising experimentally have not been efficacious in application. Ribavirin is the only drug that appears to be effective against the S. American HFs (112, 113).

AHF Vaccine

There is an attenuated vaccine for Junín virus. Referred to as Candid#1 (abbreviated from "Candidate #1"), it has been successfully used in Argentina to decrease AHF incident rates dramatically (23, 114, 115). There had been several attempts at generation of a live-attenuated JUNV vaccine strains, including some derived from the prototypical virulent XJ strain, and another from XJCl3 (116). Development of those strains was discontinued for various reasons (117-119). Candid#1 originated from the prototypical XJ strain of JUNV, which was first passaged twice in the guinea pig. Subsequently, it was passaged in the mouse brain 44 times. The mouse brain, from the last passage, was homogenized and used to inoculate fetal rhesus lung cells (FRhl-2), followed by twelve additional passages and finally cloning. Next, the resulting virus underwent one passage in FRhl-2 cells to generate the master and secondary seed stocks. One more amplification cycle in FRhl-2 cells produced the vaccine stock of Candid#1, with a cumulative total of 19 FRhl-2 passages (Figure 1.3) (120)

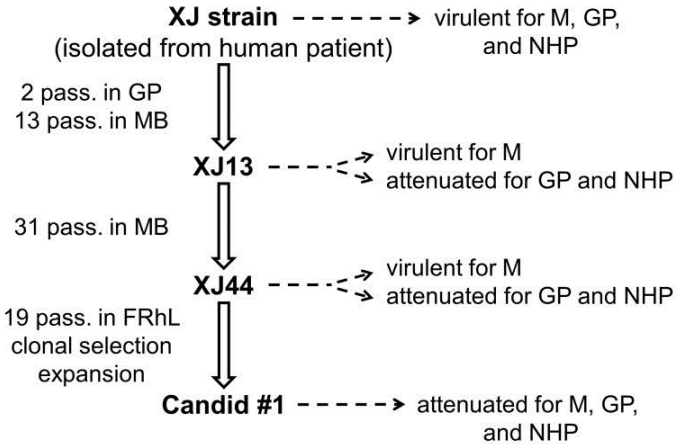

Figure 1.3 Passage History of JUNV vaccine strain, Candid#1 (reused, from Grant *et al*, 2012, with open access permission through Creative Commons). M: mouse; MB: mouse brain; GP: guinea pig; NHP: non-human primate, FRhl: fetal rhesus monkey lunc cells.

Candid#1 was found to be more effective, and was also more attenuated for mice, and non-human primates, with no detectable persistence or phenotypic reversion as well as low neurovirulence (114, 121, 122). In those vaccinated, the seroconversion rates are high and cellular immunity is stimulated as determined by lymphocyte stimulation tests (114, 121). Viral titers of Candid#1 are relatively low when compared to natural infection which may hint at a mechanism of attenuation. Phenotypic differences have also been found which may explain the attenuation including an increased susceptibility to neutralization, an increased dependence on the receptor transferrin 1, and increased sensitivity to complement when there are no antibodies present (123, 124).

In the late 1980's a field study was conducted in which approximately 6500 volunteers were given either the vaccine (3255 volunteers) or placebo (3245 volunteers) with striking results. Only one of those vaccinated was found to have a serologically confirmed case of AHF ($p<.001$) (114).

In later trials (phase II and III) Candid#1 had only minor reactogenicity and no serious reactions documented in any test subject (114, 121, 125). The vaccine would need to be effective

and safe in others beside the highest at –risk males in the population so more trials were done that included women and children. At this time, there have been no reported adverse outcomes in any of the children tested (as young as 4) and the rates of seroconversion remain high (23, 115). Although attempts were made to prevent the vaccination of pregnant women, including pregnancy testing, 49 out of 17,000 children were born to vaccinated mothers within 9 months of receiving the vaccine. Of those children born there was one documented case of anencephaly and one of meningomyelocoel which suggest caution should be used in vaccinating women in their child-bearing years (126). However, there is no direct evidence that Candi#1 crosses the placental barrier or is pathogenic to the fetus. Candid#1 is now being produced in Argentina and is being used effectively to control AHF in the endemic area (121).

There has been some evidence of the efficacy of Candid#1 against other arenaviruses. Guinea pigs and nonhuman primates are protected against challenge with Machupo when vaccinated with Candid#1 (127). In the absence of much cross-neutralization between the two viruses, the animals vaccinated show a fast antibody response upon Machupo challenge. It's possible that the vaccine is cross-priming the animals or that cellular immunity is providing cross protection.

Molecular analysis of Candid#1 indicates it has potential attenuation changes in its N-, L-, and GPC open reading frames (ORFs), compared to virulent strains. One mutation, (R[k[k), within a conserved region on the polymerase sequence, was detected at position L1156 (117, 128, 129). Additional differences were found in the Candid#1 L sequence, at position L936 (L[L[P), which falls within the structural sequence for the L protein, and L76 (H[Y[Y), which is in proximity to the putative ATP/AGP-binding P-loop (129). The Candid#1 GPC sequence contained a G1 carboxy-terminus mutation (GPC168, T[A[A), which would affect the conserved N-glycosylation sequence

(129). Data from the same study showed that the intergenic regions on both RNA segments were 100% conserved across JUNV strains (129).

The Endothelium

Overview of the endothelium

The endothelium is an organ composed of a single layer of cells that line the blood vessels. This organ can detect alterations in hemodynamic forces as well as respond to signals carried in the blood which allow it to regulate and maintain hemostasis (130-132). When the endothelium is disrupted, it can result in myriad responses including leukocyte adherence, blood vessel constriction, activation of platelets, coagulopathies, cell growth, pro-oxidation, thrombosis, vessel inflammation, and atherosclerosis (132).

Although the endothelium provides for the exchange of fluid across its barrier, it regulates other molecules more closely. Sometimes this barrier is semi-permeable; selectively allowing some molecules through. In other areas, such as the brain, the barrier is much more restrictive, protecting the vital organ from molecules or microorganisms that could cause damage (133, 134). The ability of a molecule to get through the endothelial barrier, in any particular vascular bed, is determined by the molecular weight of that molecule. Movement across the endothelium is also determined in part by the charge of the molecules and the cell as well as the ability of the molecule to be taken up by the cell. Movement of water across the barrier is determined by albumin's interactions with the extracellular matrix and glycocalyx (134). The environmental concentration of albumin lowers hydraulic conductivity of the endothelium. Furthermore, endothelial cells can change shape in response to inflammation, and alterations in cytoskeletal reorganization, causing increases in

permeability to molecules across the barrier. These cytoskeltal changes can also be mediated by other intracellular signaling events such as increases in intracellular calcium (135).

Angiogenesis

The term angiogenesis describes the process of new blood vessel formation and growth from existing vasculature (136). Vasculogenesis, on the other hand, refers to spontaneous vessel growth (137). Angiogenesis is critical in many physiological processes such as development and healing of wounds (138). Unfortunately it can also occur inappropriately to cause injury or disease and is how tumors can transition from dormant to malignant (138, 139). This has led to the development of inhibitors of angiogenesis to be used in the treatment and prevention of cancer (140-142).

For angiogenesis to occur, first, growth factors specific for angiogenesis activate endothelial cell surface receptors, thereby activating the endothelial cells (136). Next, proteases are released from the activated cells which break down the endothelial basement membrane. This provides an opportunity for the endothelial cells to move away from the vessels to which they were bound. The newly freed endothelial cells begin proliferating in the ambient matrix to form solid sprouts which connect neighboring vessels (136). Then integrins grab onto the endothelial cells as the sprouts move toward the original stimulus, causing the sprouts to form loops creating the vessel lumen. This type of angiogenesis fills in gaps between vessels by forming brand new vessels (136, 138).

A different type of angiogenesis known as intussusception, also called splitting angiogenesis, occurs when a vessel is actually split in two by the extension of a capillary wall. Intussusception is critical as it involves cells that are already present but that restructure themselves to provide needed vasculature in the absence of a parallel increase in the actual number of

endothelial cells (143). Intussusception consists of four phases. Initially, two capillary walls opposite each other must make contact. Next, the endothelial cell junction architecture is reorganized leaving small openings through which growth factors and cells can move. Third, a "core" is formed at the point of contact between the vessels which pericytes and myofibroblasts occupy where they can start to lay the foundation for the extracellular matrix upon which the vessel will grow. The last step is when the core is "fleshed out" while the general structure of the core remains stable (143).

Permeability and Adherens Junctions

As gate keepers to the passage of molecules between the blood and tissues, the endothelial cells are critical, as is the stability of the junctions which maintain the connection between them. Many diseases and other pathological states can compromise this stability and lead to inappropriate endothelial permeability. These include, but are not limited to, Clarkson disease, sepsis, ischemia, diabetes and inflammation, each of which can result in serious and often fatal outcomes (144-147). One of the most important features of endothelial cells which regulate the permeability of the barrier, are the adherens junctions (AJ) (148-150). These junctions are opened and closed as needed in response to a myriad of intracellular signaling pathways. The main protein component of endothelial specific AJs is vascular endothelial cadherin (VE-cadherin), which binds directly to several intracellular proteins in the catenin family, including beta-catenin, p120-catenin and gamma-catenin (151). When intracellular signaling initiates reorganization of AJ to allow increased permeability, it does so through different pathways which act on different AJ protein components. One way is through the activation of vascular endothelial growth factor (VEGF), which causes tyrosine phosphorylation of VE-cadherin, followed by permeability increases and leukocyte migration (152, 153). Another mechanism is through the breakdown of the AJ by the removal of VE-cadherin when it is internalized and degraded (154).

There are two pathways through which permeability of the endothelium is regulated: the "transcellular" and the "paracellular"(155). Molecules either pass through, or between, the cells respectively. For transcellular passage of molecules, there must be fenestrae, or pores through which the molecules can move (156). Alternatively this can be accomplished through vesiculo-vacuolar organelles which can fuse creating what appear to be channels across a single cell that will allow movement of molecules through the endothelial layer (157-160). Paracellular movement however, is controlled by the opening and closing of intercellular junctions. Paracellular movement is tightly controlled to maintain hemostasis because opening the junctions can expose the extracellular matrix and lead to pathogenic thrombosis (149, 161, 162). Increased vascular permeability is usually reversible. A few of the compounds that can increase vessel permeability include VEGF, histamine and thrombin, each of which do so in a way that does not compromise the viability or health of the cells (147, 163). Sometimes, this permeability increase can even be helpful to the cells or tissues especially when it provides extra nutrients or oxygen, or allows the movement of immune cells into a site of injury.

Vascular damage can also cause increased permeability. Damaged endothelial cells retract, the barrier is compromised resulting in hemorrhage, leukocyte recruitment and adhesion and possibly thrombotic events (164). Vascular damage, unlike permeability, can be irreversible leading to serious disruptions in hemostasis.

The nature of endothelial cell junctions, as well as their molecular organization, has been elucidated in previous work, providing an understanding of how the junctions respond to cell signaling events (162, 165, 166). In addition to several types of intercellular connections, there are two major types of endothelial intercellular junctions which are comprised of a network of proteins bound to cytoskeletal components interacting with signaling proteins. These are the tight junctions

(TJ) and AJ. Although TJ are critical in regulating the blood brain barrier, AJ are ubiquitous throughout the vasculature and data suggests that AJ must be present and stable before TJ can form (165).

The main protein components of AJ are proteins belong to the cadherin family. Although endothelial cells express several cadherins, the cadherin involved in the formation of endothelial AJ is VE-cadherin (165, 167). Other AJ proteins include proteins in the catenin family (p120-catenin, beta and gamma-catenin) which bind directly to VE-cadherin's cytplasmic domains. The AJ is then connected to the actin cytoskeleton through interactions of gamma and beta catenin with alpha-catenin, and then to alpha-actinin and others (168). VE-cadherin and its catenin associations are referred to as the "cadherin complex", and can affect, and be affected, by the cytoskeleton. See Figure 1.4 for a diagram.

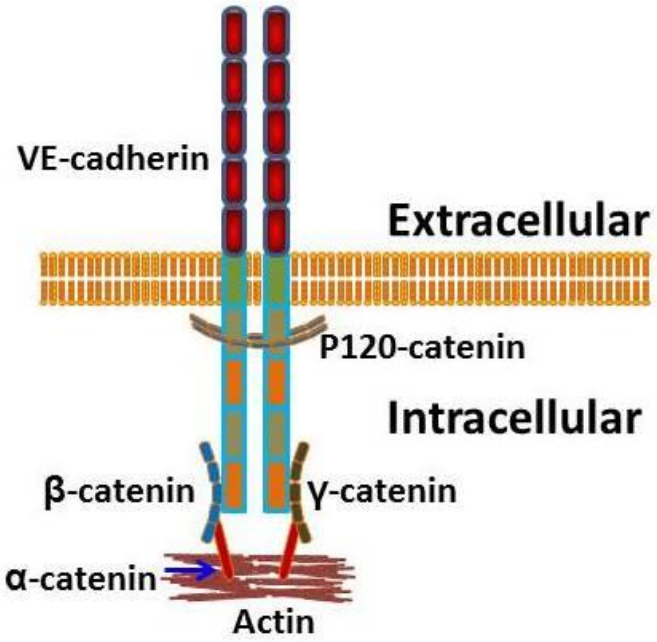

Figure 1.4: Diagrammatic representation of relevant VE-cadherin protein-protein interactions in Adherens junctions. Transmembrane VE-cadherin binds extracellularly to an adjacent VE-cadherin, and intracellularly with various catenins leading to actin associations. p120-catenin binds near the cell membrane, while beta-catenin and gamma-catenin associate more distally. Beta-catenin and p120-catenin are believed to be involved in the assembly of actin based structures.

Previously, the paradigm has been that AJ were bound to actin via alpha-catenin. But more recent data indicate that this is most likely not the case, because alpha-catenin is incapable of binding actin at the same time that it would bind beta-catenin (168).

Regardless of the mechanism, it still remains that VE-cadherin must interact with the catenins to fully regulate permeability through the AJ. When truncated VE-cadherin, that lacks the complete beta or gamma-catenin binding domain is present, the junctions are compromised (169). When done in mice, the VE-cadherin mutation results in fatal vascular reorganization (170). Anti-VE-cadherin antibodies given to adult mice results in vascular leakage and hemorrhaging (171). Compounds that only affect the adhesive properties of VE-cadherin such as histamine cause more mild, as well as reversible, effects (147).

N-cadherin is another cadherin found in endothelial cells, but it has been shown that it is distributed around the membrane rather than clustered at junctions. It has also been shown that when VE-cadherin is present, N-cadherin is excluded from the junctions (172). It is possible that when the endothelium is stable, N-cadherin functions at the membranes where endothelial cells meet pericytes (173, 174). When N-cadherin gene activation occurs in an endothelial cell specific manner, it causes a phenotype that resembles that of embryos lacking VE-cadherin. It was also described that in cultured cells, reduced N-cadherin expression results in inhibition of VE-cadherin expression (175).

Beta-catenin has been shown to play an important role in vascular permeability. Endothelial cell specific gene activation as well as the effects of beta-catenin null mouse embryos show abnormalities in the AJ formation and exhibit hemorrhage with increased blood pressure (176).

Many of the mechanisms that regulate vascular permeability involve the reorganization of AJ. Some of these mechanisms specifically target VE-cadherin by phosphorylation, while cleavage and degradation have also been shown to modulate the endothelial barrier functions (148, 157).

The current paradigm is that the AJ proteins can be modulated via tyrosine phosphorylation induced changes that compromise the endothelial barrier. Previous reports show that compounds which increase permeability (histamine, VEGF, platelet-activating factor and TNF-alpha), cause tyrosine phosphorylation of VE-cadherin as well as the catenins (beta, gamma, p120) (163, 177-180). When endothelial cells were sparse, there was more tyr phosphorylation of VE-cadherin than in confluent monolayers (181). In addition, the adhesion of immune cells, like leukocytes, can also induce phosphorylation of specific tyrosine residues on VE-cadherin, and is required for movement of the leukocytes across the endothelium (153, 182, 183).

Although the complete mechanisms of tyrosine phosphorylation of VE-cadherin have not been elucidated, the tyrosine kinase Src is a candidate. Src activation has been shown to be induced in response to VEGF and it has also been shown to directly interact with VE-cadherin (146, 184). Furthermore, Src deficient mice or those treated with Src inhibitors exhibit a decrease in Ve-cadherin tyrosine phosphorylation (147). There are contenders besides Src, however, including CSK which inhibits Src by binding VE-cadherin and phosphorylating it at a different tyrosine residue (185). PYK2 has been shown to phosphorylate beta-catenin, but it is unknown whether it can directly phosphorylate VE-cadherin (182). Kinases are not the only way in which VE-cadherin phosphorylation may be regulated. Phosphatases too, may play a role. Inhibition of phosphatases could increase VE-cadherin phosphorylation, thereby increasing permeability. Vascular endothelial protein tyrosine phosphatase (VE-PTP) is one endothelial-specific phosphatase that interacts with VE-cadherin to prevent its tyrosine phosphorylation (186). Without VE-PTP, mouse embryos can't

survive and exhibit deleterious alterations in blood vessel formation. Similar to VE-cadherin null embryos, this indicates that blood vessels are compromised in the presence of continuously phosphorylated VE-cadherin (187). There are other phosphatases, that may play a role as well by associating either directly or indirectly with VE-cadherin to affect its phosphorylation state: such as density-enhanced phosphatase-1 (DEP1), protein tyrosine phosphatase receptor type M (PTPμ), and SH2-containing phosphotyrosine phosphatase (SHP2) (188-190).

There is extensive evidence that tyrosine phosphorylation of VE-cadherin is important in regulating AJ architecture and endothelial permeability. However, it's important to understand that there are different tyrosine residues on VE-cadherin and they are phosphorylated, or dephosphorylated, in response to different intracellular signaling events. In Chinese hamster ovary (CHO) cells, the ability of VE-cadherin to bind p120- or beta-catenin can be lost if single point mutations are made (a single tyrosine-to-glutamic acid) of tyrosines 658 or 731 (respectively) (191). When VEGF activates Src in endothelial cells, it only phosphorylates VE-cadherin at tyrosine 685 (192). When ICAM1 induces neutrophil adhesion to the endothelium, VE-cadherin is phosphorylated at tyrosines 658 (Src) and 731(PYK2) (182). A different study showed that when ICAM interacted with lymphocytes it induced phosphorylation at tyrosines 645, 731 and 733, which was mediated not by Src, but by Rho, actin and Ca^{2+} (183). Differences reported might be due to differences in the conditions used for different experiments in different laboratories. More work needs to be done to address these issues and more completely elucidate the mechanisms by which VE-cadherin is differentially phosphorylated and dephosphorylated in response to different signaling pathways.

The AJ catenins can also act as substrates for the same kinases that phosphorylate VE-cadherin (180, 181). It still remains unknown, however, what effects, if any, this may have on AJ

stability or permeability of the endothelium. There is evidence that beta-catenin can also be tyrosine phosphorylated compromising its ability to bind the cytoplasmic tail of VE-cadherin and causing an increase in loss of beta-catenin at the AJ (193, 194). This may very well affect organization of the cytoskeleton and/or AJ architecture leading to an increase in permeability.

It has also been shown that the clathrin-dependent internalization of VE-cadherin can affect AJ stability, and increase vascular permeability (195). P120-catenin regulates VE-cadherin levels and stabilizes the AJ by preventing this internalization, and also by inhibiting its association with activated Src (196). It has also been shown that VE-cadherin internalization can occur through a VEGF pathway. In this pathway, VEGF activates Src which phosphorylates VAV2 which activates Rac. Activated Rac induces phosphorylation of VE-cadherin at a Serine (665) which recruits beta-arrestin-2 to VE-cadherin, a process also resulting in clathrin-dependent internalization of VE-cadherin (197).

Increased vascular permeability might also be a result of VE-cadherin lysis. VE-cadherin is susceptible to degradation by many different compounds including elastase, trypsin, cathespin G and metalloproteases (198-201). These enzymes are produced in large quantities by Leukocytes and tumor cells which could result in VE-cadherin digestion with increased cell movement and vascular permeability.

VE-cadherin has also been shown to associate with FLK1 (aka VEGFR2 or KDR) causing a decrease in proliferation signaling induced by the receptor. When this occurs, VEGF is unable to induce phospholipase Cγ (PLCγ) or activate MAP kinases to the same degree. This is due to VE-cadherin inhibition of receptor phosphorylation and subsequent internalization (202). This plays a role in VE-cadherin-induced cell growth contact inhibition and requires the phosphatase DEP1 (188, 203). Furthermore, this interaction of FLK1 and VE-cadherin may contribute to AJ protein

phosphorylation by Src inducing increased vascular permeability (147). An interesting note is that *in vivo* angiogenesis does not require Src activation by FLK, a difference that distinguishes proliferation from increased permeability (204). The mechanism of the interaction between FLK1 and VE-cadherin remains unclear. It has been shown that to bind FLK1, VE-cadherin must retain the ability to bind beta-catenin, but not p120-catenin (188).

Specific Aims

Specific Aim 1) To demonstrate that, direct Junín virus infection of primary human endothelial cells, results in decreased monolayer barrier function.

Hypothesis: The virulent strain of JUNV, Romero, will decrease endothelial cell monolayer barrier electrical resistance and increase permeability to FITC-dextran. The avirulent strain, Candid#1, will not increase monolayer permeability or decrease monolayer barrier function.

Rationale: Clinical observations of vascular dysregulation and fluid distribution problems in patients with AHF are indicative of an endothelium that has increased permeability. Based on those observations and the fact that human endothelial cells can be productively infected with JUNV, with no visible cytopathology, this study aims to determine the effects of direct JUNV infection on human endothelial cell monolayer barrier function.

Approach: Use Electric Cell-Substrate Impedance Sensing (ECIS) and transwell permeability assays to determine if infection of human endothelial cells with either a virulent (Romero) or avirulent (Candid#1) strain alters monolayer barrier integrity or increases monolayer permeability.

<u>Specific Aim 2)</u> To demonstrate that, direct Junin virus infection of primary human endothelial cells, results in the disruption of endothelial adherens junctions and alters levels of one or more of the protein components of these junctions.

Hypothesis: (1) Adherens junctions will be disrupted during Romero infection, but not Candid#1 infection of human endothelial cells, which will be evidenced by either changes in the levels or localization of any (or all) of the major adherens junction proteins, and/or by disruption of the VE-cadherin/beta-catenin complexes. (2) Romero infection and not Candid#1 infection will also affect the actin architecture of the infected cells.

Rationale: Adherens junctions play a major role in regulating vascular permeability. Unlike tight junctions, AJ are found in all endothelial cells and are necessary for tight junction formation. They also stabilize the cells by anchoring the cytoskeleton to the junctions. For those reasons, this study focuses on examining the effects of JUNV infection on the adherens junctions of human endothelial cell monolayers.

Approach: Immunocytochemistry, Immunoprecipitations and western blotting will be used to determine changes in the major protein components of adherens junctions: vascular endothelial cadherin (VE-cadherin), beta-catenin, and p120-catenin as well as actin, one of the major components of the cytoskeleton.

<u>Specific Aim 3)</u> To demonstrate that Junin virus induced alterations in endothelial adherens junctions is modulated by at least one Src kinase family member and can be ameliorated by its inhibition.

Hypothesis: The mechanism of JUNV Romero-induced disruption of endothelial barrier function involves the activation of Src kinase and can be prevented by its inhibition.

Rationale: Src family kinases have been shown to play a key role in regulating adherens junction function to regulate permeability during angiogenesis, wound healing and in response to VEGF and TNF-alpha. Based on this data, this study aims to examine the role of Src kinase in JUNV mediated endothelial cell barrier dysfunction and whether this can be ameliorated with Src inhibitors.

Approach: (1) Use ELISA to examine levels of activated Src in endothelial monolayers infected with JUNV. (2) RNAi or pharmaceutical Src inhibitors will be used during JUNV infection of human endothelial cells to determine the effects of Src inhibition on virus-induced barrier dysfunction.

Chapter 2. Materials and Methods

Cells

Endothelial Cells

Primary, single donor HUVEC and HMVEC-L (Lonza, Walkerville, MD, USA) were cultured in endothelial cell basal medium (EGM-2 and EGM-2 MV bulletkits respectively; Lonza, Walkerville, MD, USA) plus 20% fetal bovine serum (Gibco, Aukland, New Zealand) supplemented with L-glutamine, antibiotics on plates coated with type I rat tail collagen (Millipore/Upstate, Temecula, CA) at 10µg/cm^2. Cells were used at passages 3-7 in all experiments. HUVEC and HMVEC-L cells were infected with Candid#1 or Romero at an MOI of 4 unless otherwise indicated. At selected time points after infection, whole cell lysates and cell culture supernatants were collected.

Vero Cells

Vero E6 cells are a clone of Vero 76 cells from African green monkey kidney epithelial cells. These cells were cultured in DMEM plus 10% fetal bovine serum supplemented with L-glutamine and antibiotics/antimycotics (Gibco). These cells were used to grow viral stocks and to titer the virus using plaque assays for this study.

Viruses

Candid#1 was initially developed as a human vaccine.(122) We acquired it from Dr. Robert Tesh of the University of Texas Medical Branch at Galveston, after 1 passage in suckling mice. It was passaged again in Vero E6 cells, at 35C, which generated the highest stock titers, to create a working stock for infections. The Junín Romero strain was initially isolated from a fatal AHF case using MRC5 cells.{Kenyon, 1986 #325} We obtained it from Dr. Mike Holbrook of the University of Texas Medical Branch at Galveston. The virus stock underwent 2 passes in Vero

cells at 37C, and then an additional passage in Vero cells at 37C was done to generate the working stock (passage 3). All work using the virulent Romero strain of JUNV was performed in the University of Texas Medical Branch BSL4 facility according to all institutional health and safety guidelines.

Plaque Assay

Plaquing Candid#1 and Romero posed a considerable challenge and the following protocol was strictly adhered to. Serial ten-fold dilutions of unknown samples and known controls were generated. 6-well plates of barely-confluent Vero E6 cells (<passage 40) were inoculated with 100ul of each sample dilution and allowed to incubate 1 hour at 37C with gentle rocking every 15 minutes to distribute the virus inoculum over the monolayer. After the incubation, the wells were gently overlaid with 3ml per well of a 1:1 solution of 2X MEM and 1% SeaKem agarose. Plates were left undisturbed until the overlay polymerized, at which point they were moved to a 37C incubator and allowed to remain undisturbed until the second overlay. The second overlay was the same as the first, with the addition of 2% neutral red indicator dye to the solution. This overlay was added to the 6-well plates, gently on day 6 after the first overlay for Candid#1, and on day 5 for Romero. Again the plates were allowed to remain undisturbed until the second overlay polymerized, after which they were moved to the 37C incubator. Plates were examined between 12-24 hours post second overlay, or the plaques would not be visible. PFU/ml was calculated by:

(Average number of plaques) X (dilution factor) X (inoculum size) = PFU/ml

Infection of monolayers

HUVEC and HMVEC cells were seeded at 3.3 X 10^4 cells/cm^2 and allowed to reach confluency. Confluency was defined as the point at which the monolayer barrier function reached stable levels as determined by ECIS. When seeded at this density, the monolayers needed 108

hours post seeding to reach confluence. Within 6 hours of reaching confluence, monolayers were infected as follows with either the Candid#1 or Romero strain of JUNV at an MOI = 4, or were mock infected with Vero cell culture supernatant. All work using the virulent Romero strain of JUNV was performed in the University of Texas Medical Branch BSL4 facility according to all institutional health and safety guidelines

To infect the monolayers, culture medium was aspirated from cell culture dishes and inoculum added. Infection was allowed to proceed for 1 hour at 37C in a 37C incubator. Every 15 minutes, culture plates were gently rocked to redistribute the virus. After the incubation time, the inoculum was removed and fresh culture media was added to the plates which were then returned to the incubator.

Electric cell-substrate impedance sensing (ECIS™)

For determining alterations in transendothelial electrical resistance, the ECIS™ system Model 1600R and electrode arrays (Applied Biophysics Inc, Troy, NY) were utilized. Specifically, 8W10E+ arrays were used. The array chambers were coated with 10µg/cm^2 of type I rat tail collagen for 30 minutes at 37°C. HUVEC and HMVEC-L cells were seeded at a density of 3.3X10^5 cells/cm^2 and infected 108 hours post seeding at MOI of 4. ECIS measurements immediately following seeding at that density indicated that 108 hours post-seeding was the time when confluence had been reached and remained stable, for both HUVEC and HMVEC-Ls. Resistance, capacitance, and impedance information was collected continuously for five days post infection. Each experiment was repeated 3 times in sextuplicate.

Transwell permeability assays

Collagen-coated (10 μg/cm^2) Transwell polycarbonate filters (pore size 0.4 μm, exposed area 1 cm^2; Costar, Brumath, France) were used. HUVECs and HMVEC-Ls were seeded at passage 5 at a density of 3.3X10^5 cells/cm^2 on the filter surface. The upper chamber of the transwell contained 0.5 mL culture medium and the lower 1.5 mL of culture medium. Infection was done 108 hours post-seeding**.** Fluorescein isothiocyanate (FITC)-labeled dextran (molecular weight of 70 kDa Sigma) was used as an index of macromolecular diffusion. After infection with Candid#1 at MOI=4, 1 mg/ml FITC-dextran in HUVEC medium, was added to the upper chamber of the Transwell system. 100μL samples were taken from the lower chamber at 24h intervals and the same volume of HUVEC medium was replaced in this chamber to prevent fluid movement due to hydrostatic pressure. The fluorescence was measured with a spectrophotometer (Fluoroskan Ascent, Thermo-Scientific) using 480 nm and 520 nm as the excitation and emission wavelengths, respectively. The quantities of all abluminal dextrans were estimated using a standardization curve.

Immunocytochemistry

HUVECs and HMVEC-Ls were seeded at 3.3X10^4 cells/cm^2 on collagen coated Permanox chamber slides (Nalge Nunc Internationsl, Rochester, NY) and infected 108 hours post seeding. Preliminary studies of ECIS growth kinetics indicated 108 hours post seeding was the peak time of electrical resistance. Chamber slides were fixed in 4% paraformaldehyde in PBS for 10 minutes at room temperature. And then permeabilized in 0.2% TritonX-100 in PBS for 5 minutes at room temperature. Alexa Fluor 488 and Alexa Fluor 594 (both at 1:500; Molecular Probes, Leyden, Netherlands) labeled secondary antibodies were used for fluorescence detection. Slides were mounted using Prolong Gold anti-fade reagent with DAPI (Invitrogen, Eugene, OR) to stain for

nuclei. Confocal images were acquired using Zeiss LSM 510 w.s. software on a Zeiss Axiovert 200M inverted microscope (both from Carl Zeiss, Oberkochen, Germany). All images are representative of 3-5 independent experiments. Table 2.1 contains designated primary antibodies along with the dilutions and secondary antibodies used for all immunofluorescence and immunoblotting in this study.

Target	Species	Specificity	Clone#	Stock Concentration	Vendor	Working Dilution	Use	Secondary Reagent
PECAM	Mouse	h	E-8	200ug/ml	Santa Cruz Biotech	1:200	Western Blot	Anti-mouse HRP
Beta-catenin	Mouse	m, r, h	E-5	200ug/ml	Santa Cruz Biotech	1:200	Immunofluorescence/ Western Blot	Anti-mouse Alexafluor 488/Anti-mouse HRP
VE-cadherin	Goat	m, r, h	C-19	200ug/ml	Santa Cruz Biotech	1:100	Immunofluorescence/ Western Blot	Anti-goat Alexafluor 488/Anti-goat HRP
P120 Isoform1	Mouse	m, h	G-7	200ug/ml	Santa Cruz Biotech	1:100	Immunofluorescence/ Western Blot	Anti-mouse Alexafluor 488/Anti-mouse HRP
P120 Isoform 2	Rabbit	m, h	H-90	200ug/ml	Santa Cruz Biotech	1:100	Western Blot	Anti-rabbit HRP
Beta-actin	Mouse	h	9	200ug/ml	Santa Cruz Biotech	1:100	Western Blot	Anti-mouse HRP
*Phalloidin Alexafluor 488	n/a	broad	A12379	300 units	Molecular Probes/Invitrogen	1:100	Immunofluorescence	n/a

Table 2.1: List of primary antibodies, working dilutions and secondaries used. *Phalloidin is not an antibody, it is an Alexafluor conjugated, high affinity F-actin probe.

Immunoprecipitations

Immunoprecipitations were performed after cells were lysed in RIPA buffer (Thermo Scientific, Rockford, IL) with Halt Phosphatase Inhibitor (Thermo Scientific) and protease

inhibitor cocktail tablets (Roche, Mannheim, Germany). 400μg of protein was used with 4 μg of primary antibody and was gently agitated overnight at 4°C. 40 μL of protein A/G beads (Pierce, Rockford, IL) were then added to the mixture and gently agitated overnight at 4°C. The beads were resuspended by boiling in 6X Laemmli buffer and run on an SDS-PAGE gel and transferred to nitrocellulose membranes. The membranes were then probed with various antibodies.

Western Blot

Detection of proteins was performed by western blotting whole cell lysates from HUVECs or HMVEC-Ls grown on 100-mm tissue-culture plates. Lysates from mock infected cells were used as a control. Protein concentrations were determined by using the BCA Protein Assay Kit (Thermo Scientific). Using the results from the BCA protein assay the amount of protein added for each sample was normalized. Cell lysates or immunoprecipitations were run on SDS-PAGE gels (Biorad, Hercules, CA) and transferred onto nitrocellulose membranes (Biorad). The membranes were blocked with 5% non-fat milk powder diluted in TBST (20mM Tris, pH 7.6, 140 mM NaCl, 0.2% Tween-20) for 1 hour at room temperature. Proteins were detected using antibodies listed above and incubated for 1 hr at room temperature with gentle agitation or overnight at 4°C. The blots were then incubated with goat anti-rabbit, anti-mouse or anti-goat horseradish peroxidase-conjugated secondary antibody (Santa Cruz). Supersignal West Pico (Pierce, Rockford, IL) was used to visualize the proteins. ImageJ software from the NIH was used to quantitate bands normalized to beta-actin.

Cytokine Analysis

Supernatant samples from HUVEC and HMVEC-L monolayers infected with either Candid#1, Romero or mock infected, were collected at 24 hour time points for 5 days post

infection and analyzed either via Bioplex (Bio-Rad, Hercules, CA), VeriKine ELISAs (41100-1 or 41410-1, PBL, Piscataway, NJ) or an interferon bioassay. The Bioplex and VeriKine assays were performed according to manufacturer's protocols. For the interferon bioassay, Vero cells were seeded in 96 wells plates at 1.5x105 cells/ml and kept in 37C CO2 incubator. After 24 hours, the plates were decanted and 110 µl EMEM with 2% FBS was added to each well. 50µl of each cell supernatant was added to the wells in duplicate and serially diluted to 1:3. The plates were incubated for 24 hours at 37C after which they were decanted and washed 3X with HBSS. After the last wash 25µl of a sindbis virus dilution was added to each well except for the cell controls which received 25µl of EMEM 2%. Plates were incubated 1 hour at 37C then decanted and 100ul of methylcellulose was added. After another 24 hour incubation at 37C, the plates were evaluated for plaques which were then stained with crystal violet and counted if present.

ELISAs

PhosphoSrc or VEGF: To measure levels of activated Src kinase or VEGF in the infected or mock infected HUVEC and HMVEC-L monolayers the PathScan phosphor Src (Tyr416) sandwich ELISA kit (#7953 Cell Signaling Technology, Danvers, MA), or the Human VEGF ELISA kits (#EHVEGF, Thermo Scientific, Rockford, Il), were used. Cell lysates from cells either infected with Candid#1, Romero or mock infected were analyzed for phosphoSrc tyr416 or VEGF levels according to the manufacturer's protocols for the ELISA kits.

Chapter 3. Junín virus infection causes decreased endothelial cell monolayer barrier integrity and increased monolayer permeability

Summary

Endothelial dysregulation is a key component of the hemorrhagic fever caused by Junín virus, although the pathogenesis of this dysfunction is unclear (87, 91). One study demonstrated that JUNV infection altered endothelial cell nitric oxide production and adhesion molecule expression, with no cytopathology, but that study did not address the effects of JUNV infection on permeability or cell-cell junction integrity (87). This study reports that direct JUNV infection of human endothelial cells with either the virulent Romero strain, or the non-virulent Candid#1 strain, does decrease monolayer barrier electrical resistance and increase permeability.

Introduction

The endothelium is the primary barrier maintaining separation of blood and tissues. As such, it is critical that it not be compromised so that it can effectively regulate the exchange of nutrients and molecules into and out of the blood. A healthy, properly functioning endothelium is the gatekeeper: a powerful semi-permeable sentry that is responsible for, among other things, allowing the transmigration of leukocytes during immune responses, preventing anything unwelcome from crossing over into the brain and maintaining tissue fluid balances. Endothelial *permeability* refers to the movement of solutes through paracellular junctions, a process regulated by diffusion and dynamic function of interendothelial junctions (205). The junctions must be able to respond as needed to extrinsic and intrinsic cellular signals, often concomitant, which can induce the intercellular contacts between cells to dissolve or reform as needed. Permeability is critical in many normal physiological processes such as wound healing, immune cell recruitment and

angiogenesis. Inflammation cannot occur without permeability, but it can contribute to disease when it occurs inappropriately, such as during lead poisoning, sepsis and cancer metastasis (145, 147). Some pathogenic permeability is a result of endothelial damage while some instances are more subtle, the result of inappropriate signaling which results in the opening of intercellular junctions rather than cell damage or death. This can compromise vascular homeostasis and otherwise deleteriously affect the surrounding tissues.

JUNV has been shown to productively infect human umbilical vein endothelial cells (HUVECs) without causing overt cell damage, and several questions regarding JUNV pathogenesis have been addressed using HUVECs as a model but most are limited to the attenuated Candid#1 because the virulent strains of JUNV are CDC category A agents that must be handled in BSL4 facility. The effects of JUNV infection, on the barrier function of an endothelial monolayer, have not yet been investigated. It has been reported that patients infected with JUNV exhibit increased levels of TNF-alpha and INF-alpha, which can contribute to endothelial permeability, and may play a role during disease progression (94). It is possible that direct infection of the endothelium could contribute to the vascular syndrome associated with AHF, so this study aims to determine if and how JUNV infection impacts endothelial cell monolayers.

To determine if direct infection plays a role in pathogenesis of JUNV infection, primary, single donor human endothelial cells were infected with either the attenuated vaccine strain, Candid#1, or the virulent Romero strain of JUNV and monolayer barrier function was assessed via ECIS and transwell permeability assays. Because HUVECs are a well-established and highly characterized model of endothelial function they were chosen as the initial model in which to examine the questions posed in this study. However, because JUNV most likely infects the microvascular cells of the lungs upon initial exposure, which is most often inhalation of aerosols,

HUVECs may not be considered the most physiologically relevant of the endothelial cell subtypes for this investigation. For that reason, this study also used human microvascular endothelial cells from the lungs (HMVEC-Ls) as an additional model of endothelial JUNV infection.

Results

Infection with JUNV decreases HUVEC and HMVEC-L monolayer electrical resistance

To determine whether JUNV infection could disrupt endothelial cell monolayer barrier integrity, electric cell-substrate impedance sensing (ECIS) was used to measure trans-endothelial resistance. Using ECIS, infected HUVEC and HMVEC-L monolayers were continuously evaluated for barrier integrity after infection. Confluent monolayers of passage 4 HUVECs or HMVEC-Ls were infected with JUNV and monitored via the ECIS system. In this model, the cell membranes *impede* the electrical current as they grow on the electrodes. This forces the current to flow between or under the cells, resulting in increased *impedance*. Impedance data are converted to resistance (ohms, Ω) and capacitance and reported and documented using the ECIS software. Monolayers were seeded and allowed to reach confluency. Pre-infection resistance levels were used to verify that confluence was achieved and maintained and that the cells exhibited normal low levels of resistance variations. Decreased resistance indicates reduced monolayer barrier integrity. Mock infection was performed using uninfected Vero cell culture supernatant. As shown in Figure 3.1, at approximately 60 hours post infection, electrical resistance of both the HUVEC (3.1 A) and HMVEC-L (3.1B) monolayers infected JUNV decreased relative to mock-infected cells. Productive infection was verified by using supernatant samples to generate growth curves which are depicted in Figure 3.2.

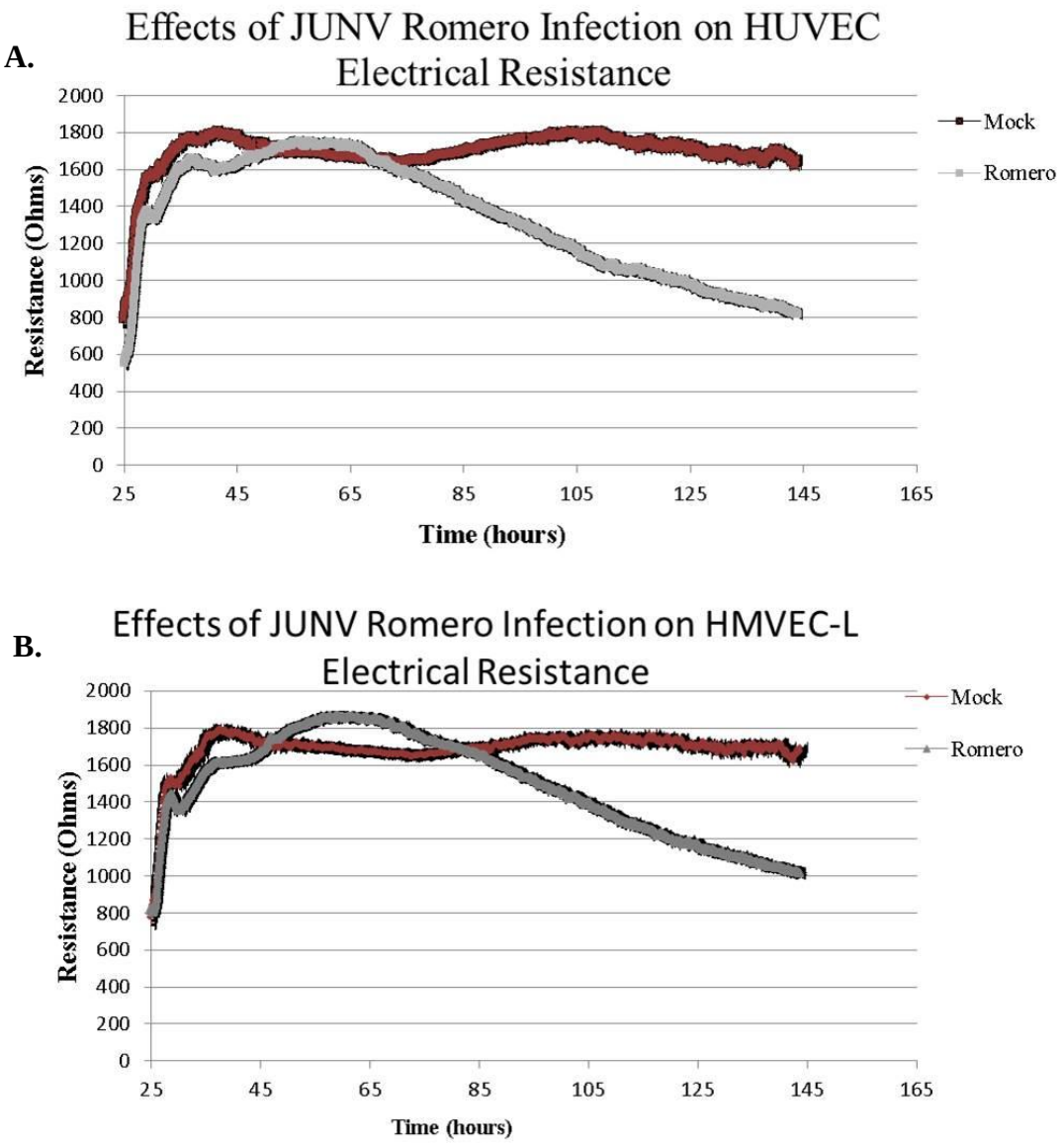

Figure 3.1. JUNV Decreases HUVEC and HMVEC-L Electrical Resistance. Cells were seeded onto collagen-coated gold electrode arrays and allowed to reach confluence (108h post seeding). Monolayers were then infected with JUNV or mock infected and evaluated by ECIS. HUVECs **(A)** or HMVEC-Ls **(B)** infected with JUNV show decreased electrical resistance beginning at approximately 60 hours post infection (~85 hours after plates were connected to ECIS machine.). Mock infected show no decrease in electrical resistance. Images are representative of 3 or more independent experiments.

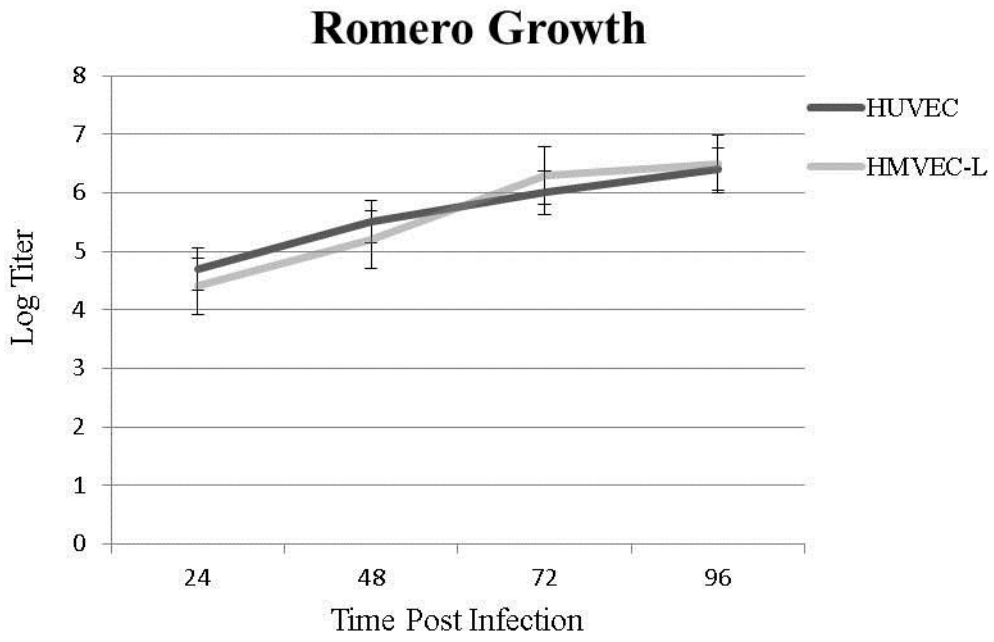

Figure 3.2 Growth curve of JUNV Romero in HUVECs and HMVEC-Ls indicate productive infection and viral titer during ECIS experiments. Each point represents the mean ± standard deviation from three experiments

Infection with JUNV increases HUVEC and HMVEC-L monolayer permeability to 70kD FITC-dextran

To establish the physiological relevance of the ECIS data, transwell permeability assays were performed to determine if the drop in electrical resistance coincided with increased permeability of the HUVEC or HMVEC-L monolayer to FITC-dextran. Confluent monolayers of passage 4 HUVECs or HMVEC-Ls were infected with JUNV or mock infected with Vero cell culture supernatant. After the infection, 70 kDa FITC-dextran was added to the upper chambers and samples from the lower chambers were taken at 24 hour intervals. Any fluorescence detected in the lower chambers was attributed to movement of the FITC-dextran from the upper chamber through the monolayer. This allowed us to evaluate whether molecules approximately the size of albumin would be able to move through the monolayer during JUNV infection. JUNV infection significantly increased the amount of 70 kDa FITC-dextran allowed to pass through HUVEC and HMVEC-L monolayers compared to mock infected cells (Figure 3.3). Supernatant samples were also taken to calculate viral titers over the time course of the experiment. Viruses were productively infecting the monolayers of both cell types, as shown in Figure 3.4.

A.

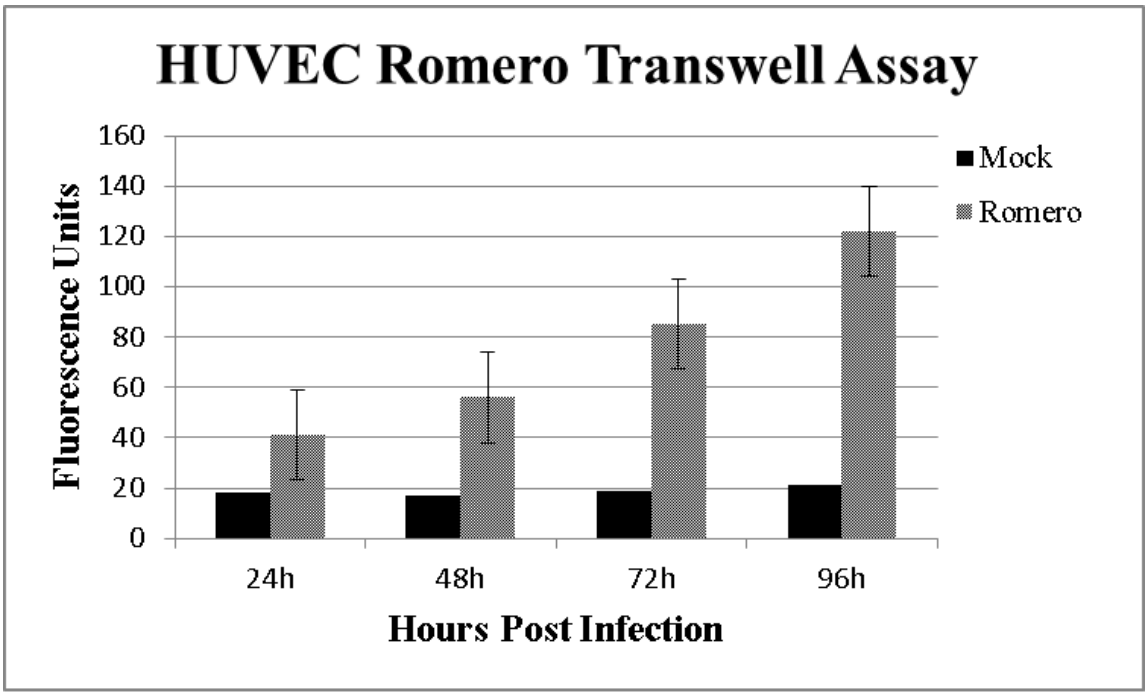

B.

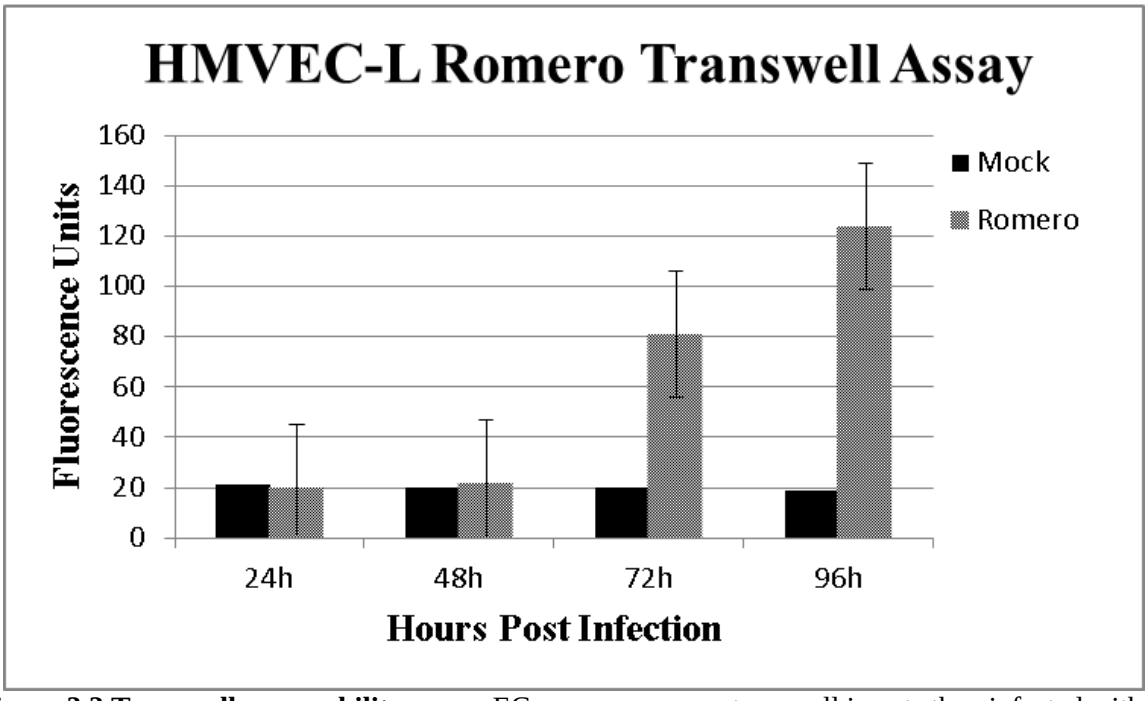

Figure 3.3 Transwell permeability assay. ECs were grown on transwell inserts then infected with JUNV. Samples were taken every 24h for 5 days. HUVECs **(A)** or HMVEC-Ls **(B)** infected with JUNV show an extremely significant increased permeability to 70 kDa FITC-Dextran in the absence of visible cytopathology ($P<0.0001$ by paired t-test). Data are the mean ± standard deviation from three experiments.

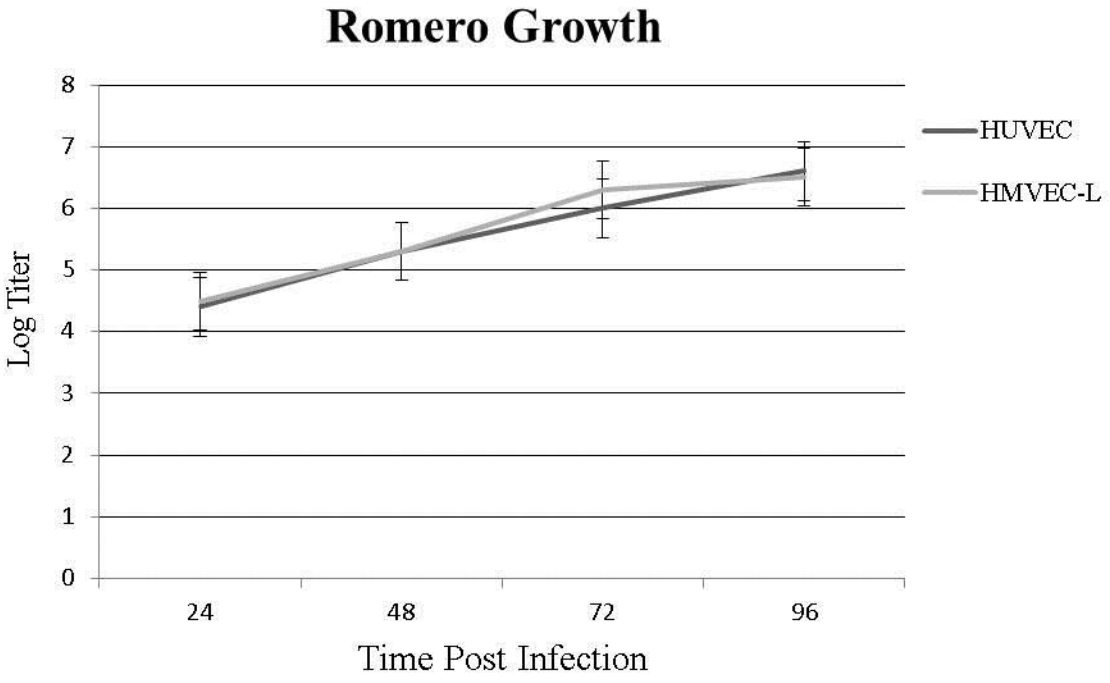

Figure 3.4 Growth curves of JUNV indicate productive infection and viral titer during transwell experiment. Growth of JUNV Romero in HUVECs and HMVEC-Ls during the first 96 hours of the transwell experiment. Each point represents the mean ± standard deviation from three experiments.

Gamma irradiation of JUNV prevents the decrease in electrical resistance in HUVEC and HMVEC-L monolayers

To determine if viral replication and productive cellular infection are necessary for the increase in permeability, gamma irradiated virus was used to infect the cells. Although this question as not within the original scope of this study, the results would give us important information about the nature of the virus/cell interaction that is occurring to cause increased permeability. There was no detectable decrease in electrical resistance with infection with killed JUNV, in either endothelial cell type tested (Figure 3.5).

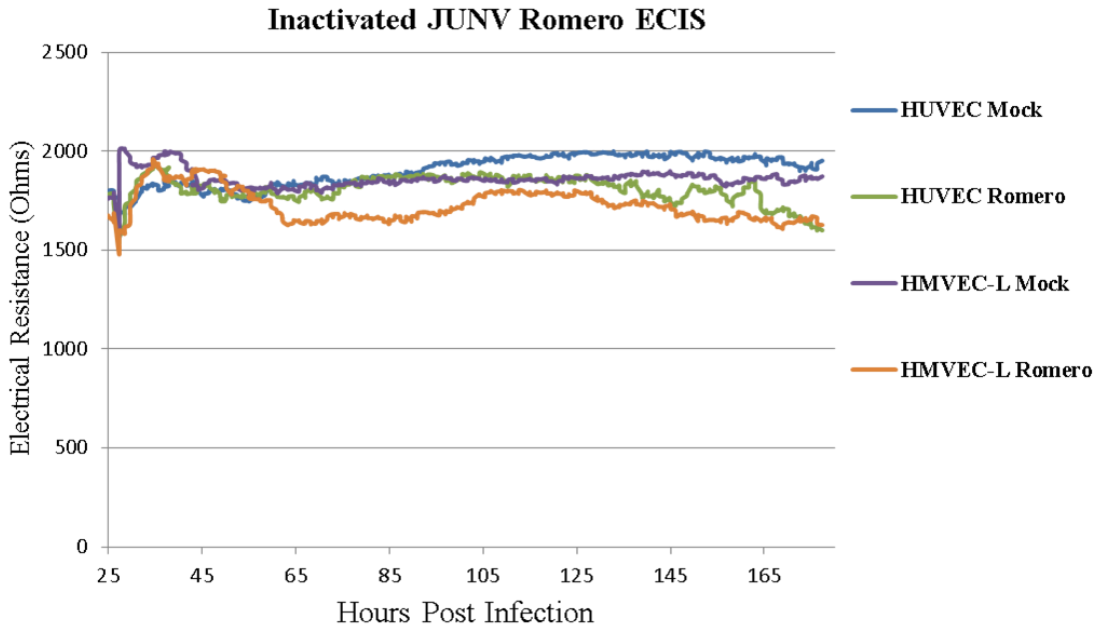

Figure 3.5 Killed JUNV Does Not Decrease HUVEC and HMVEC-L Electrical Resistance. Cells were seeded onto collagen-coated gold electrode arrays and allowed to reach confluence (108h post seeding). Monolayers were then infected with JUNV Romero killed with gamma irradiation (5MRad) and evaluated by ECIS. Gamma irradiated JUNV infection does not decrease HUVEC and HMVEC-L monolayer electrical resistance. Data are representative of 3 independent experiments.

HUVEC and HMVEC-L monolayers exhibit no overt visible cytopathology during infection with JUNV

It has been reported that JUNV infection in HUVECs causes no cytopathology, an observation confirmed in this study, by phase contrast microscopy and immunoblotting for platelet–endothelial cell adhesion molecule (PECAM), an endothelial cell marker that is present in healthy monolayers (206). As is seen in Figure 3.6, the relative amounts of PECAM detected in cell lysates of HUVECs and HMVEC-Ls infected with JUNV are the same at 48 and 72 hours post infection. Densitomtery of the western blot bands confirm the visual assessment (3.6 B). Because permeability and resistance changes occurred after 60 hours post infection, the western blot data in this dissertation includes 72 and 96 hours post infection.

Visual confirmation of healthy, confluent HUVEC and HMVEC-L monolayers is seen in Figure 3.5, which shows phase contrast microscope images of the monolayers infected with either JUNV Romero at 72 hours post infection. Viral titers were also calculated to verify productive infection during the experiment in which the phase contrast photos were taken and PECAM samples generated (Figure 3.7).

A.

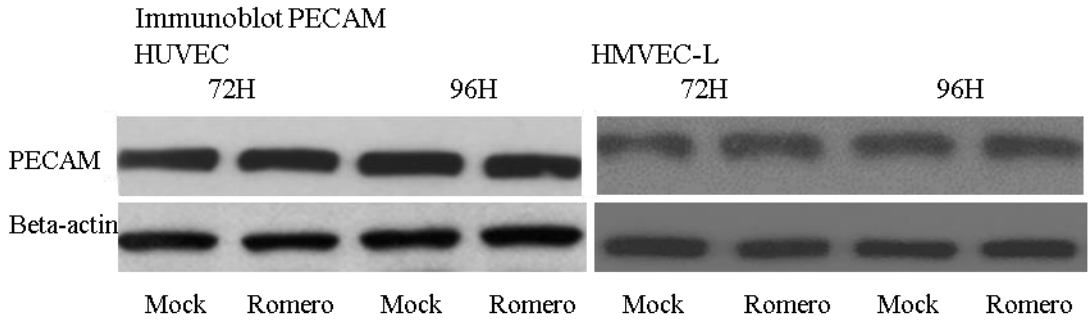

B.

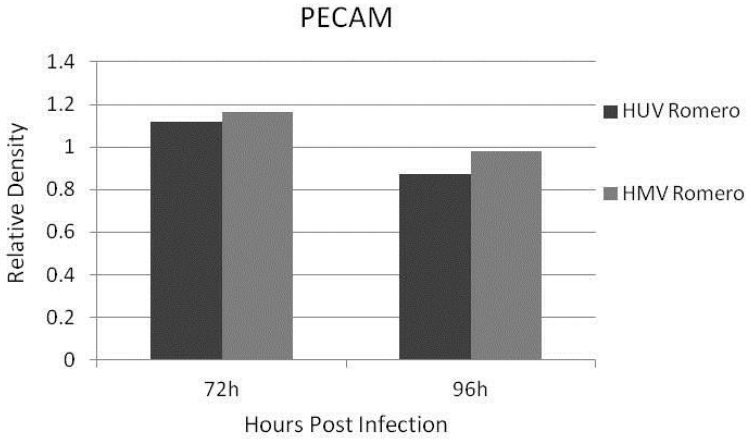

Figure 3.6 (A.) Western blot of PECAM. There are no detectable differences in PECAM between Romero-infected and mock in both cell types. **(B.)** ImageJ Analysis of immunoblotted bands was used to measure relative band density. The results were normalized to beta-actin and are representative of 3-5 independent experiments.

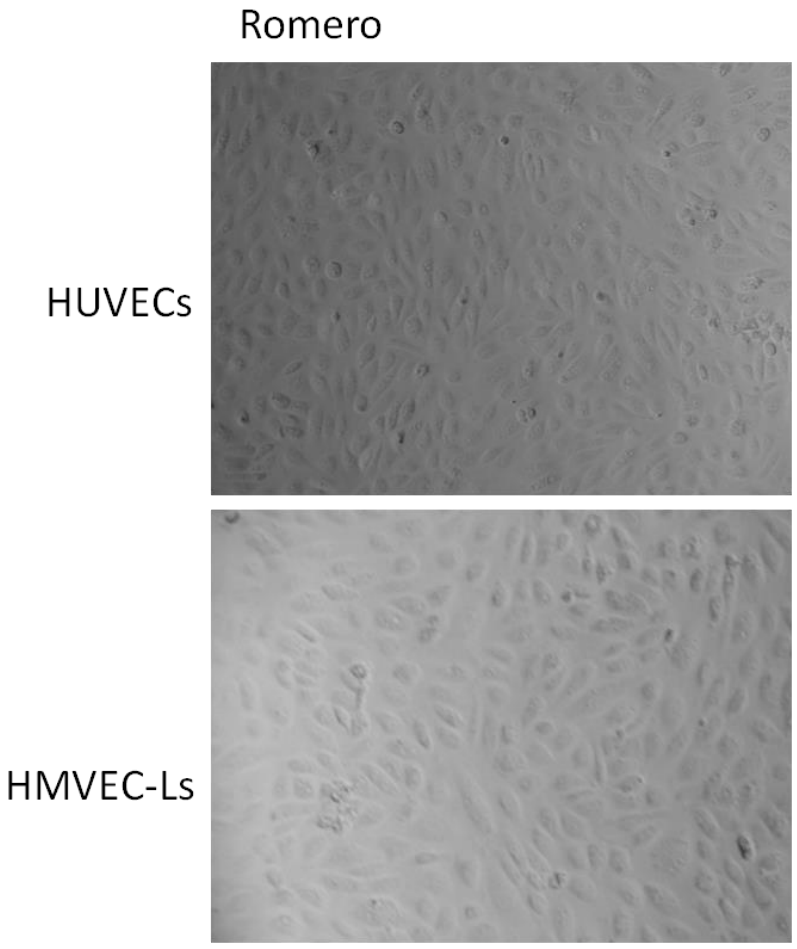

Figure 3.7 Phase contrast microscope observations of HUVEcs and HMVEC-Ls during infection with JUNV. Cells were seeded onto collagen-coated cell culture plates and allowed to reach confluency before infected with JUNV. Both cell types exhibit healthy monolayers during infection with JUNV Ronmero at 72 hours post infection. Images are representative of 3-5 independent experiments.

Discussion

Clinical manifestations of AHF indicate vascular dysregulation with increased vascular permeability in the absence of overt endothelial damage. Patients exhibit thrombocytopenia, leucopenia, proteinuria and fluid distribution problems. Vomiting and dehydration can cause rising hematocrits, but even hospitalized patients receiving fluid replacements experience hemoconcentration (94). Hemorrhage occurs, but clinically is usually more than ITP or other non VHF conditions at similar levels of thrombocytopenia. These observations implicate an endothelium which, although not visibly damaged, is altered enough to perhaps initiate a permeability increase that, when combined with other physiological factors during infection, may contribute to development of disease. The presence of a vascular syndrome, in the absence of overt vascular damage, reminds us that it is possible for a viral infection to affect cellular processes without overt cellular injury. For example, LCMV, another arenavirus, alters growth hormone levels in the pituitaries of CH3/ST mice while leaving housekeeping functions undisturbed (89, 207, 208). It is possible that the endothelial cellular response to JUNV infection contributes to disease progression and understanding that response is necessary to effectively prevent and treat AHF.

For that reason, the role of direct infection of endothelial cells with JUNV was investigated, with results indicating that JUNV infection alone does, in fact, decrease HUVEC and HMVEC-L monolayer barrier function, and increase HUVEC and HMVEC-L monolayer permeability to FITC-dextran in the absence of visible cytopathology. Because JUNV infection decreases endothelial barrier function, it is important to find out the mechanism so that possible therapeutic targets can be identified. Since approximately 90% of the outcomes in patients with AHF who enter the hemorrhagic phase are fatal, finding treatments that target the vascular

syndrome is critical in saving lives. To achieve this, the mechanisms underlying these changes in barrier function need to be elucidated.

Although the results indicate that the permeability observed allows 70kD dextran to move through the monolayer, there are many things to consider when evaluating this information. The ability of a molecule to move through gaps in the endothelium is dependent on several things, and size is merely one factor. The shape as well as the charge of a molecule can also affect its ability to move through the monolayer. So although this data indicates the relative size of the molecules measured, moving through the monolayer, it does not definitely indicate which physiologically relevant molecules might actually make it across if this were to occur during disease development.

The fact that inactivated virus does not cause the same changes in permeability or resistance, indicates that productive viral infection and replication within the cells is required for these changes in endothelial barrier integrity. This is not surprising based on reports that viral replication requires interaction with the actin cytoskeleton (209, 210). It is possible that it is this very interaction which initiates the intracellular signaling changes to disrupt the monolayer. Adherens junctions are directly connected to the actin cytoskeleton via catenins, so disruptions in the actin network could affect the junctional architecture. The actin data presented in Chapter 4 indicates that there are alterations in actin that, although not enough to compromise the overall health of the cells, may be sufficiently altered that it would not be unexpected to be mechanistically involved in the increased permeability seen here.

These experiments were also carried out using the non-virulent vaccine strain of the JUNV, Candid#1. There were no differences found between Candid#1 and the virulent Romero strain in these studies, so the Candid#1 data has been included in the appendix at the end of this dissertation. Although the lack of any differences between the two strains here was unexpected, it is revealing in

that it indicates that the attenuation of Candid#1 may be due to reasons other than an inability to cause the same intra-endothelial cellular changes as the virulent strain. Some possible explanations include that attenuation of the vaccine strain may be due to a decreased ability of that strain to replicate and disseminate in a human. This could either be due to deficiencies in the virus's ability to replicate in a human, or an increase in susceptibility to the innate immune response; two important aspects of JUNV pathogenesis that we are unable to replicate in this *in vitro* model.

Chapter 4. JUNV infection differentially alters endothelial cell monolayer adherens junction protein levels and actin architecture in the absence of overt cytopathology

Summary

Because adherens junctions (AJ) are ubiquitous and critical in regulating permeability, this study focused on elucidating any changes specifically within AJ, rather than tight or gap junctions. AJ are also directly connected to the cytoskeleton through the catenins, an interaction which could affect changes in monolayer permeability during infection with JUNV. It has been reported that JUNV replication within the cell requires interaction with actin so actin was also investigated in this study (209, 210). The data shows that *in vitro* JUNV infection of HUVEcs and HMVEC-Ls causes changes in adherens junction protein levels and affects the protein interactions within the junctions. VE-cadherin and p120-catenin levels are decreased while beta-catenin levels remain unchanged. The data also indicate that the actin architecture of infected cells may be altered sufficiently that it would not be unexpected that this be mechanistically involved in the increased permeability seen in the absence of visible cytopathology.

Introduction

The endothelium contains different types of junctions that function in different ways to regulate the semi-permeable state of the vasculature: gap junctions, tight junctions (TJ) and adherens junctions (AJ). Unlike the epithelium, within the endothelium the AJ can be found intermingled with TJ along the intercellular cleft . Although AJ and TJ junctions are formed by different molecules they share some characteristics. For example in either junction, homophilic adhesion is through transmembrane proteins that form zipper-like structures along the cell border (166). TJ are crucial in maintaining vascular integrity, especially in tissues such as the brain which require strict regulation of permeability. However, only AJ are ubiquitous throughout the vasculature and there is substantial evidence that AJ and TJ are interconnected and that AJ may influence TJ organization (149). AJ are formed early in vessel development followed by TJ, once the AJ are stabilized. Furthermore, many substances known to increase vascular permeability have been shown to directly alter AJ organization by activation of specific tyrosine kinases and/or phosphatases (148). For these reasons, the studies here focused on adherens junctions.

VE-cadherin is the endothelial cell specific cadherin. VE-cadherin proteins on adjacent cells bind each other via their extracellular domains. The cytoplasmic domain binds to beta-catenin, gamma-catenin and p120-catenin which link VE-cadherin to the actin network via alpha-catenin. A delicate balance between kinases and phosphatases controls adherens junction stability, disruption of which can cause junction discohesion (150).

To determine if the changes in endothelial permeability and resistance that were observed, were a result of changes in AJ, immunocytochemistry, immunoprecipitations and western blotting were performed on HUVEc and HMVEC-L monolayers either infected with JUNV Romero or mock infected. The diagram from Figure 1.4 has been included again here for convenience.

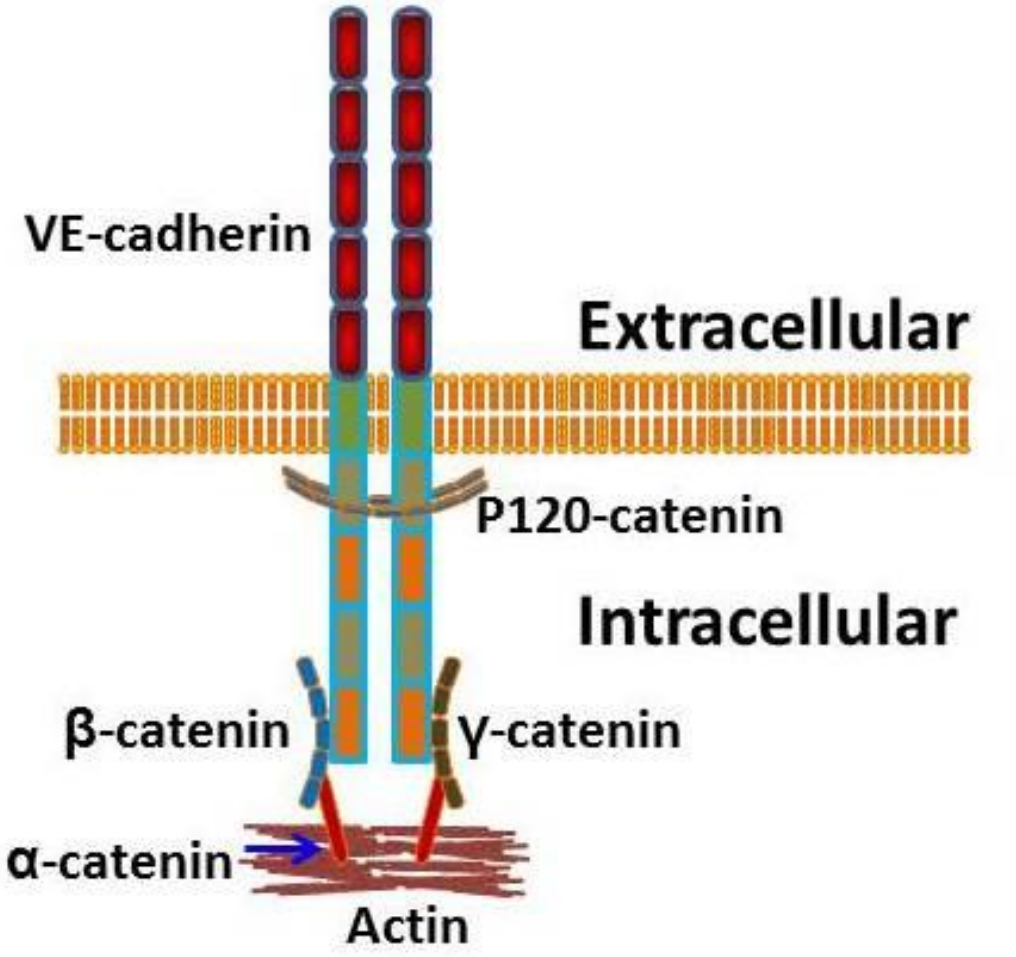

Figure 1.4: Diagrammatic representation of relevant VE-cadherin protein-protein interactions in Adherens junctions. Transmembrane VE-cadherin binds extracellularly to an adjacent VE-cadherin, and intracellularly with various catenins leading to actin associations. p120-catenin binds near the cell membrane, while beta-catenin and gamma-catenin associate more distally. Beta-catenin and p120-catenin are believed to be involved in the assembly of actin based structures.

Results

JUNV infection corresponds to a reduction in VE-cadherin/bet-catenin complexes in HUVEC and HMVEC-L monolayers

In addition to being a crucial component of the Wnt nuclear signaling cascade, beta-catenin participates in anchoring AJ to the cytoskeleton by associating directly with VE-cadherin. Disruption of this complex affects cell-cell adhesion and barrier function so the stability of this interaction was examined during infection of HUVEc and HMVEC-Ls during infection with JUNV. To determine if the AJ association between VE-cadherin and beta-catenin is disrupted during JUNV infection, confluent monolayers were infected. Because the barrier function changes occurred after 60 hours post infection, cell lysates were made at 72 and 96 hours post infection. Cell lysates were immunoprecipitated for beta-catenin and immunoblotted for VE-cadherin.

The data gathered indicate that during infection with JUNV, the complexes between VE-cadherin and beta-catenin are disrupted. Less VE-cadherin is pulled down with beta-catenin in infected cell lysates, than in mock infected cell lysates (Figure 4.1A). Densitometry on the bands indicates that the levels of VE-cadherin pulled down with beta-catenin in infected cell lysates is less than half than that pulled down in mock infected lysates (Figure 4.1B).

Representative viral titers corresponding to infections in which VE-cadherin IP data were gathered are shown in Figure 4.2 and indicate that there was productive viral infection during these experiments.

A.

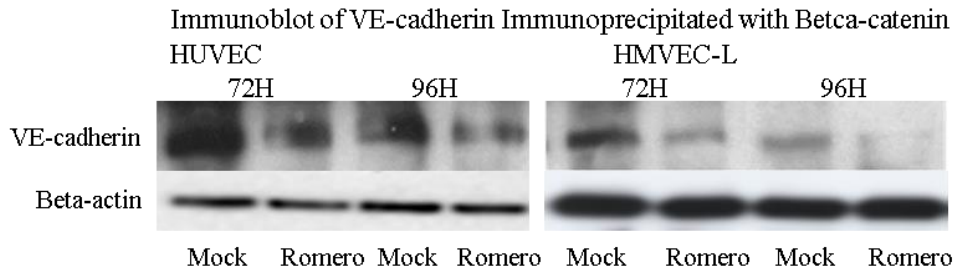

B.

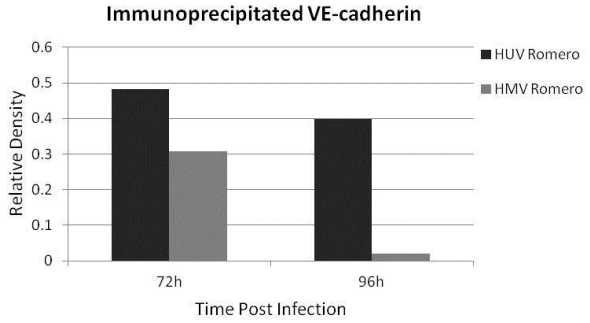

Figure 4.1. (A.) Western blot of VE-cadherin pulled down with beta-catenin. Mock infected immunoprecipitates show more VE-cadherin pulled down with beta-catenin than infected IPs do. **(B.)** ImageJ Analysis of immunoblotted bands was used to measure relative band density compared to mock. The results were normalized to beta-actin and are representative of 3-5 independent experiments.

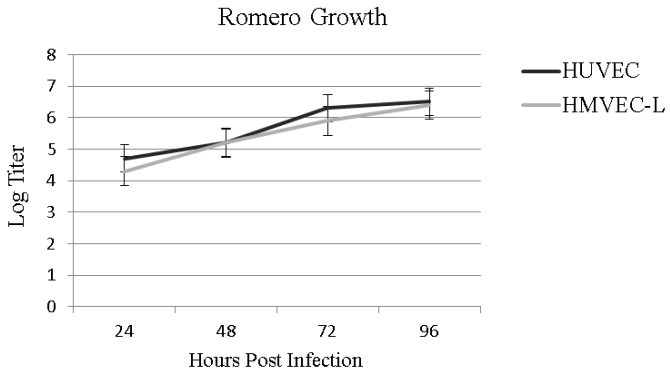

Figure 4.2 Growth curves of JUNV indicate productive infection and viral titer. Growth of Romero in HUVECs and HMVEC-Ls during the first 96 hours of the beta-catenin IP experiment. Data are representative of 3-5 independent experiments. Each point represents the mean ± standard deviation from three experiments.

In HUVEC and HMVEC-L monolayers, JUNV infection corresponds to reduced levels of VE-cadherin, and p120-catenin; does not change beta-catenin levels and modifies the actin architecture without decreasing overall actin levels

Adherens junctions are critical in maintaining endothelial barrier integrity and VE-cadherin is the main protein component of these junctions. Under normal physiological conditions VE-cadherin is degraded and resynthesized as cellular and tissue requirements demand. P120-catenin is a critical component of adherens junctions and has been shown to play a role in vascular permeability during metastasis of certain tumor types (211). It binds to the juxtamembrane domain of VE-cadherin and has been shown to modulate intracellular levels of VE-cadherin by regulating clathrin-mediated endocytosis (195, 212). Immunofluorescent staining of infected HUVECs and HMVEC-Ls was used to determine whether JUNV infection alters the levels of VE-cadherin or p120-catenin. As early as 24 hpi, infected cells show decreased VE-cadherin (Figure 4.3) and p120-catenin (Figure 4.4). As increasing viral antigen is detected, expression of both proteins decreases until levels are nearly below visualization levels at 96 hpi. This contrasts with mock-infected cells in which VE-cadherin and p120-catenin expression remain strong throughout the time course.

Viral titers were calculated during the experiments to indicate virus levels in supernatants during the infections that corresponded to the VE-cadherin data and the p120-catenin data (Figure 4.3 C and 4.4 C, respectively).

. **A** **B**

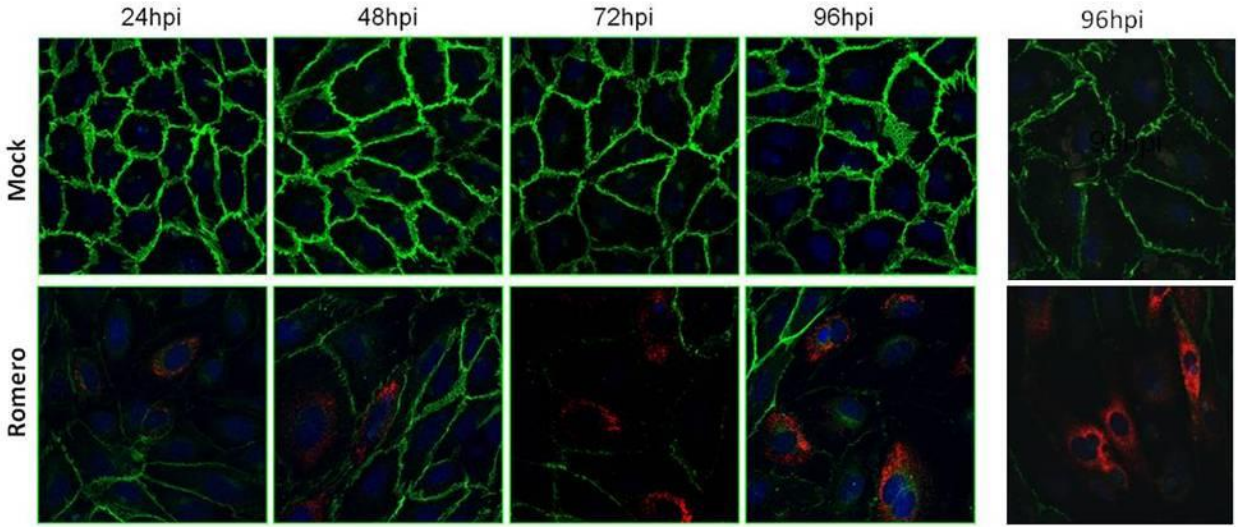

C. **D.**

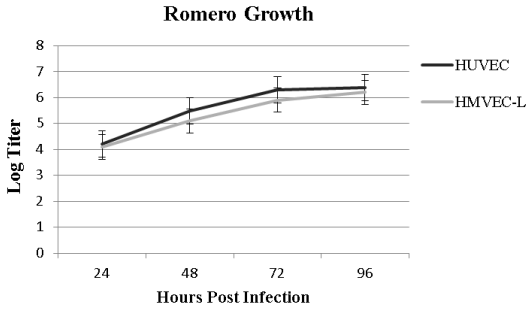

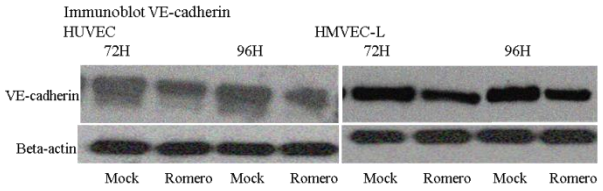

E.

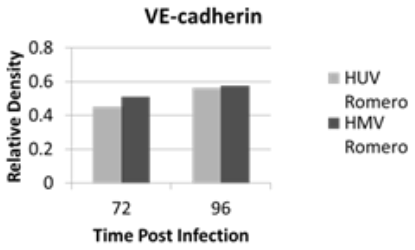

Figure 4.3 Immunocytochemistry of VE-cadherin. JUNV infection greatly decreases VE-cadherin staining in HUVECs **(A)** and HMVEC-Ls **(B).** Cell monolayers were infected at an MOI of 4 or mock infected and fixed at 24 hour time points for 5 days. Alexafluor 488 green: VE-cadherin; Alexafluor 594 red: Junin virus and blue: DAPI. HPI is hours post infection. All time points for HUVECs are shown and a representative time point is shown for HMVEC-Ls. All images are 40X magnification. **(C)**. Growth curves of JUNV Romero in HUVECs and HMVEC-Ls during the first 96 hours of the experiment in which the VE-cadherin data was gathered**. (D.) and (E)** Western blots and Image J analysis of density relative to mock-infected, and normalized to beta-actin, confirm imaging data. Each point represents the mean ± standard deviation from three experiments.

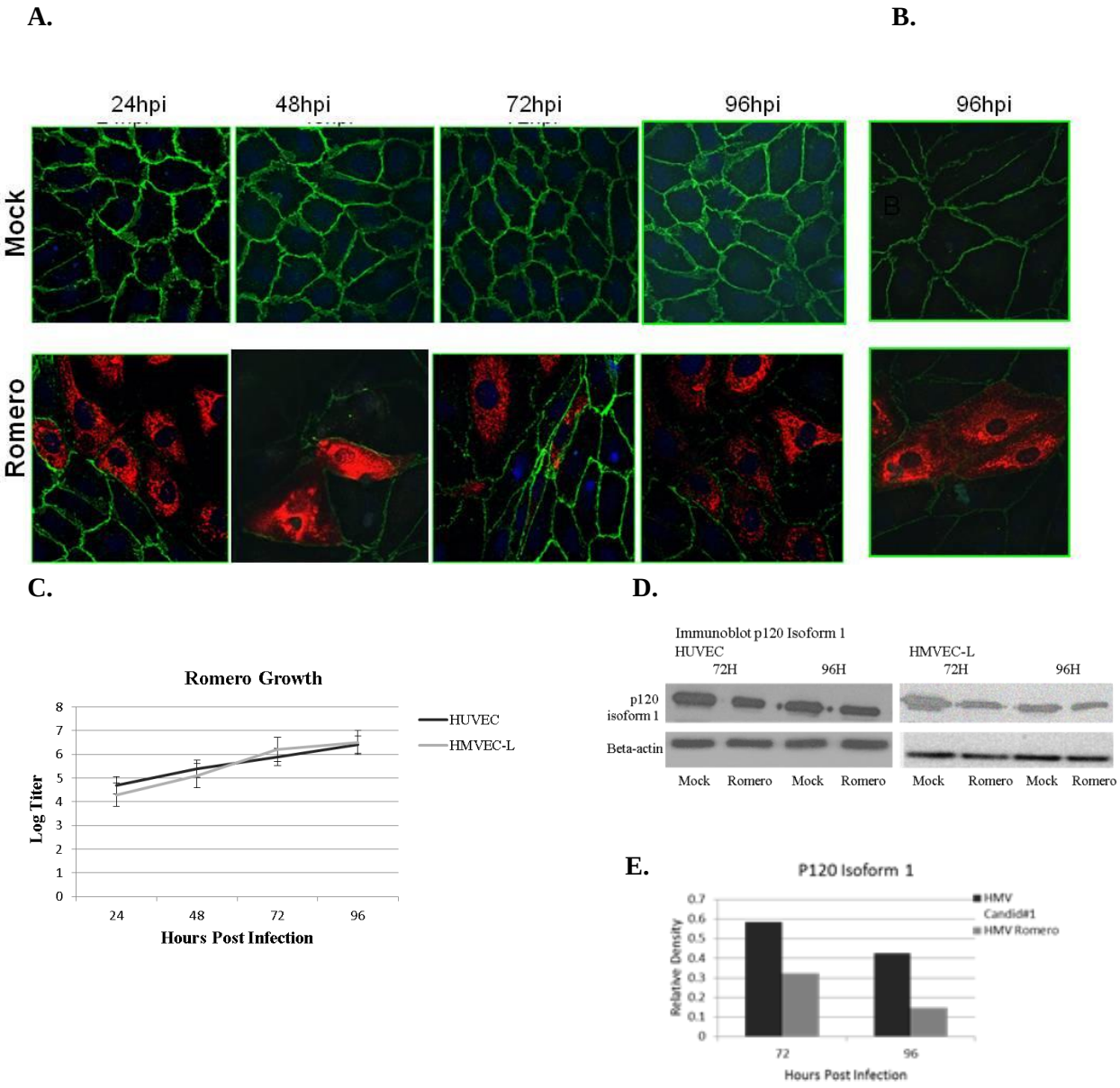

Figure 4.4 Immunocytochemistry of p120-catenin isoform 1. JUNV infection greatly decreases p120-catenin isoform 1 staining in HUVECs **(A)** and HMVEC-Ls **(B).** Cell monolayers were infected at an MOI of 4 or mock infected and fixed at 24 hour time points for 5 days. Alexafluor 488 green: p120-catenin; Alexafluor 594 red: JUNV and blue: DAPI. HPI is hours post infection. All time points for HUVECs are shown and a representative time point is shown for HMVEC-Ls. All images are 40X magnification **(C.)** Growth curves of JUNV Romero in HUVECs and HMVEC-Ls during the first 96 hours of the experiment in which p120-catenin data was gathered. **(D.)** and **(E)** Western blots and Image J analysis of density relative to mock-infected, and normalized to actin, confirm imaging data. Each point represents the mean ± standard deviation from three experiments.

Beta-catenin is another important component of adherens junctions. It binds directly to VE-cadherin and connects the junction to the actin cytoskeleton via alpha-catenin. Immunostaining of infected or mock infected HUVEC and HMVEC-L monolayers was used to see if beta-catenin levels were altered during JUNV infection. JUNV infection did not result in reduced beta-catenin levels relative to mock-infected HUVECs (Figure 4.6A) or HMVEC-Ls (4.6B).

Immunocytochemistry of actin filaments was also used to visualize the effects of JUNV infection on cellular architecture. Because the actin cytoskeleton is so important in cellular architecture, the effects of JUNV infection on actin staining were evaluated in infected HUVECs or HMVEC-Ls. As shown in Figure 4.7 we found no alterations in the relative amounts of actin staining, although we did see a difference in the relative distribution of actin. EC monolayers infected with JUNV, show small, distinct gaps between the cells as well as apparent minor alterations in the overall shape of the actin cytoskeleton. For example, if you look more closely at the cells you can see that in infected cells, the actin fibers stretch across the center of the cells rather than remain more distinctly near the perimeter (Figure 4.7C). This is characteristic of a monolayer that would allow the passage of small molecules through the junctions while maintaining the overall health of the monolayer.

JUNV titers were calculated from supernatant samples taken during the course of the experiments to determine virus growth. Growth curves of samples taken during beta-catenin and actin experiments are shown in Figure 4.6C and 4.7D respectively.

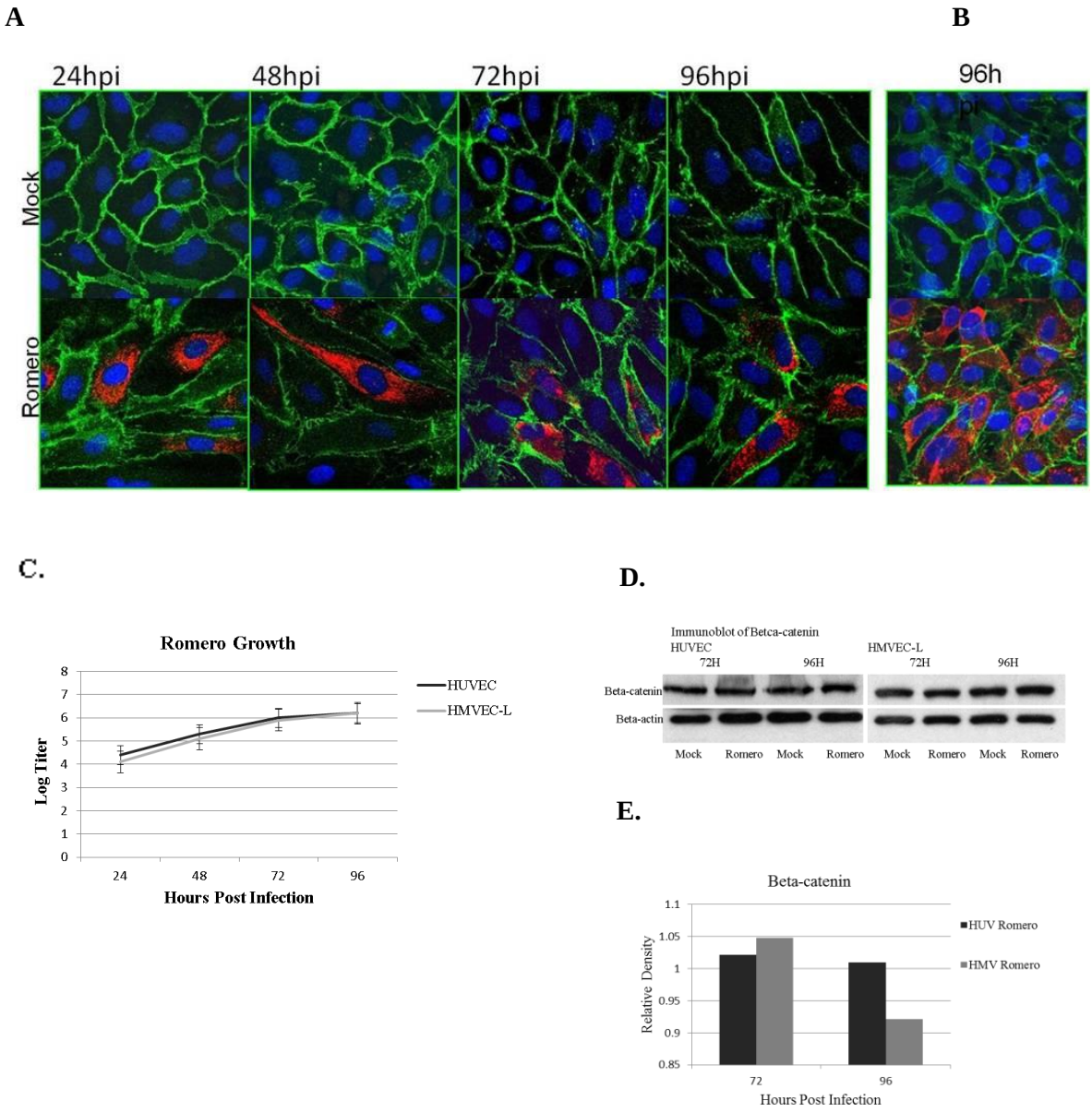

Figure 4.6. Immunocytochemistry of beta-catenin. JUNV infection does not reduce beta-catenin staining in HUVECs **(A)** or HMVEC-Ls **(B).** Cell monolayers were infected at an MOI of 4 or mock infected and fixed at 24 hour time points for 5 days. Alexafluor 488 green: beta-catenin; Alexafluor 594 red: Junin virus Romero and blue: DAPI. HPI is hours post infection. All time points for HUVECs are shown and a representative time point is shown for HMVEC-Ls. All images are 40X magnification **(C.)** Growth curves of JUNV Romero in HUVECs and HMVEC-Ls during the first 96 hours of the experiment in which beta-catenin data was gathered. **(D.)** and **(E)** Western blots and Image J analysis of density relative to mock-infected, and normalized to actin, confirm imaging data. Each point represents the mean ± standard deviation from three experiments. Each point represents the mean ± standard deviation from three experiments.

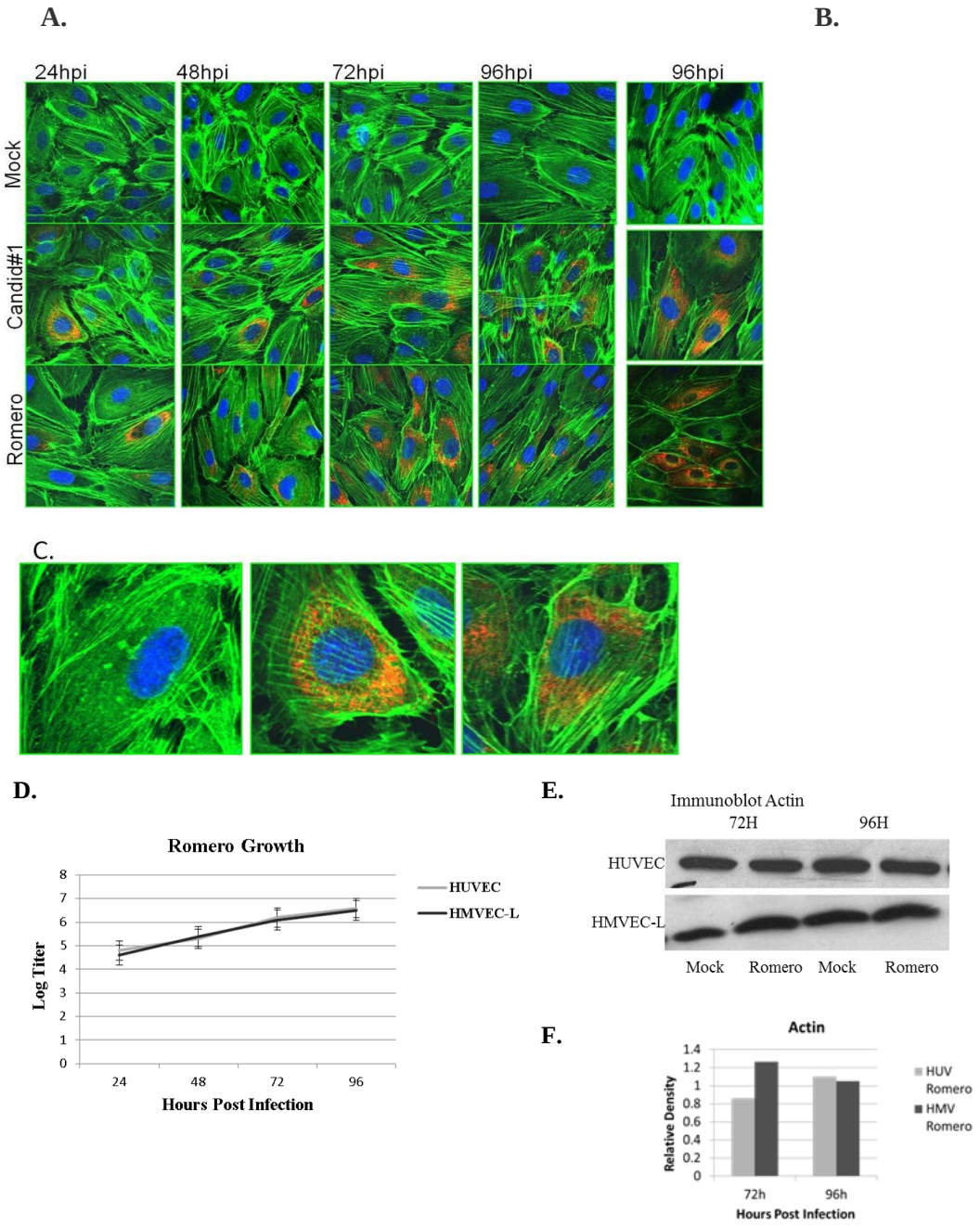

Figure 4.7 Immunocytochemistry of F-actin. JUNV infection alters the actin architecture of HUVECs **(A)** and HMVEC-Ls **(B**) without compromising overall actin levels. Cell monolayers were infected at an MOI of 4 or mock infected and fixed at 24 hour time points for 5 days. Alexafluor 488 green: phalloidin; Alexafluor 594 red: Junin virus Romer and blue: DAPI. HPI is hours post infection. All time points for HUVECs are shown and a representative time point is shown for HMVEC-Ls. Insets depicting close up views of a few representative cells is also shown **(C).** All images are 40X magnification. **(D.)** Growth of JUNV Romero in HUVECs and HMVEC-Ls during the first 96 hours of the experiment in which the actin data was gathered**. (E.)** and **(F.)** Western blots and Image J analysis of density relative to mock-infected, and normalized to actin, confirm imaging data. Each point represents the mean ± standard deviation from three experiments.

Discussion

Determining the involvement of adherens junctions in JUNV induced endothelial dysfunction is an important step in defining the mechanisms underlying the pathogenesis of the vascular syndrome seen during AHF. This study reports that this dysfunction is associated with changes in adherens junction stability including loss of VE-cadherin, disruption of adherens junction protein complexes and alterations in the actin cystoskeleton. These findings indicate that direct viral infection contributes to endothelial cell function alterations resulting in increased endothelial dysfunction and decreased endothelial barrier integrity.

VE-cadherin functions in numerous ways to dynamically regulate vascular permeability under normal physiologic processes such as angiogenesis and wound healing (213, 214). Myriad pathways are involved and finely regulated by cellular signaling events. The specific signaling events involved determine the exact nature of the junctional remodeling. Many of the AJ proteins play more than one role in the endothelial cells and can be activated, inactivated or degraded based on the specific signaling cascade involved. In addition to functioning at the membrane within AJ, beta-catenin is critical in the nuclear Wnt cascade. p120-catenin wears more than one hat as well and the function of its individual isoforms is only recently being investigated.

Many disease processes involving adherence junction disruption and inappropriate permeability, such as lead poisoning, involve VEGF signaling and Src kinase activation (215). TNF-alpha activates Fyn during sepsis which opens the AJ and contributes to multi-organ failure (216). P120-catenin mismanages the turnover of VE-cadherin allowing the permeability required for some kinds of tumor metastasis (217). More recently it was demonstrated that Andes hantavirus-induced endothelial permeability was due to VEGFR2 signaling via Src which destabilized the VE-cadherin junctional complex and could be decreased through Src and VEGFR2 inhibitors (218, 219). Because the data shows that AJ are compromised during JUNV infection, the

next logical step would be to investigate whether Src kinase is involved in the intracellular signaling that leads to AJ disruption. If it is, then it would be possible to address the issue by testing FDA approved Src inhibitors as potential therapies to ameliorate the vascular syndrome seen during AHF.

Based on reports that JUNV interacts with the actin cytoskeleton and that this interaction is necessary for viral entry and replication, it was important to investigate the effects of JUNV on the actin cytoskeleton in this model (209, 210). Here, alterations in the actin framework of infected cells, correlates to increases in permeability and decreases in electrical resistance that were observed. The alterations shown here, in the actin cytoskeleton during JUNV infection, speak to the interactions others have shown, as well as provide a possible role for actin in the increased permeability and decreased electrical resistance demonstrated here.

Again, it must be noted, that both virus strains, the virulent Romero and the attenuated Candid#1, caused similar changes in the adherens junctions proteins examined, as well as in actin (Data in appendix). This lends more support to the conclusion that the attenuation of Candid#1 is through some mechanism other than the pathogenic effects on the endothelium.

Chapter 5. JUNV infection alters intracellular HUVEC and HMVEC-L signaling and cytokine profiles to induce alterations in adherens junctions, without inducing Src kinase activation

Summary

To better understand the intracellular signaling occurring during JUNV infection that results in adherens junction disruption, two major regulators of permeability were investigated first: VEGF and Src kinase. Unexpectedly, this study reports that there is no increase in VEGF production during *in vitro* infection of HUVEC and HMVEC-Ls with either the virulent or attenuated strains of JUNV. As a critical component in regulating VE-cadherin levels intracellulary, p120-catenin became a logical target for further study. The data reported here indicates that there is an isoform switch of p120-catenin during JUNV infection, from isoform 1 to isoform 2. Although many cytokines were examined during JUNV infection, including but not limited to TNF-alpha and type I and type II interferons, the only cytokine profile changes reported in this study are that during *in vitro* infection of HUVEC and HMVEC-Ls with either Candid#1 or Romero, MCP-1 and IL-6 production increases.

Introduction

VEGF is made by endotheial cells to stimulate the formation of new blood cells and can also act mitogenically to induce the endothelial cells to divide and multiply. It also functions to facilitate vascular permeability which is critical in angiogenesis and wound healing (220). There are several members of the VEGF family: VEGF-(A), B, C, D, E, F and PlGF. The identification of these different isoforms brings the possibility of therapeutic targets, for diseases in which angiogenesis is critical, such as rheumatoid arthritis and cancer (221). VEGF inhibitors might be appropriate targets for some conditions, but the side effects for such a broad inhibitor could present

serious problems. It has been reported that anti-VEGF treatments have adverse effects on coagulation, as is evidenced by bleeding and thrombotic events (222, 223). VEGF-defective mice exhibit progressive motor neuron degeneration, which might be another concern in therapies directed at inhibiting VEGF (224). Finally, it's possible, although not documented, that VEGF inhibition during ischemic heart disease could aggravate it by preventing the development of compensatory vasculature. A more specific therapeutic alternative to VEGF inhibition would be Src kinase, which has been shown to be critical in cellular signaling involving VEGF and TLR2 and its inhibition has already been shown to ameliorate some instances of pathogenic increases in vascular permeability (146). Determining the role of both VEGF and Src kinase in JUNV induced permeability might prove quite useful in developing novel therapeutic targets, so this study aimed to define the roles of each during *in vitro* JUNV infection of endothelial cells.

P120-catenin has also been shown to play a critical role in maintaining levels of VE-cadherin in healthy endothelial cells and this role is only beginning to be well understood. In some cases, p120-catenin affects internalization of VE-cadherin and subsequent junction opening, while in other situations p120-catenin appears to direct phosphorylation changes of VE-cadherin which causes the junctions to open in the absence of VE-cadherin internalization (196, 225). There are four possible isoforms of p120-catenin, based on different splicing events during translation and the roles of these isoforms in AJs organization and control is only beginning to be understood (226). It has been reported that the p120-catenin isoform profile can affect tumor metastasis, possibly through opening AJ (217). The loss of p120-catenin seen earlier in this study was, in fact, the specific loss of isoform 1. For this reason, it was important to follow up by examining other p120-catenin isoforms during JUNV infection.

Results

Infection with JUNV does not increase VEGF levels

There are many documented instances in which inappropriate permeability is caused by the iunduction of VEGF: myocardial infarction, lead poisoning and stroke among others. Some infectious organisms also induce VEGF production in endothelial cells, such as rickettsia and dengue virus. VEGF functions to increase permeability through Src kinase action on adherens junctions, so determining if endothelial cells infected with JUNV showed an increase in VEGF production would indicate if Src kinase might be involved. Suprisingly, the data from this study shows no increase in VEGF levels in HUVECs or HMVEC-Ls infected with JUNV (Figure 5.1).

Supernatant samples were also used to calculate virus titer during the infection from which samples were taken for VEGF analysis. Virus growth indicates a productive infection as has been observed in all previous infections and are shown in Figure 5.1 C.

A.

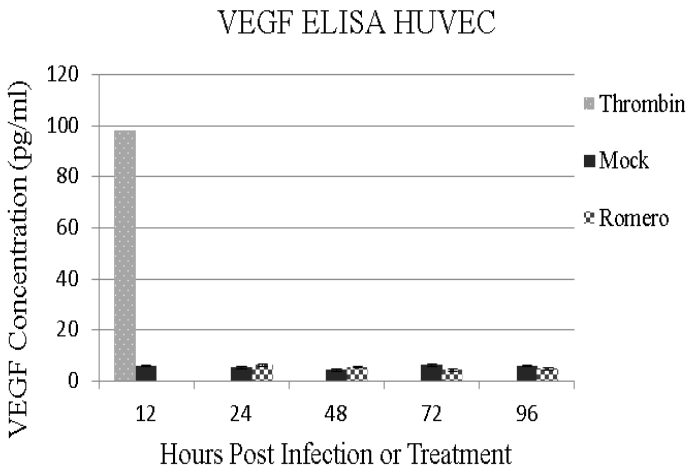

B.

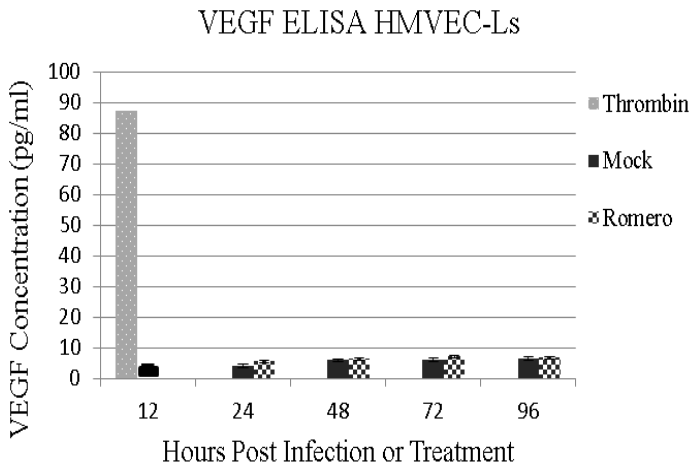

C.

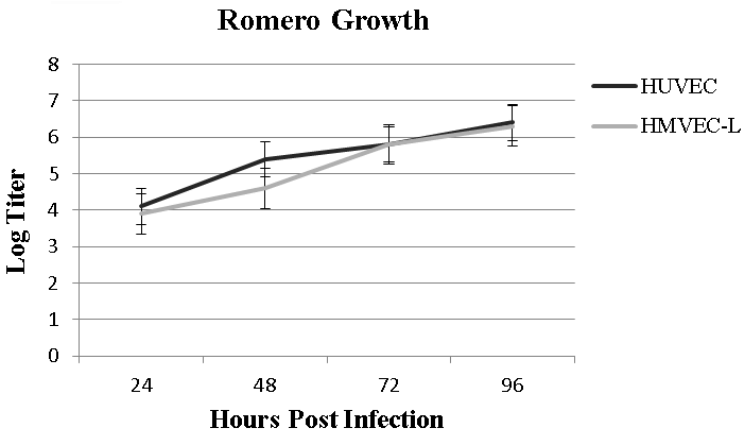

Figure 5.1 VEGF ELISA. Infected or mock infected HUVEC **(A)** or HMVEC-L **(B)** cell lysates were analyzed by ELISA to determine levels of VEGF. Activation of cells with thrombin at 1 IU/ml for 12 hours was used as a positive control for VEGF induction. JUNV did not increase VEGF levels in either cell type. **(C.)** Growth curves of JUNV Romero in HUVECs and HMVEC-Ls during the first 96 hours of the experiment**.** Each point or bar represents the mean ± standard deviation from three experiments.

Infection with JUNV does not increase Src kinase activity

Adherens junctions are regulated by complicated intracellular signaling cascades that often involve Src kinase and there are approved Src inhibitors that are in clinical trials for the treatment of inappropriate permeability during different disease processes. It has also been reported that Src inhibition can prevent increased permeability in HUVECs by hantaviruses (218, 219). To see if Src was involved in the changes seen during JUNV infection, cell lysates were analyzed by ELISA specific for c-Src phosphorylated at the active site (tyr416). As is seen in Figure 5.2, there was no increase in the levels of phosphorylated c-Src in JUNV infected HUVEC (**A**) or HMVEC-L (**B**) lysates compared to mock. Cells stimulated with VEGF, a known inducer of c-Src activity, were used as a positive control. Virus growth curves indicate productive infection as has been observed in all previous infections and are shown in Figure 5.2 C.

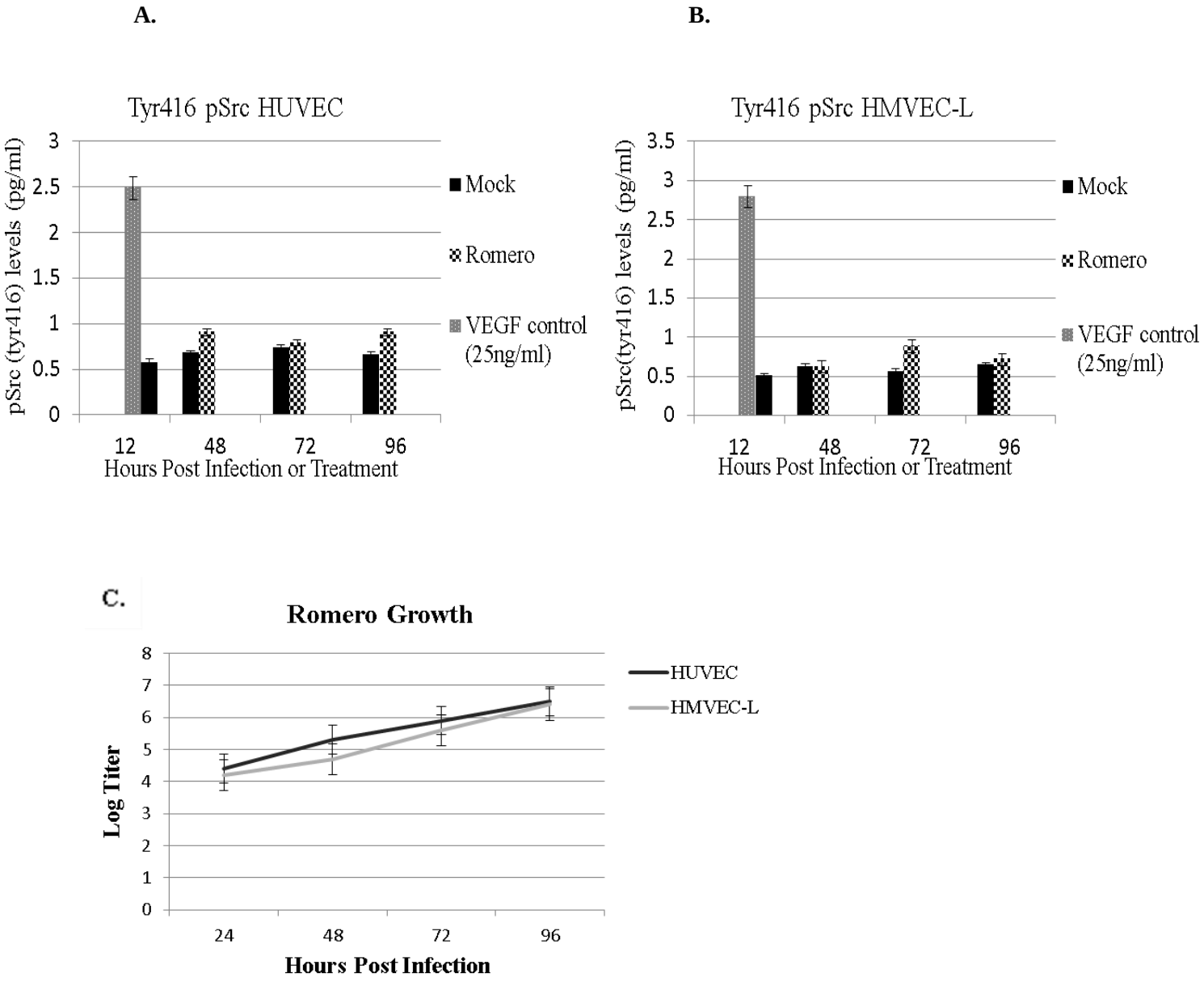

Figure 5.2 Phospho-Src ELISA. Infected or mock infected HUVEC **(A)** or HMVEC-L **(B)** cell lysates were analyzed by ELISA to determine levels of activated pSrc (Tyr416). VEGF at 25ng/ml for 12 hours was used as a positive control. JUNV did not increase pSrc levels in either cell type. Data are means ± SEM representing 3-5 independent experiments. **(C.)** Growth of JUNV Romero in HUVECs and HMVEC-Ls during the first 96 hours of the experiment**.** Each point or bar represents the mean ± standard deviation from three experiments.

Infection with JUNV alters the p120-catenin isoform profiles of HUVEC and HMVEC-Ls

P120-catenin has been shown to be critical in regulating VE-cadherin levels and adherens junction stability (195, 227). Binding directly to VE-cadherin, p120-catenin helps maintain appropriate levels of VE-cadherin and contributes to regulation of endothelial cell phenotype switching from adhesive to motile (227). In addition, p120-catenin isoform switching has been shown to differentially affect some cellular processes including cancer metastasis. For these reasons the levels and isoform profiles of p120-catenin were investigated in this study. The initial evaluation of p120-catenin levels was done using an antibody specific for isoform 1, so the levels of other p120-catenin isoforms, during JUNV infection of HUVECs and HMVEC-Ls, were investigated. The data show that during infection with JUNV, in both endothelial cell types, p120-catenin isoform 1 (Figure 5.5) decreases while isoform 2(Figure 5.6) increases.

A.

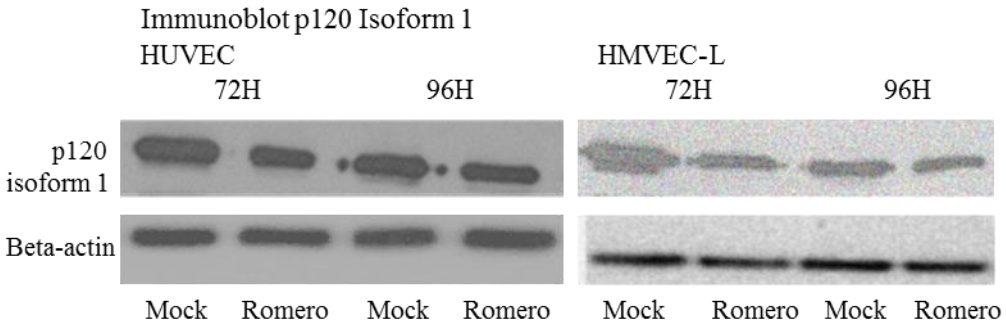

B.

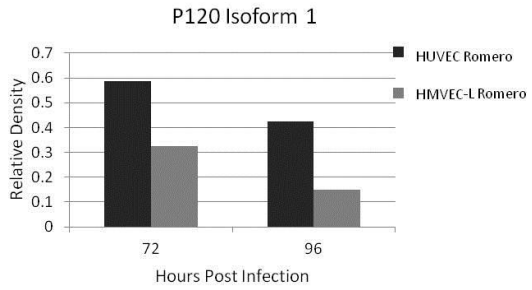

C.

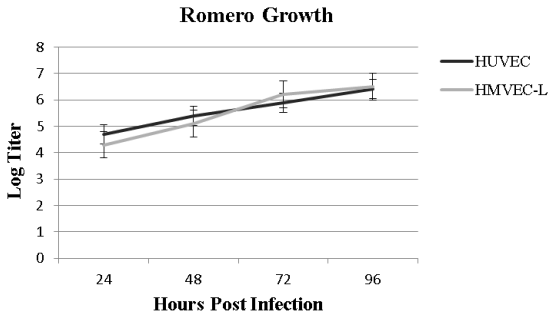

Figure 5.3 P120-catenin Isoform 1 decreases over time compared to mock infected cells. Cell monolayers were infected at an MOI of 4 or mock infected and lysates made at 24 hour intervals**. (A.)** Western blots show an increase in p120-catenin isoform 1 in infected cell lysates compared to mock infected. **(B.)** Image J analysis of density relative to mock-infected, and normalized to actin, confirm imaging data. **(C.)** Growth curves of JUNV Romero in HUVECs and HMVEC-Ls during the first 96 hours of the experiment**.** Each point represents the mean ± standard deviation from three experiments.

A.

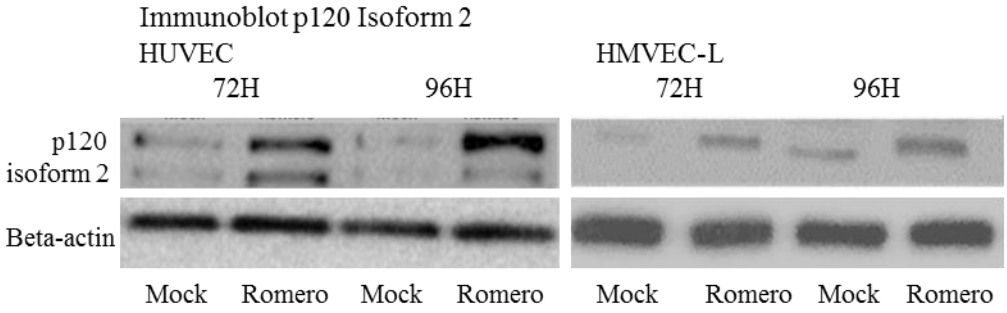

B.

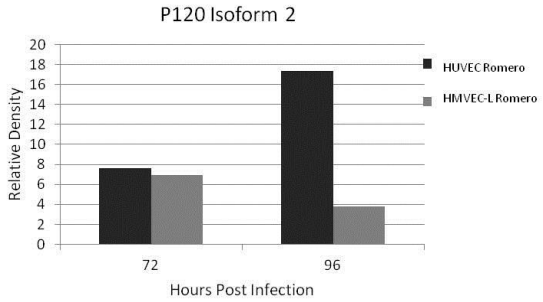

C.

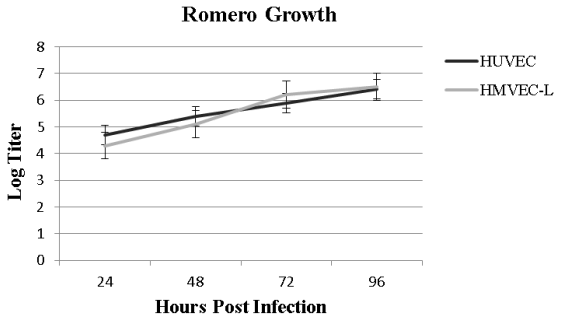

Figure 5.4 P120-catenin Isoform 2 increases over time compared to mock infected cells. Cell monolayers were infected at an MOI of 4 or mock infected and lysates made at 24 hour intervals**. (A.)** Western blots show an increase in p120-catenin isoform 2 in infected cell lysates compared to mock infected. **(B.)** Image J analysis of density relative to mock-infected, and normalized to actin, confirm imaging data. **(C.)** Growth curves of JUNV Romero in HUVECs and HMVEC-Ls during the first 96 hours of the experiment**.** Each point represents the mean ± standard deviation from three experiments.

Infection with JUNV induces HUVEC and HMVEC-L production of MCP1

Because there was no evidence that the adherens junction alterations seen in this study were due to increased VEGF production or Src kinase activation, cytokine levels in cell culture supernatants were determined using Bio-Plex® bead array system. Table 5.1 shows the cytokine data measured. Many of the cytokines were below detectable levels including TNF-alpha, while some showed no changes compared to mock infected cells, including INF-gamma, INF-beta and INF-alpha. Only two of the cytokines measured were found to be significantly different in infected cells than in mock infected cells: MCP-1 and IL6.

Undetected Cytokines	Unchanged Cytokines	Increased Cytokines
TNF-a	IFN-g	MCP-1
IL-1b	IL-4	IL-6
IL-2	IL-8	
IL-5	IL-12(p70)	
IL-7	IL-17	
IL-1-	G-CSF	
IL-13	GM-CSF	

Table 5. 1 Cytokine analysis. HUVEC and HMVEC-L supernatants were analyzed for cytokine levels during infection with JUNV or mock infected. Supernatant samples were taken every 24 hours post infection and subjected to either Bioplex cytokine analysis, ELISA or the interferon bioassay. The only cytokines measured that were changed compared to mock infected cells were IL-6 and MCP1, which were both significantly increased compared to mock infected cells. Data are representative of 3-5 independent experiments.

To confirm comparable, productive JUNV infection during the experiment in which samples were taken for cytokine analysis, viral growth was calculated and is shown in Figure 5.7. Virus growth indicates similar titers as in all previous infections.

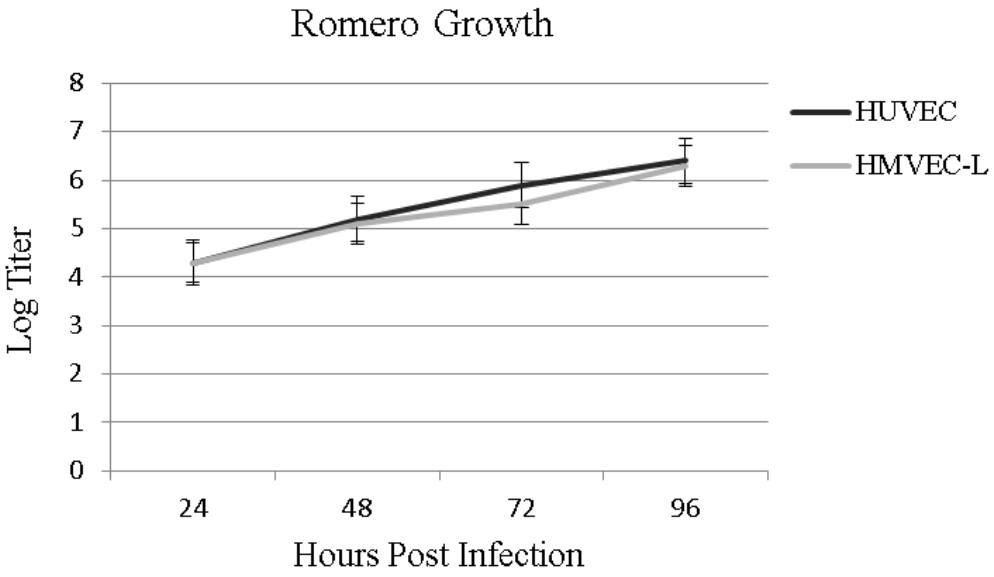

Figure 5.5 Growth curves of JUNV indicate productive infection and viral titer. Growth of Romero in HUVECs and HMVEC-Ls during the first 96 hours of the cytokine experiment. Each point represents the mean ± standard deviation from three experiments.

Monocyte chemotactic protein-1, (MCP-1) is a member of the small inducible gene (SIG) family of proteins. MCP-1 recruits leukocytes when needed at injury or infection sites. The MCP1 gene is located on chromosome 17 (17q11.2-q12). MCP-1 has been implicated in inflammation, leukocyte recruitment and signaling to open tight junctions in the brain (228). It has also been found to be elevated in patients with dengue shock although its role in endothelial permeability is still largely unclear. Interestingly, this study reports that MCP-1 was elevated in cell supernatant samples infected with JUNV Romero (Figure 5.6).

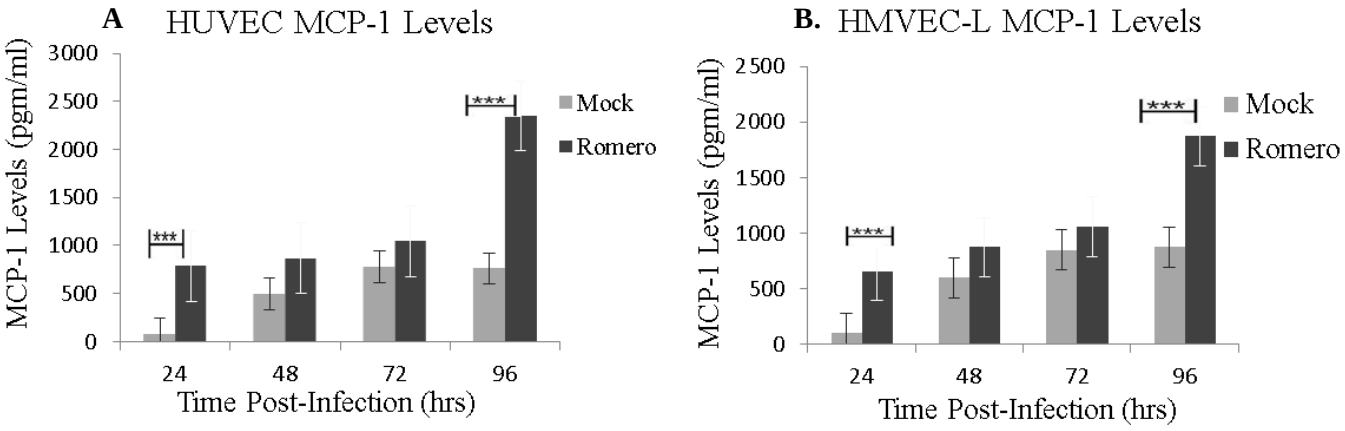

Figure 5.6 MCP-1 production in JUNV Infected Endothelial Cells. HUVECs **(A)** and HMVEC-Ls **(B)** infected with JUNV Romero show an increase in MCP-1. Cell monolayers were infected at an MOI of 4 or mock infected and supernatant samples were taken every 24 hours post infection and subjected to Bioplex cytokine analysis. Data are extremely significant by a two-way repeated measure ANOVA test (***p-value<0.0001). Each bar represents the mean ± standard deviation from three experiments.

Infection with JUNV induces HUVEC and HMVEC-L production of IL-6

Il-6 is a pro-inflammatory cytokine that is a marker of vasculitis, can increase permeability and is associated with adverse outcomes in many diseases including the prototypical VHF, yellow fever (229). IL-6 is released in response to different cytokines including IL-1 and TNF-b. The IL-6 receptor is found on many cell surfaces and can lead to the transcription of a wide variety of proteins through three major signaling cascades: protein kinase C (PKC), cAMP/protein kinase A, and the calcium release pathway (230). IL-6 has several isoforms and each one serves a different function when secreted by different cells in distinct situations (231).

In this study, an increase in IL-6 levels in the cell culture supernatants of endothelial cells infected with JUNV (Figure 5.7) is reported.

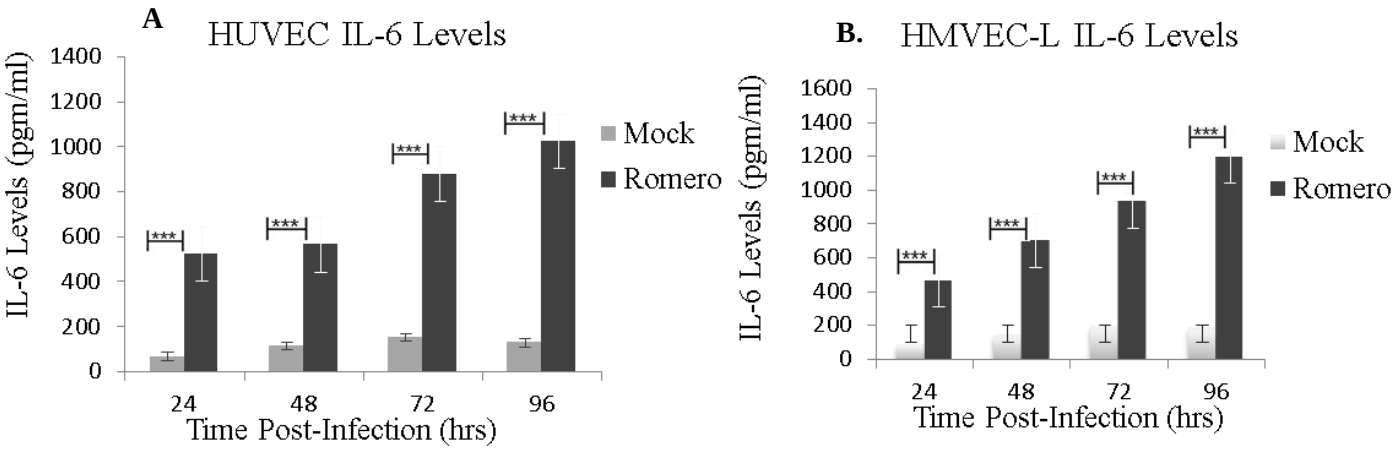

Figure 5.7 IL-6 production in JUNV Infected Endothelial Cells. HUVECs **(A)** and HMVEC-Ls **(B)** infected with JUNV Romero show an increase in IL-6. Cell monolayers were infected at an MOI of 4 or mock infected and supernatant samples were taken every 24 hours post infection and subjected to Bioplex cytokine analysis. Data are extremely significant by a two-way repeated measure ANOVA test (***p-value<0.0001). Each bar represents the mean ± standard deviation from three experiments.

Discussion

VEGF is a well-established inducer of vascular permeability in many situations including wound healing and angiogenesis (197). It has also been shown to cause inappropriate permeability that leads to disease in situations such as myocardial infarction (146). Increased VEGF levels were expected in light of the data indicating adherens junction dissociation and increased permeability during JUNV infection. It is somewhat surprising that VEGF is not increased in this system. Nevertheless, Src levels were measured because Src kinase is involved in several intracellular signaling pathways, only one of which involves VEGF. Finding no increase in Src kinase activation in this study was also rather surprising, since most of the adherens junction proteins have been identified as Src substrates. Needless to say, these data indicate that the JUNV induced permeability seen in this study must be the work of an as of yet unidentified signaling cascade. P120-catenin has been shown to be critical in regulating VE-cadherin levels, so it was the logical target of the next investigation in this study. The isoform switch seen in p120-catenin during infection with JUNV may indicate the involvement of one of many signaling pathways specific for p120-catenin, which are still poorly understood. To more closely examine the signaling occurring during JUNV infection, cytokine profiles of the infected endothelial cells were examined.

The only cytokines found altered following JUNV infection in this study, were MCP-1 and IL-6. In the endothelium, IL-6 is a known inducer of angiogenesis, and can also cause endothelial permeability and induce the production of MCP-1, which was also found increased during infection with JUNV (232-234). MCP-1 plays a role in angiogenesis and wound repair, has been shown to induce permeability and is found significantly increased in dengue hemorrhagic fever patients as well as in human endothelial cells infected with Rickettsia in vitro (235, 236). Increased levels of both MCP-1 and IL-6 are not surprising considering that increased production of reactive oxygen species can increase levels of both in endothelial cells (237). Although Gomez *et al* only found

increased NO in HUVECs infected with the virulent Junin strain, NO is only one ROS and it is possible that other ROS are produced in JUNV infected endothelial cells as well (87). Levels of both MCP-1 and IL-6 were increased, and the biphasic nature of this increased expression is not completely unexpected as it has been seen with IL-6 and MCP-1 in other pathogenic circumstances such as irradiation, and a mouse model of otitis media with effusion (238, 239). Considering that these two cytokines have been shown to function synergistically to increase vascular inflammation, it is likely that they function together during JUNV infection to induce signaling which leads to adherens junction dysregulation with subsequent permeability increases (240). Because visible changes were only observed in cells infected with JUNV and expressing viral proteins, the mechanism of action on the adherens junction proteins appears to involve an *intra*cellular cascade rather than *inter*cellular signaling, with no paracrine effect. Studies using neutralizing antibodies against MCP-1 or IL-6 could help define their role here. Again, an *in vivo* system is needed to more closely investigate the role of these cytokines during JUNV infection.

Circulating interferon levels play important roles in arenavirus caused diseases. Increased levels of circulating interferon correlate to increased severity of the disease (241-244). In the studies presented here, IFN-alpha, beta or gamma were not detected in ECs infected with JUNV. Although this means that the ECs themselves are not responding to infection with JUNV by expressing interferon, it does not mean that circulating interferons do not play a role in pathogenesis. *In vivo* studies will be critical in addressing this issue.

Again, these studies were repeated using the vaccine strain of JUNV, Candid#1 and no differences were found between it and the virulent Romero strain. (Data in appendix).

Chapter 6. Discussion And Future Directions

Discussion

AHF is a public health concern for those who live or work in the endemic area, as well as for anyone traveling to such areas, or who might be targeted and/or respond in the event of a bioweapons attack. It is imperative that the pathogenesis of this disease is better understood, so that it can be successfully prevented, accurately diagnosed, and effectively treated. The etiological agent of AHF is Junín virus, the pathogenesis of which is still poorly understood. Because it is highly infectious by aerosol with a high mortality rate, it is a CDC category A agent and must be handled in a BSL4 facility. This makes it much more difficult to study, and consequently limits not only the amount of information available already, but also the scope of research being performed.

Clinical manifestations of AHF such as rising hematocrits, edema and tissue congestion indicate vascular dysregulation with increased vascular permeability in the absence of overt endothelial damage. Patients exhibit thrombocytopenia, leucopenia, proteinuria and fluid distribution problems (94). Vomiting and dehydration can cause rising hematocrits, but even hospitalized patients receiving fluid replacements experience hemoconcentration. Hemorrhage occurs, but clinically is usually more than ITP or other non VHF conditions at similar levels of thrombocytopenia. These observations implicate an endothelium which, although not visibly damaged, is altered enough to perhaps initiate a permeability increase that, when combined with other physiological factors during infection, may contribute to development of disease.

The presence of a vascular syndrome in the absence of overt vascular damage reminds us that it is possible for a viral infection to affect cellular processes without overt cellular injury. For example, LCMV, another arenavirus, alters growth hormone levels in the pituitaries of CH3/ST mice while leaving housekeeping functions undisturbed.(207, 208) It is possible that the

endothelial cellular response to JUNV infection contributes to disease progression, and understanding that response is necessary to effectively prevent and treat AHF.

Recently, Cuevas *et al* reported that viral infection and replication are not required for Candid#1 to induce the immune response in macrophages; that interaction with the macrophages via TLR2 is enough (245). Endothelial cells, including HUVEcs and HMVEc-Ls express TLR2 so it is possible that Candid#1 or Romero might interact with the endothelial cells in the same way, initiating some kind of intracellular response (246, 247). Inducible TLR tyrosine phosphorylation has been linked to activation of Src family kinases, which seem to be an integral part of the TLR2 and TLR3 signaling complex (248). The fact that productive viral infection is needed for the changes seen in barrier function, and that Src kinase is not activated, it seems plausible that the signaling involved in this study is not through a TLR2/Src dependent pathway. This is not to say that JUNV/TLR2 signaling does not affect pathogenesis on some level, perhaps even synergistically with the intracellular viral inductions that are likely responsible for the replication-dependent changes reported here.

In addition to the VEGF/Src kinase pathways, other signaling cascades affect and help regulate adherens junctions. P120-catenin is a critical component of VE-cadherin regulation at the junctions; it regulates VE-cadherin levels and controls its availability, but the functions and signaling cascades in which p120-catenin are involved are not fully understood (195). There is significant data indicating that p120-catenin both suppresses tumors and promotes metastasis, perhaps through modulating adhesion at adherens junctions (227). However, p120 alone is not sufficient to stabilize adhesion, and in fact, signaling through its amino-terminal domain has been shown to disrupt adhesion (227). This study reports an isoform switch of p120-catenin during infection with JUNV, which lends support to the idea that the VE-cadherin loss seen during JUNV infection is a result of p120-catenin signaling rather than VEGF signaling. The specific roles of

p120-catenin isoform 2 in junction maintenance are not well known and more research is needed in this area.

Endothelial cells can produce different cytokines in response to different physiological conditions, including infection. The cytokine profile of infected endothelial cells in this study, show that JUNV infection stimulates production of IL-6 and MCP-1, but not TNF-alpha or interferons. IL-6 and MCP-1 have been reported to increase endothelial permeability, either on their own or synergistically (240). The data presented here provide evidence that IL-6 and MCP-1 are working in a bi-phasic, synergistic manner to affect adherens junction changes. AHF patients have high levels of circulating TNF-alpha and INF-gamma from immune cells during disease. Those cytokines, combined with the data here, suggest that the combination of circulating cytokines and endothelial expressed cytokines are working together to exacerbate permeability and worsen the vascular syndrome.

Finally, the fact that the attenuated vaccine strain causes the same changes in endothelial cell permeability and adherens junctions during infection is unexpected and very interesting. It indicates that Candid#1 attenuation is not due to pathogenic mechanism attenuation – in so far as pathogenic mechanisms relate to direct endothelial cell infection and alterations in barrier function. Instead, it appears that Candid#1 must not be able to disseminate, and or replicate, to the same degree as the wild-type, virulent Romero strain. Perhaps this involves some level of temperature sensitivity or less successful mechanisms for evading immune responses. Recently, a study to rescue JUNV strains from Cloned cDNAs, suggests that Candid#1 does, in fact, replicate more slowly than Romero (249). This is also supported by the fact that, in these studies at 37C, Romero consistently reached approximately 0.5 log higher than Candid#1, and to get high enough titer stocks of Candid#1 for these experiments , the virus had to be grown at 35C, instead of 37C, which is the temperature at which Romero stocks were generated. Of course, in this *in vitro* system, there

are no immune responses of any kind, so *in vivo* studies need to be done to evaluate the effects of immune responses to Candid#1 replication and dissemination within a live, immune competent organism.

Future Directions

This study reports an unexpected absence of VEGF and Src kinase signaling during JUNV infection. Instead, p120-catenin appears to be playing a role, as do the interactions of actin with adherens junction and perhaps with the virus itself. More studies need to be done to elucidate exactly how p120-catenin might be functioning in this process of opening adherens junctions in the absence of Src signaling, and also to determine how and when the virus interacts with the actin cytoskeleton, and if altering these interactions changes the kinetics junctional changes. High resolution imaging studies, in which co-localization of p120 with actin, and actin with the virus, would be very helpful in answering these questions. Another effective approach for delineating these interactions would be to generate mutant viruses lacking specific virion components, and assessing their ability to co-localize with cellular components or induce changes in adherens junctions. Additionally, microarray analysis would help to further define the signaling cascades that are involved and could help narrow down the search for potential therapeutic targets.

Testing the addition of cytokines alone, in this system, would most certainly cause permeability and adherens junction changes, but because the effects seen during JUNV infection in this study were limited to cells expressing viral antigens, it does not appear that a paracrine effect plays a role. A more effective approach for future studies would be to add exogenous antibodies, directed against IL-6 and MCP-1, to help define the extent to which they are affecting the adherens junction changes and barrier function disruption. Ideally, doing this with each cytokine alone, and also together, at different time points, would help define the role each plays in

junction disruption during infection, and also if this effect can be reduced, or ameliorated, with antibodies against the cytokines.

3-dimensional modeling of the adherens junctions during infection would offer more insight into the role that virus/actin interaction might be playing in junction disassembly. In addition to allowing better special and temporal investigations into the protein interactions, it would also allow modeling to include intravascular forces such as sheer stress and flow dynamics, as well as perhaps help identify more specific protein-protein interactions that were not investigated here, or that might not even be considered relevant in the current permeability paradigm.

As more animal models are developed for studying Junín virus, it will become easier to get *in vivo* data that can substantiate or refute the *in vitro* data that has been generated. Monitoring the endothelium in an infected animal over time, would provide answers to many questions still unanswered about the vascular dysfunction during JUNV infection, such as how much of the endothelium gets infected? Is the extracellular matrix playing a role? Can the endothelium be successfully targeted for therapeutics? Immunohistochemistry and cutting-edge *in vivo* imaging systems would provide an entirely new perspective for answering these questions that simply cannot be done using an *in vitro* system.

This study has provided solid footing on which to further explore the mechanisms of vascular dysfunction seen in arenavirus hemorrhagic fevers, but finding the answers to these questions, as well as those yet to be asked, will require animal studies and, ideally, evaluation of human tissue samples from patients who have either survived, or succumbed to, disease. Moving forward with this line of research will be critical in understanding JUNV pathogenesis and transmission, strengthening preventative measures, and generating treatments that include therapies that will provide better outcomes for patients stricken with AHF.

Appendix

All of the studies presented in this dissertation were also performed using the attenuated JUNV vaccine strain Candid#1. There were no significant differences found between these studies and those with the virulent Romero strain. Because there were no differences found and so as not to confuse the reader, the Candid#1 data are presented here rather than in the main body of the dissertation.

CANDID#1 RESULTS

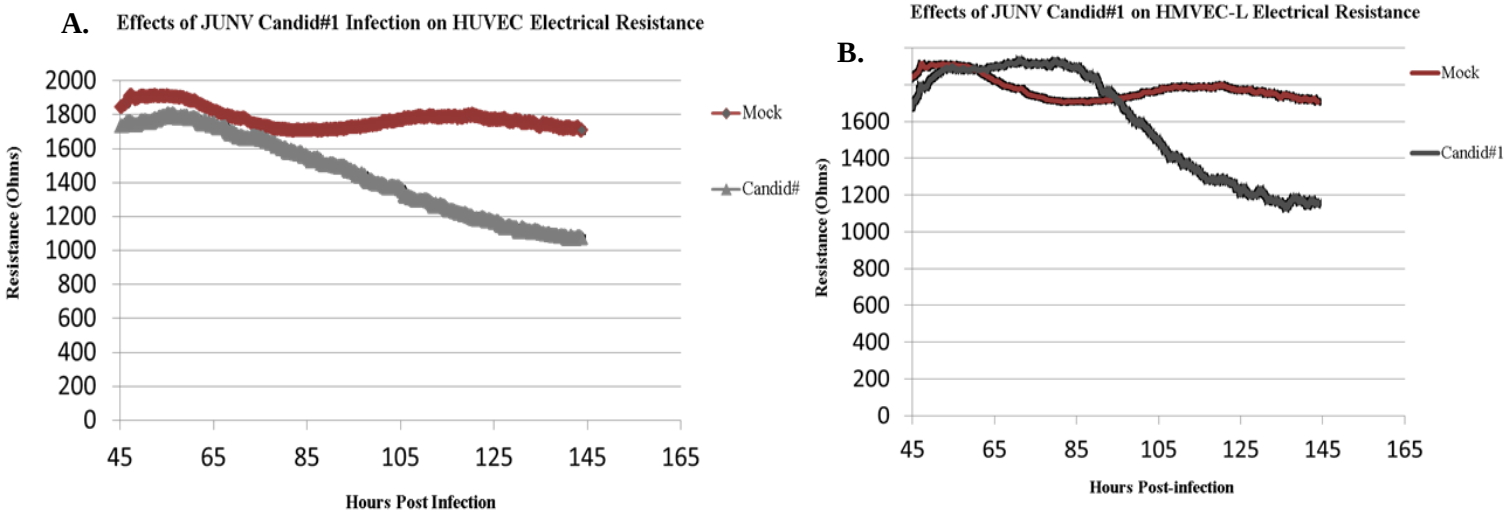

C. **Infection with Candid#1 decreases HUVEC and HMVEC monolayer electrical resistance**

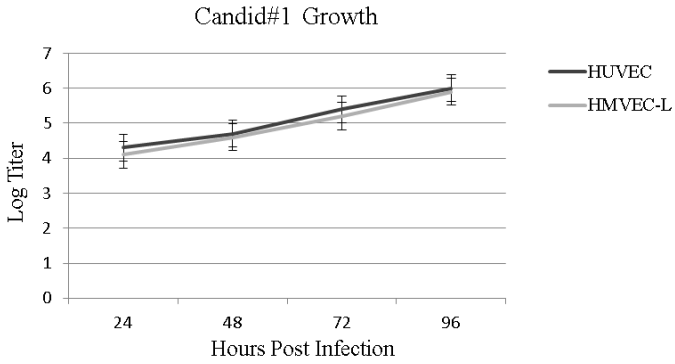

Figure A.1 Candid#1 Decreases HUVEC and HMVEC-L Electrical Resistance. Cells were seeded onto collagen-coated gold electrode arrays and allowed to reach confluence (108h post seeding). Monolayers were then infected with JUNV Candid#1 or mock infected and evaluated by ECIS. HUVECs **(A)** or HMVEC-Ls **(B)** infected with JUNV Candid#1 show decreased electrical resistance beginning at approximately 60 hours post infection (~85 hours after plates were connected to ECIS machine). **(C.)** Growth of Candid#1in HUVECs and HMVEC-Ls during the first 96 hours of the IP experiment. Each point represents the mean ± standard deviation from three experiments.

Infection with Candid#1 increases HUVEC and HMVEC-L monolayer permeability to 70kD FITC-dextran.

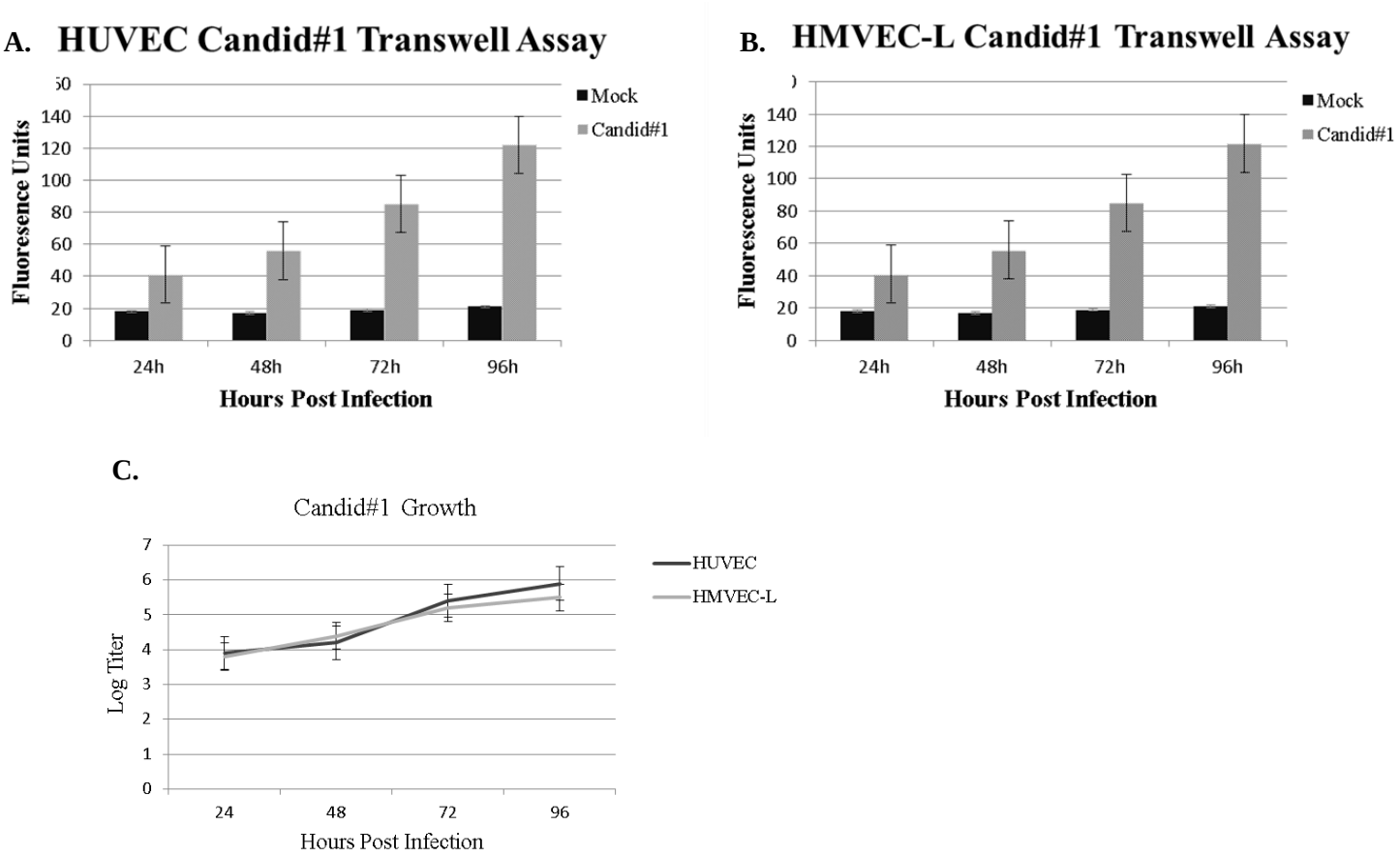

Figure A.2 Transwell permeability assay. Cells were seeded onto transwell inserts and infected with JUNV Candid#1. Samples were taken every 24h for 5 days. HUVECs **(A)** or HMVEC-Ls **(B)** infected with Candid#1 show an extremely significant increased permeability to 70 kDa FITC-Dextran in the absence of visible cytopathology ($P<0.0001$ by paired t-test). **(C.)** Growth of Candid#1in HUVECs and HMVEC-Ls during the first 96 hours of the IP experiment. Data are representative of 3 or more independent experiments. Each point represents the mean ± standard deviation from three experiments.

Gamma irradiation of Candid#1 prevents the decrease in electrical resistance.

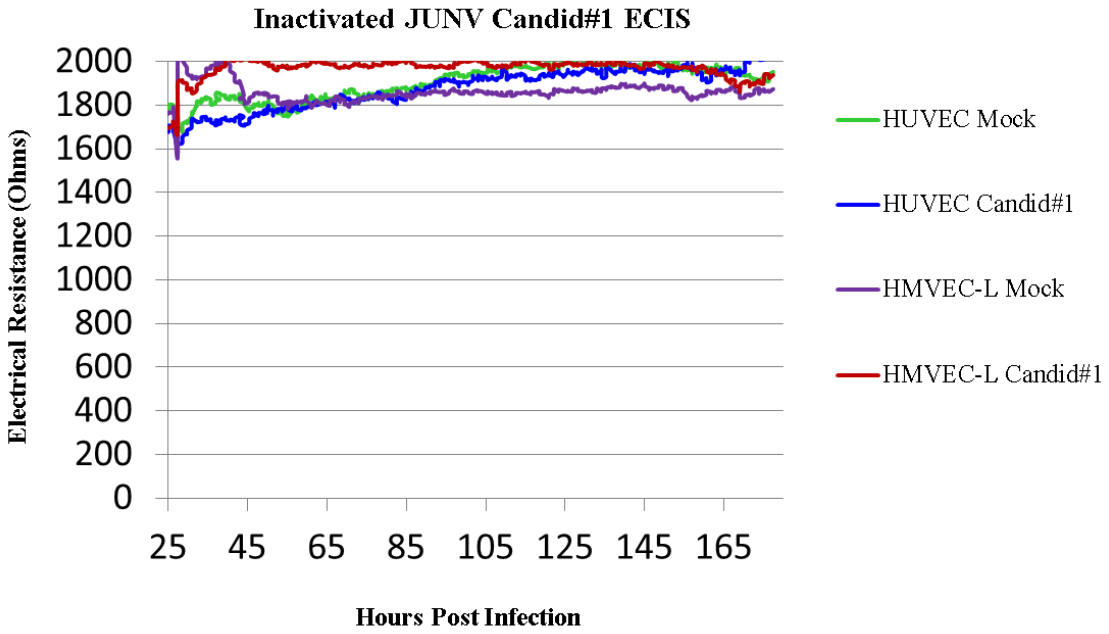

Figure A.3 Killed JUNV Does Not Decrease HUVEC and HMVEC-L Electrical Resistance. Cells were seeded onto collagen-coated gold electrode arrays and allowed to reach confluence (108h post seeding). Monolayers were then infected with JUNV Romero killed with gamma irradiation (5MRad) and evaluated by ECIS.. Gamma irradiated JUNV infection does not decrease HUVEC and HMVEC-L monolayer electrical resistance. Data are representative of 3 independent experiments.

HUVEC and HUMVEC-L monolayers exhibit no overt cytopathology during infection with JUNV Candid#

A. **B.**

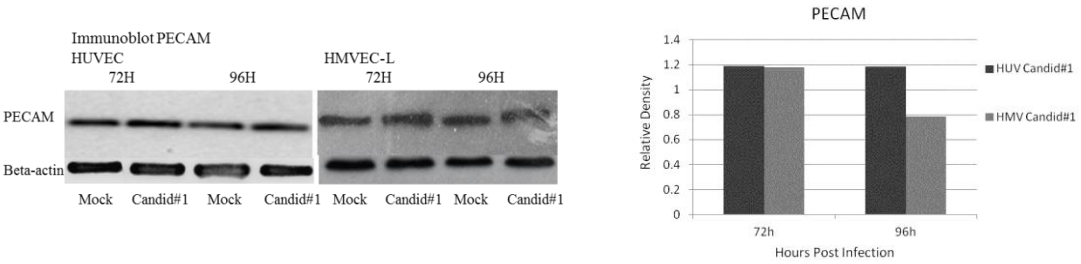

Figure A.4 (A.) Western blot of PECAM. There are no detectable differences in PECAM between Candid#1-infected and mock in both cell types. **(B.)** Image J analysis of density relative to mock-infected, and normalized to actin, confirm imaging data and are representative of 3-5 independent experiments.

HUVEC and HMVEC-L monolayers appear healthy when observed with phase-contrast microscopy during JUNV Candid#1 infection.

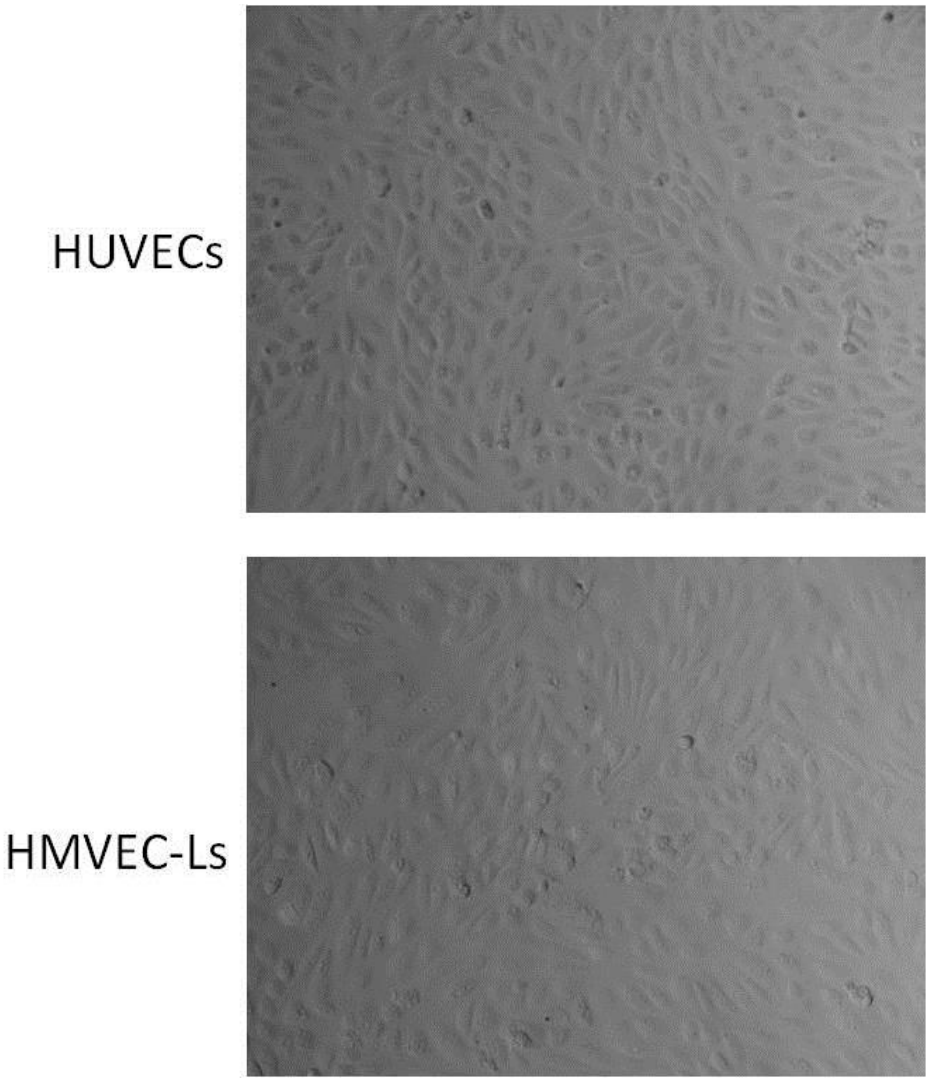

Figure A.5 Phase contrast microscope observations of HUVECs and HMVEC-Ls during infection with JUNV Candid#1. Cells were seeded onto collagen-coated cell culture plates and allowed to reach confluency before infected with JUNV Candid#1. Both cell types exhibit healthy monolayers at 72 hours post infection. Images are representative of 3-5 independent experiments.

Infection with Candid#1 corresponds to a reduction in VE-cadherin/beta-catenin complexes in HUVEC and HMVEC-L monolayers.

A.

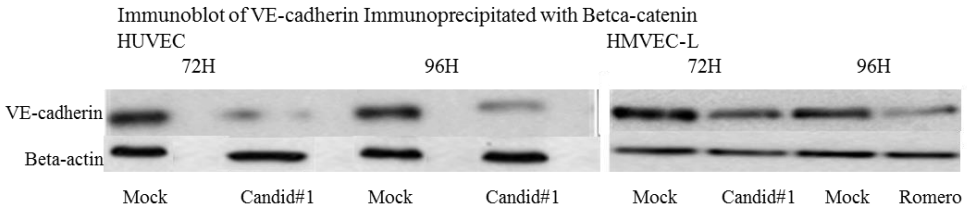

B.

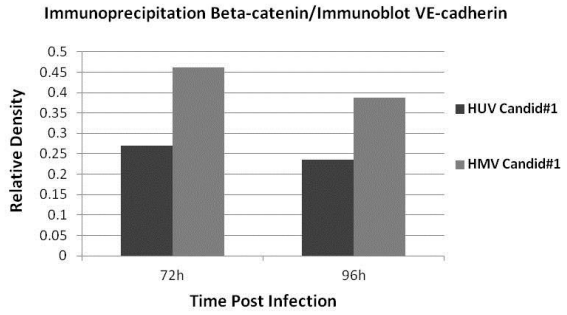

C.

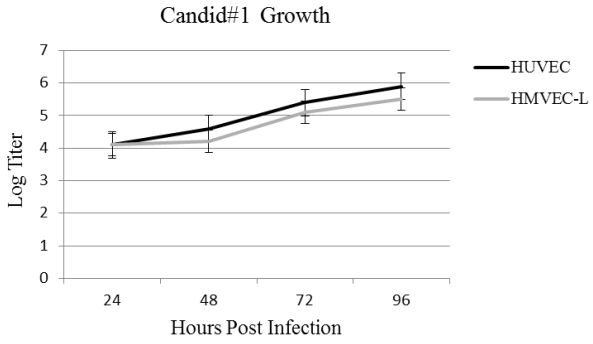

Figure A.6 Western blot of VE-cadherin pulled down with beta-catenin. **(A.)** Mock infected immunoprecipitates show more VE-cadherin pulled down with beta-catenin than infected IPs. **(B.)** Image J analysis of density relative to mock-infected, and normalized to actin, confirm imaging data. **(C.)** Growth of Candid#1in HUVECs and HMVEC-Ls during the first 96 hours of the IP experiment. Each point represents the mean ± standard deviation from three experiments.

Infection with Candid#1 in HUVEC and HMVEC-L monolayers decreases VE-cadherin staining.

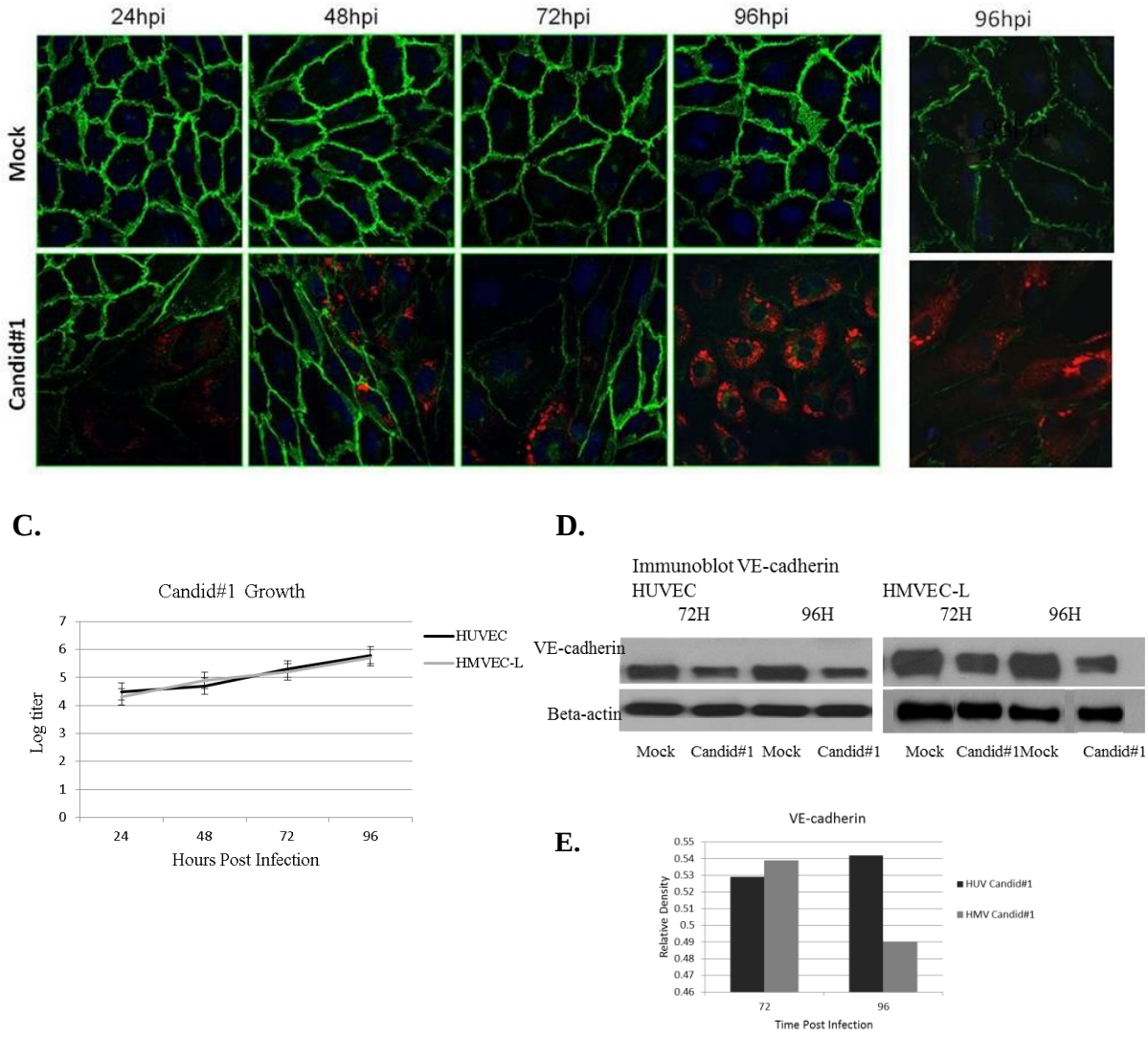

Figure A.7 Immunocytochemistry of VE-cadherin. JUNV Candid#1 infection greatly decreases VE-cadherin staining in HUVECs **(A)** and HMVEC-Ls **(B).** Cell monolayers were infected at an MOI of 4 or mock infected and fixed at 24 hour time points for 5 days. Alexafluor 488 green: VE-cadherin; Alexafluor 594 red: Junin virus and blue: DAPI. HPI is hours post infection. All time points for HUVECs are shown and a representative time point is shown for HMVEC-Ls. All images are 40X magnification**. (C.)** Growth curves of JUNV Candid#1 in HUVECs and HMVEC-Ls during the first 96 hours of the experiment in which the VE-cadherin data were gathered. Each point represents the mean ± standard deviation from three experiments. **(D.)** and **(E)** Western blots and Image J analysis of density relative to mock-infected, and normalized to actin, confirm imaging data.

Infection with Candid#1 in HUVEC and HMVEC-L monolayers decreases p120-catenin isoform 1 staining.

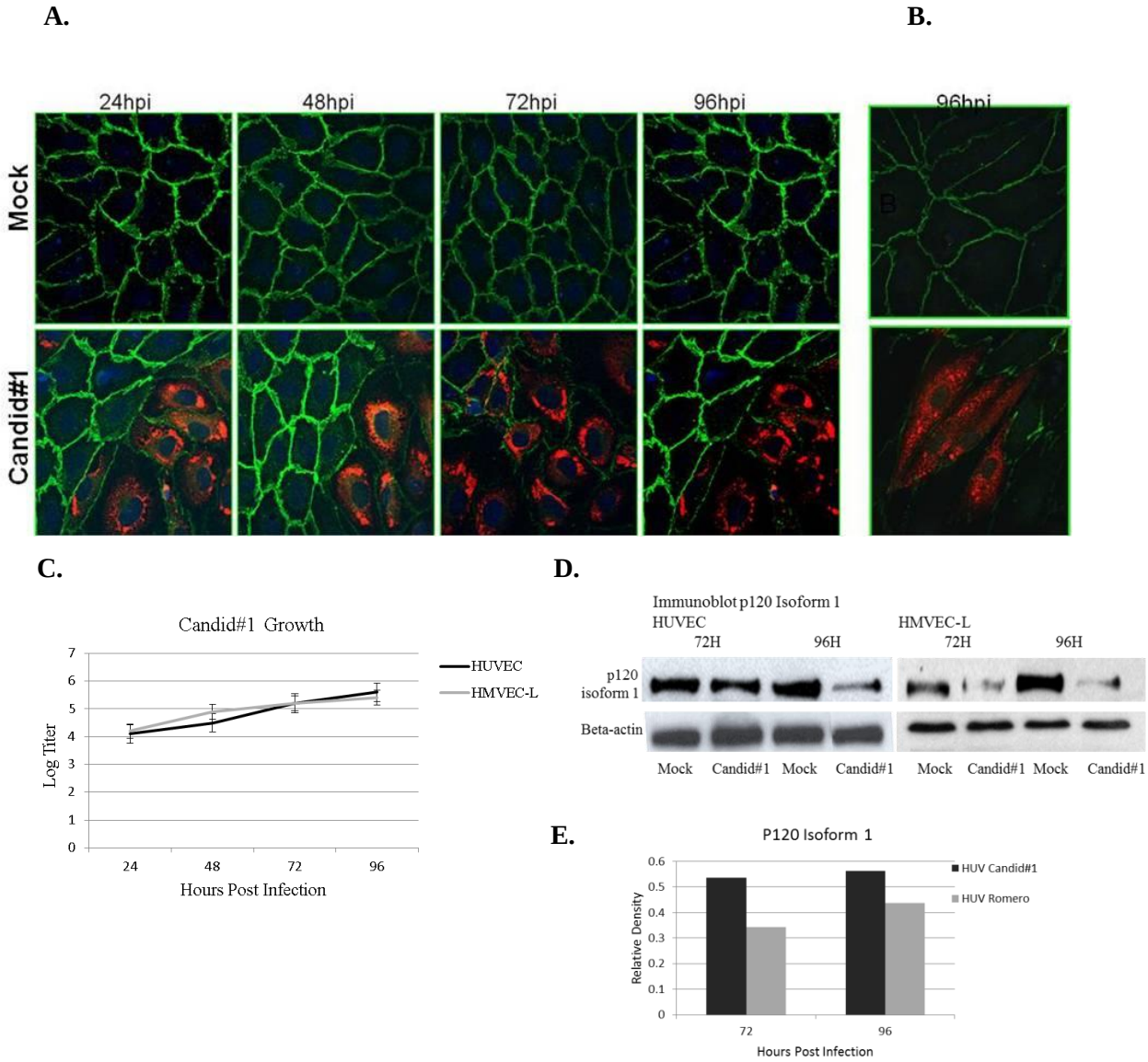

Figure A.8 Immunocytochemistry of p120-catenin isoform 1. JUNV Candid#1 infection greatly decreases p120-catenin isoform 1 staining in HUVECs **(A)** and HMVEC-Ls **(B).** Cell monolayers were infected at an MOI of 4 or mock infected and fixed at 24 hour time points for 5 days. Alexafluor 488 green: p120-catenin; Alexafluor 594 red: JUNV and blue: DAPI. HPI is hours post infection. All time points for HUVECs are shown and a representative time point is shown for HMVEC-Ls. All images are 40X magnification (**C.)** Growth curves of JUNV Candid#1 in HUVECs and HMVEC-Ls during the first 96 hours of the experiment in which p120-catenin data were gathered. Each point represents the mean ± standard deviation from three experiments. **(D.)** and **(E)** Western blots and Image J analysis of density relative to mock-infected, and normalized to actin, confirm imaging data.

Infection with Candid#1 in HUVEC and HMVEC-L monolayers does not alter beta-catenin staining.

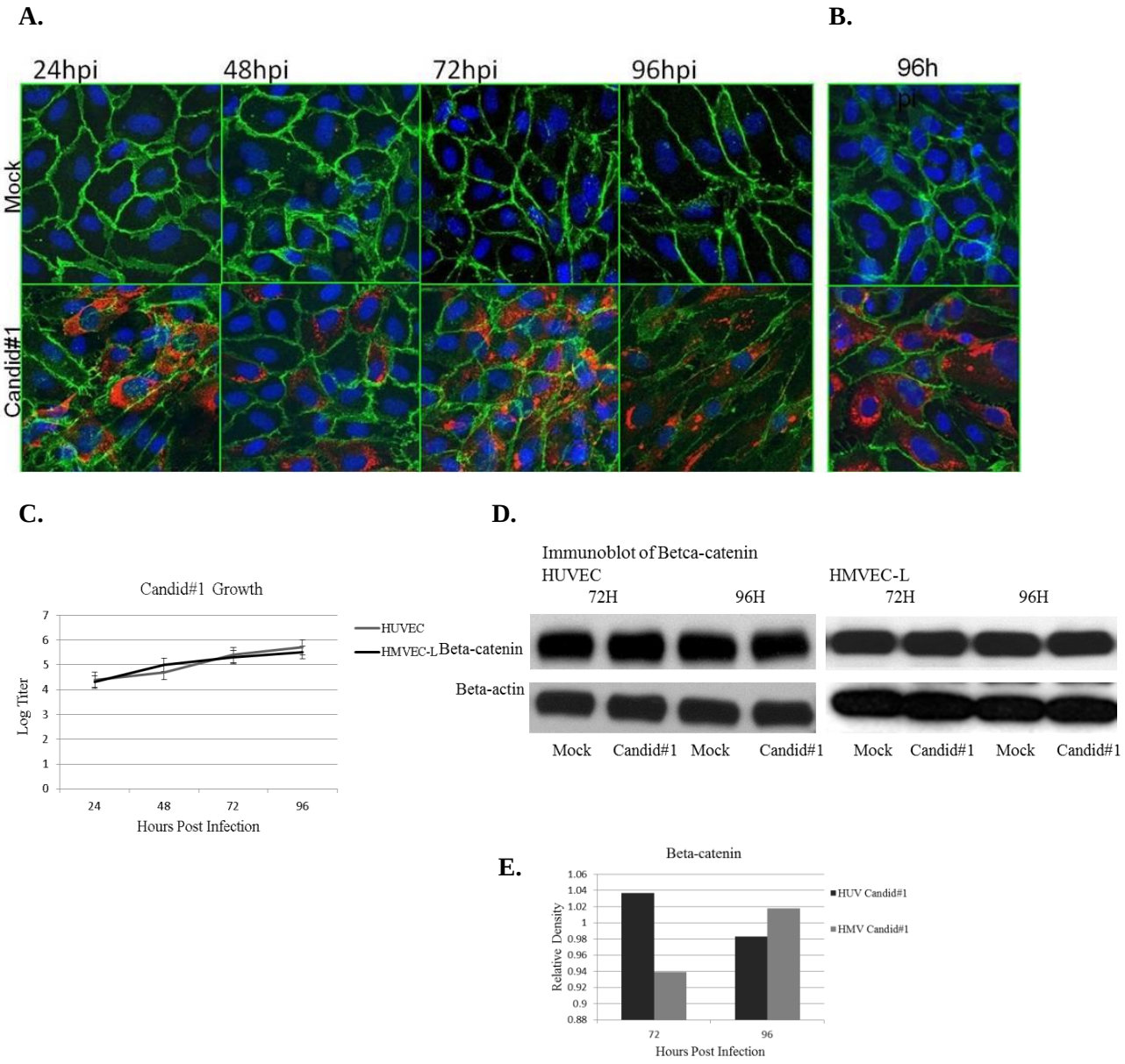

Figure A.9. Immunocytochemistry of beta-catenin. JUNV Candid#1 infection does not reduce beta-catenin staining in HUVECs **(A)** or HMVEC-Ls **(B).** Cell monolayers were infected at an MOI of 4 or mock infected and fixed at 24 hour time points for 5 days. Alexafluor 488 green: beta-catenin; Alexafluor 594 red: Junin virus Candid#1 and blue: DAPI. HPI is hours post infection. All time points for HUVECs are shown and a representative time point is shown for HMVEC-Ls. All images are 40X magnification **(C.)** Growth curves of JUNV Candid#1 in HUVECs and HMVEC-Ls during the first 96 hours of the experiment in which beta-catenin data were gathered. Each point represents the mean ± standard deviation from three experiments. **(D.)** and **(E)** Western blots and Image J analysis of density relative to mock-infected, and normalized to actin, confirm imaging data.

Infection with Candid#1 in HUVEC and HMVEC-L monolayers modifies actin architecture without affecting the overall level of staining.

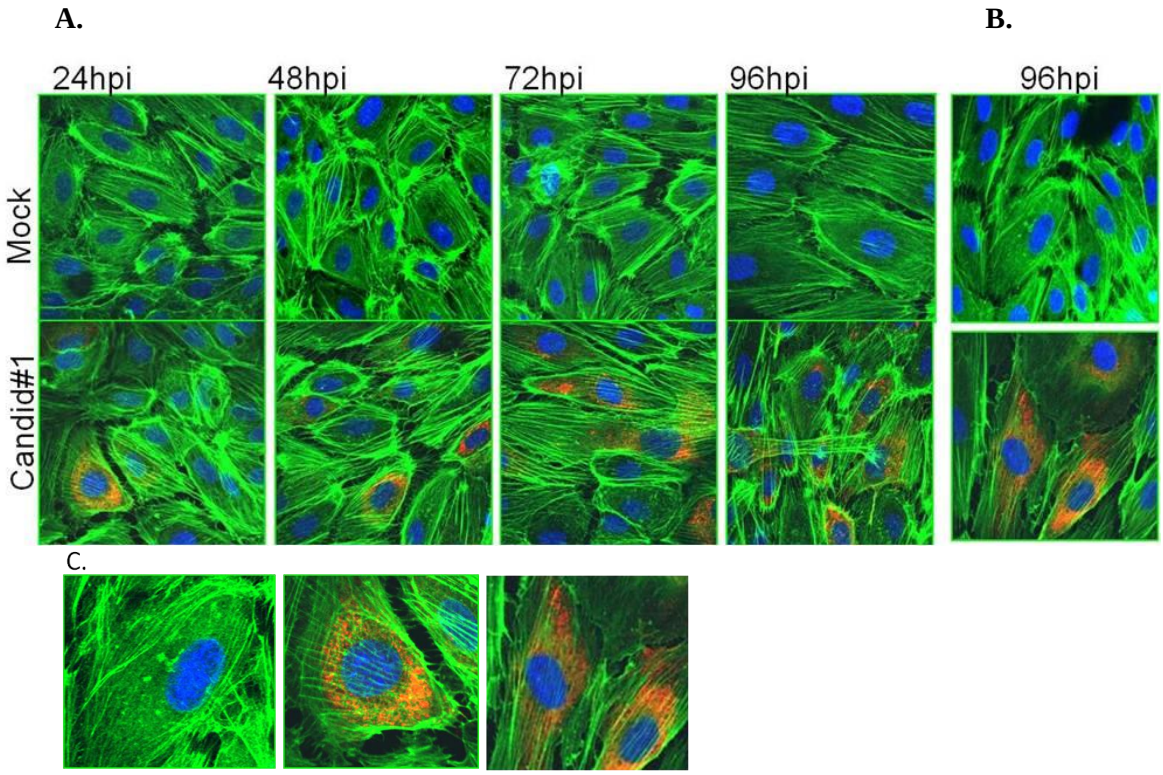

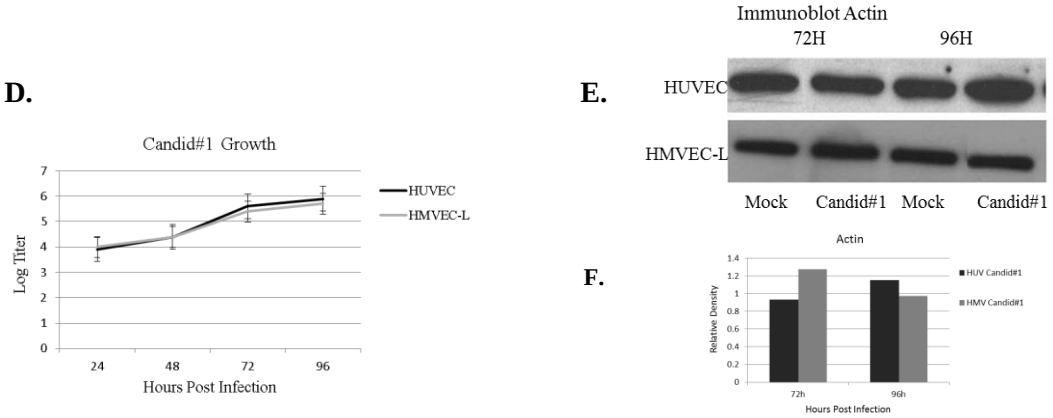

Figure A.10 Immunocytochemistry of F-actin. JUNV Candid#1 infection alters the actin architecture of HUVECs **(A)** and HMVEC-Ls **(B)** without changing overall levels of actin staining. Cell monolayers were infected at an MOI of 4 or mock infected and fixed at 24 hour time points for 5 days. Alexafluor 488 green: phalloidin; Alexafluor 594 red: Junin virus Candid#1 and blue: DAPI. HPI is hours post infection. All time points for HUVECs are shown and a representative time point is shown for HMVEC-Ls. Insets depicting close up views of a few representative cells is also shown **(C).** All images are 40X magnification. **(D.)** Growth of JUNV Candid#1 in HUVECs and HMVEC-Ls during the first 96 hours of the experiment in which the beta-catenin data was gathered**.** Each point represents the mean ± standard deviation from three experiments. **(E.)** and **(F.)** Western blots and Image J analysis of density relative to mock-infected, and normalized to actin, confirm imaging data.

Infection with Candid#1 in HUVEC and HMVEC-L monolayers does not increase VEGF levels.

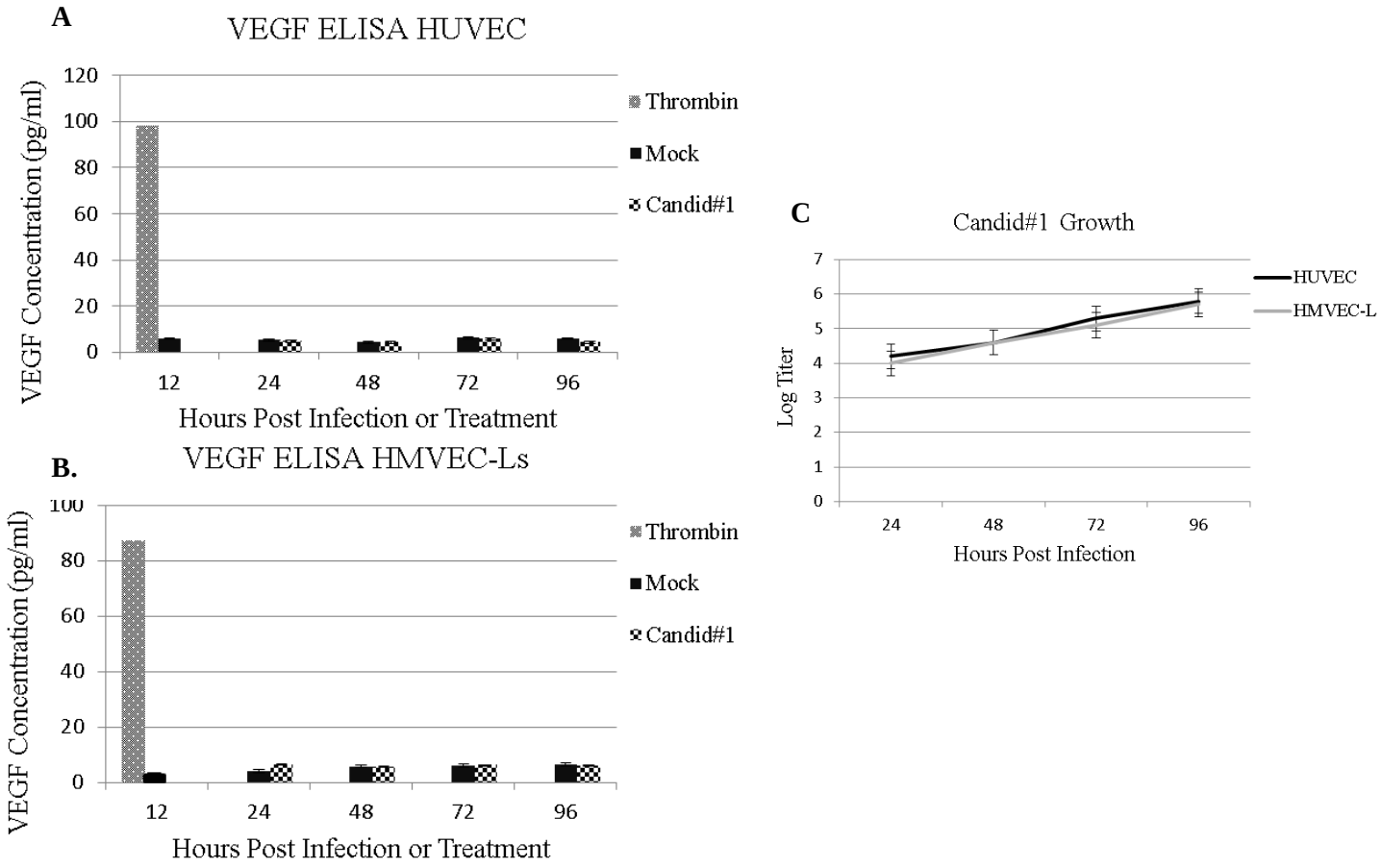

Figure A.11 VEGF ELISA. Infected or mock infected HUVEC **(A)** or HMVEC-L **(B)** cell lysates were analyzed by ELISA to determine levels of VEGF. Activation of cells with thrombin at 1 IU/ml for 12 hours was used as a positive control for VEGF induction. JUNV Candid#1 did not increase VEGF levels in either cell type. Data are means ± SEM representing 3-5 independent experiments. **(C.)** Growth curves of JUNV Candid#1 in HUVECs and HMVEC-Ls during the first 96 hours of the experiment. . Each point represents the mean ± standard deviation from three experiments.

Infection with Candid#1 in HUVEC and HMVEC-L monolayers does not increase Src activity.

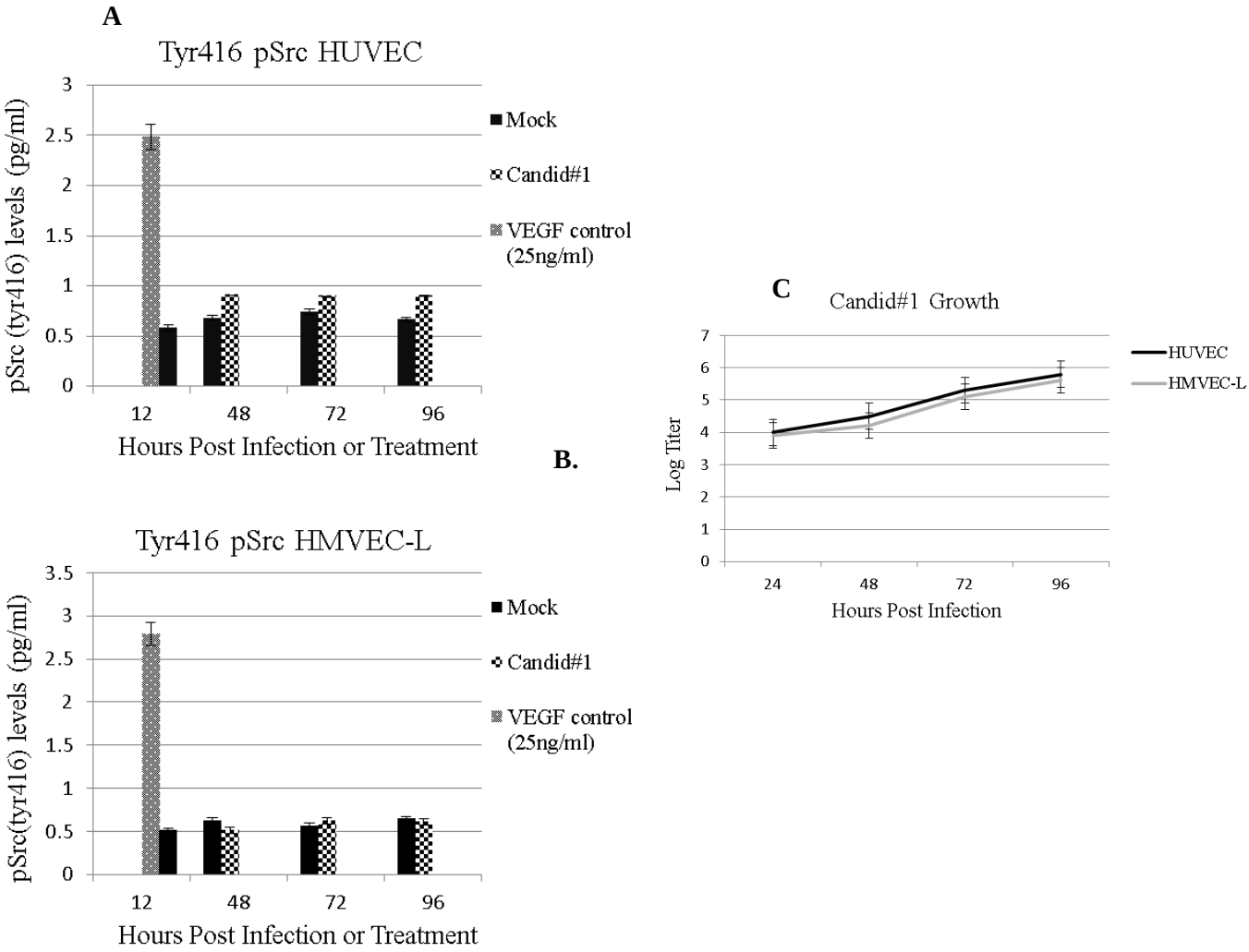

Figure A.12 Phospho-Src ELISA. Infected or mock infected HUVEC **(A)** or HMVEC-L **(B)** cell lysates were analyzed by ELISA to determine levels of activated pSrc (Tyr416). VEGF at 25ng/ml for 12 hours was used as a positive control. JUNV Candid#1 did not increase pSrc levels in either cell type. Data are means ± SEM representing 3-5 independent experiments. **(C.)** Growth of JUNV Candid#1 in HUVECs and HMVEC-Ls during the first 96 hours of the experiment**.** Each point or bar represents the mean ± standard deviation from three experiments.

Infection with Candid#1 in HUVEC and HMVEC-L monolayers decreases p120-catenin isoform 1.

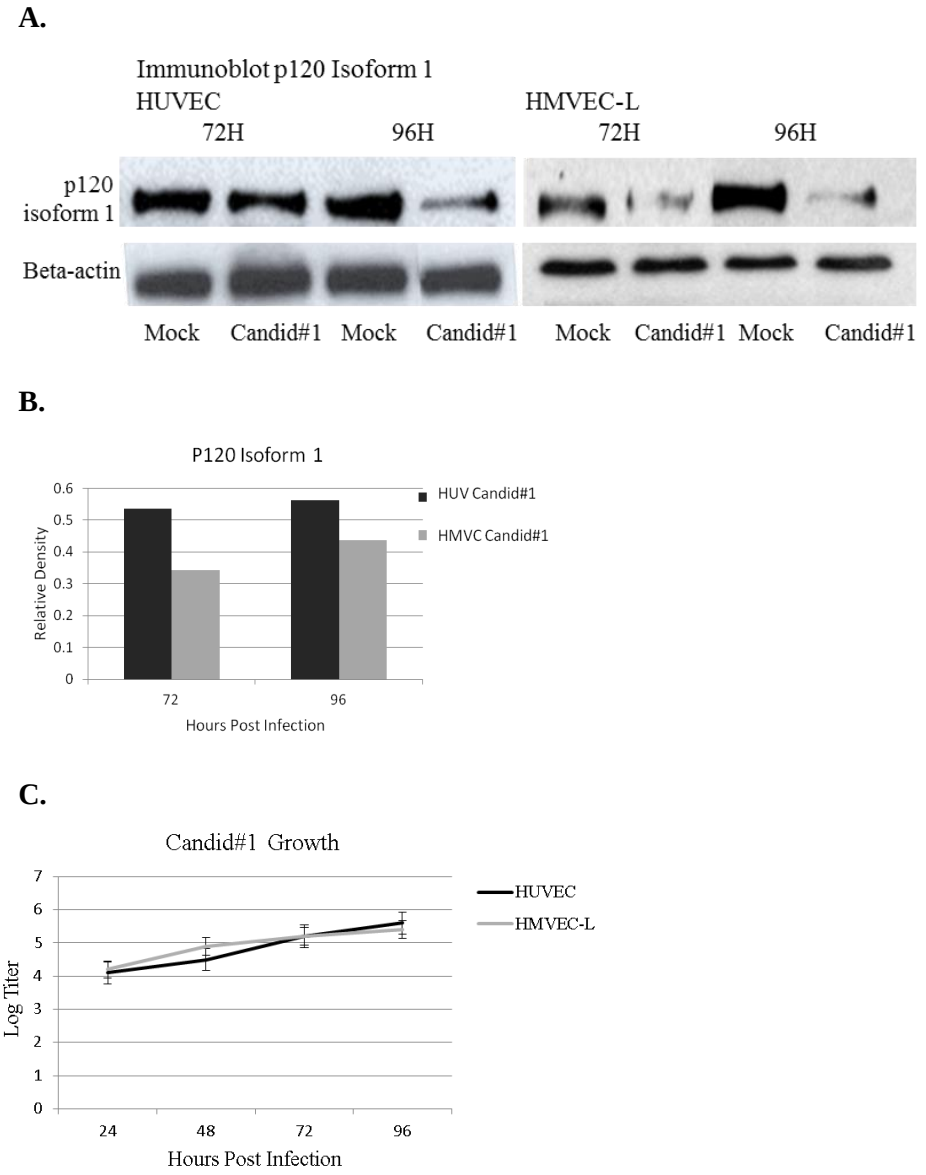

Figure A.13 p12-catenin Isoform 1 decreases over time compared to mock infected cells. Cell monolayers were infected with JUNV Candid#1 at an MOI of 4 or mock infected and lysates made at 24 hour intervals**. (A.)** Western blots show an increase in p120-catenin isoform 1 in infected cell lysates compared to mock infected. **(B.)** Image J analysis of density relative to mock-infected, and normalized to actin, confirm imaging data. **(C.)** Growth curves of JUNV Candid#1 in HUVECs and HMVEC-Ls during the first 96 hours of the experiment**.** Each point represents the mean ± standard deviation from three experiments.

Infection with Candid#1 in HUVEC and HMVEC-L monolayers increases p120-catenin isoform 2.

A.

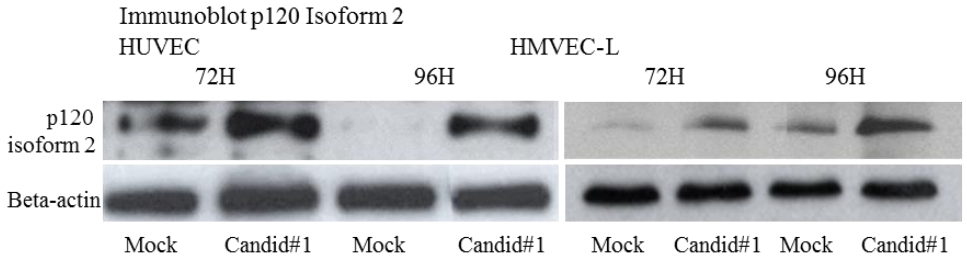

B.

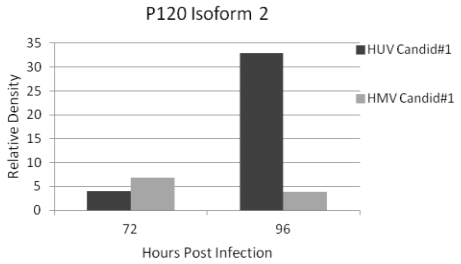

C.

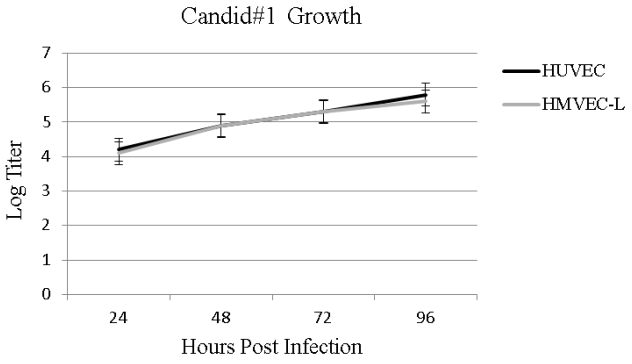

Figure A.14 P120 Isoform 2 increases over time compared to mock infected cells. Cell monolayers were infected with JUNV Cnadid#1 at an MOI of 4 or mock infected and lysates made at 24 hour intervals**. (A.)** Western blots show an increase in p120-catenin isoform 2 in infected cell lysates compared to mock infected. **(B.)** Image J analysis of density relative to mock-infected, and normalized to actin, confirm imaging data. **(C.)** Growth curves of JUNV Candid#1in HUVECs and HMVEC-Ls during the first 96 hours of the experiment**.** Each point represents the mean ± standard deviation from three experiments.

Infection with Candid#1 in HUVEC and HMVEC-L monolayers induces production of MCP1.

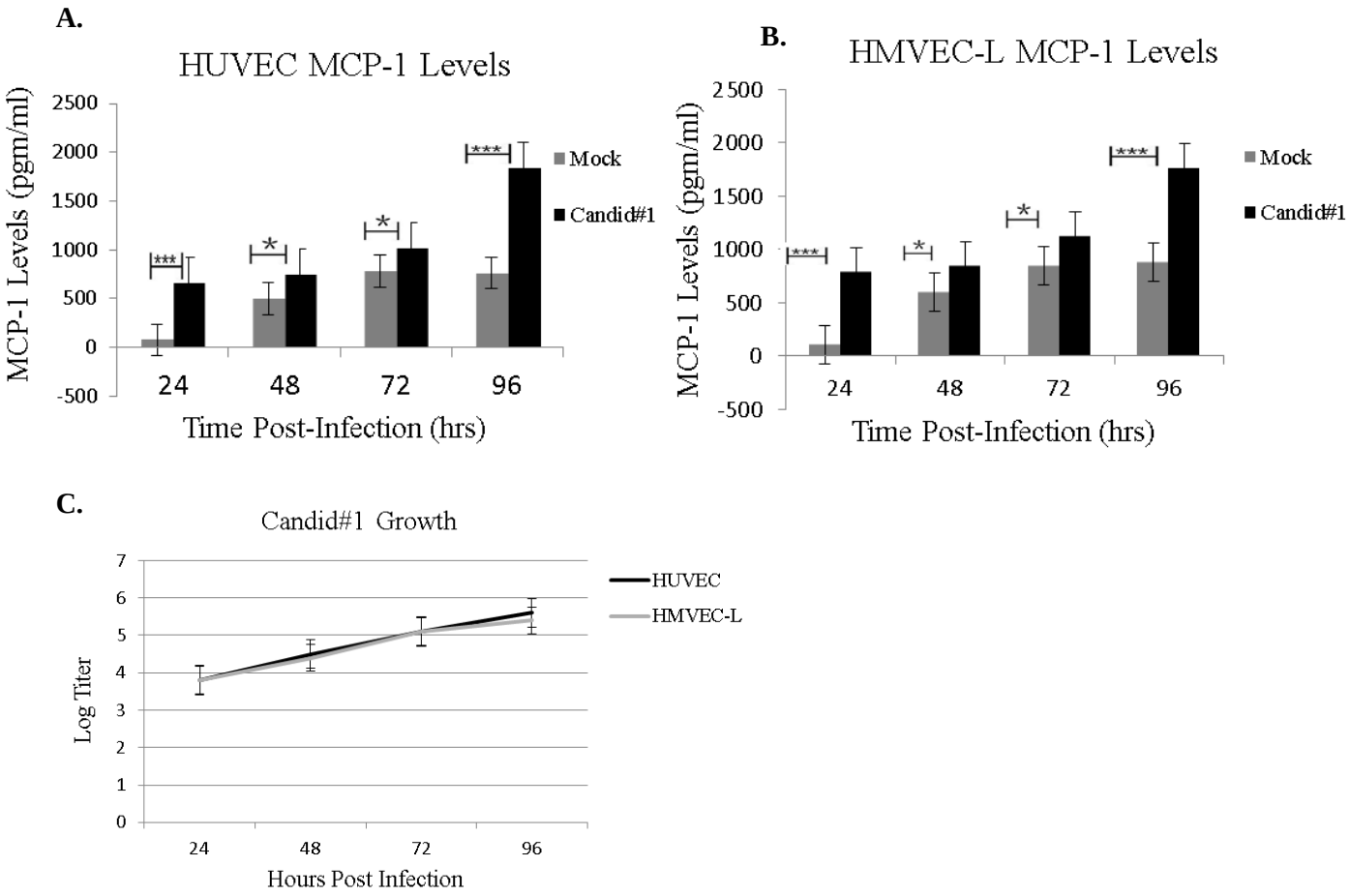

Figure A.15 MCP-1 production in JUNV Candid#1 Infected Endothelial Cells. HUVECs **(A)** and HMVEC-Ls **(B)** infected with JUNV Candid#1 show an increase in MCP-1. Cell monolayers were infected at an MOI of 4 or mock infected and supernatant samples were taken every 24 hours post infection and subjected to Bioplex cytokine analysis. Data is extremely significant by a two-way repeated measure ANOVA test (***p-value<0.0001). **(C.)** Growth curves of JUNV Candid#1in HUVECs and HMVEC-Ls during the first 96 hours of the experiment**.** Each point or bar represents the mean ± standard deviation from three experiments.

Infection with Candid#1 in HUVEC and HMVEC-L monolayers induces production of IL-6.

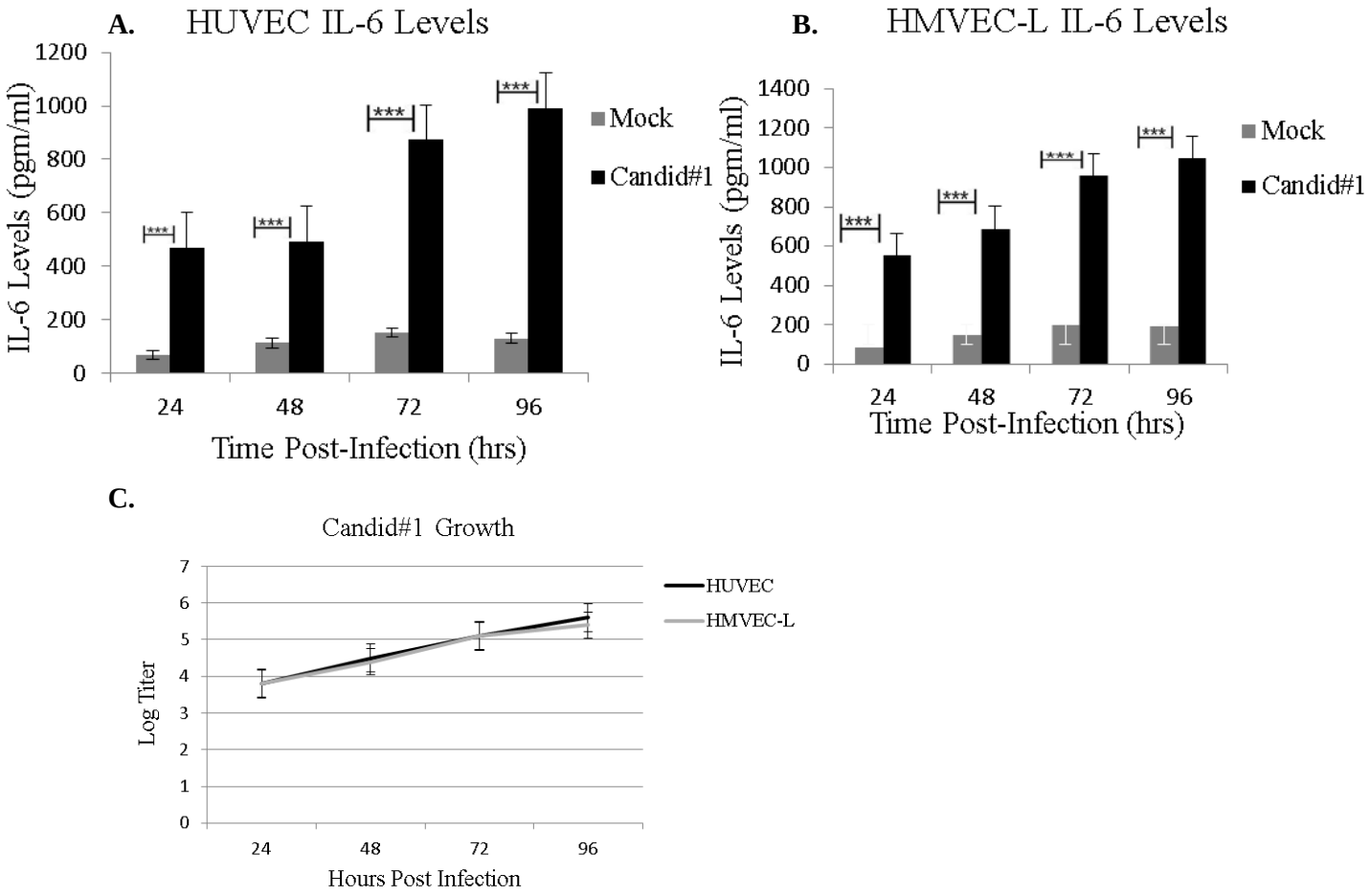

Figure A.16 IL-6 production in JUNV Candid#1 Infected Endothelial Cells. HUVECs **(A)** and HMVEC-Ls **(B)** infected with JUNV Candid#1 show an increase in MCP-1. Cell monolayers were infected at an MOI of 4 or mock infected and supernatant samples were taken every 24 hours post infection and subjected to Bioplex cytokine analysis. Data is extremely significant by a two-way repeated measure ANOVA test (***p-value<0.0001). **(C.)** Growth curves of JUNV Candid#1in HUVECs and HMVEC-Ls during the first 96 hours of the experiment**.** . Each point or bar represents the mean ± standard deviation from three experiments.

References

1. Marty AM, Jahrling PB, Geisbert TW. Viral hemorrhagic fevers. Clin Lab Med. 2006;26(2):345-86, viii. doi: 10.1016/j.cll.2006.05.001. PubMed PMID: 16815457.
2. LeDuc JW. Epidemiology of hemorrhagic fever viruses. Rev Infect Dis. 1989;11 Suppl 4:S730-5. PubMed PMID: 2546247.
3. Ftika L, Maltezou HC. Viral haemorrhagic fevers in healthcare settings. Journal of Hospital Infection. 2013;83(3):185-92. doi: http://dx.doi.org/10.1016/j.jhin.2012.10.013.
4. Chumakov. Studies of virus haemorrhagic fevers. J Hyg Epidemiol Microbiol Immunol. 1963. p. 125-35 .
5. Johnson KM, Peters, C.J. Viral hemorrhagic fevers. In: RBC, editor. Current diagnosis. Philadelphia, PA: Saunders; 1985. p. 212–8.
6. Perng G, Solbrig M. Viral Hemorrhagic Fevers. In: Jackson AC, editor. Viral Infections of the Human Nervous System: Springer Basel; 2013. p. 337-68.
7. McCormick JB, Webb PA, Krebs JW, Johnson KM, Smith ES. A Prospective Study of the Epidemiology and Ecology of Lassa Fever. Journal of Infectious Diseases. 1987;155(3):437-44. doi: 10.1093/infdis/155.3.437.
8. Vitullo AD, Hodara VL, Merani MS. Effect of persistent infection with Junin virus on growth and reproduction of its natural reservoir, Calomys musculinus. The American journal of tropical medicine and hygiene. 1987;37(3):663-9.
9. Sang R, Kioko E, Lutomiah J, Warigia M, Ochieng C, O'Guinn M, Lee JS, Koka H, Godsey M, Hoel D, Hanafi H, Miller B, Schnabel D, Breiman RF, Richardson J. Rift Valley Fever Virus Epidemic in Kenya, 2006/2007: The Entomologic Investigations. The American Journal of Tropical Medicine and Hygiene. 2010;83(2 Suppl):28-37. doi: 10.4269/ajtmh.2010.09-0319.
10. Martins GF, Guedes BAM, Silva LM, Serrão JE, Fortes-Dias CL, Ramalho-Ortigão JM, Pimenta PFP. Isolation, primary culture and morphological characterization of oenocytes from Aedes aegypti pupae. Tissue and Cell. 2011;43(2):83-90. doi: http://dx.doi.org/10.1016/j.tice.2010.12.003.
11. Peterson AT, Carroll DS, Mills JN, Johnson KM. Potential mammalian filovirus reservoirs. Emerging infectious diseases. 2004;10(12):2073-81. doi: 10.3201/eid1012.040346. PubMed PMID: 15663841; PubMed Central PMCID: PMC3323391.
12. Borio L, Inglesby T, Peters CJ, et al. Hemorrhagic fever viruses as biological weapons: Medical and public health management. JAMA. 2002;287(18):2391-405. doi: 10.1001/jama.287.18.2391.
13. Manzione Nd, Salas RA, Paredes H, Godoy O, Rojas L, Araoz F, Fulhorst CF, Ksiazek TG, Mills JN, Ellis BA, Peters CJ, Tesh RB. Venezuelan Hemorrhagic Fever: Clinical and Epidemiological Studies of 165 Cases. Clinical Infectious Diseases. 1998;26(2):308-13. doi: 10.1086/516299.
14. Salas R, Pacheco ME, Ramos B, Taibo ME, Jaimes E, Vasquez C, Querales J, de Manzione N, Godoy O, Betancourt A, Araoz F, Bruzual R, Garcia J, Tesh RB, Rico-Hesse R, Shops RE. Venezuelan haemorrhagic fever. The Lancet. 1991;338(8774):1033-6. doi: http://dx.doi.org/10.1016/0140-6736(91)91899-6.
15. Aleksandrowicz P, Wolf K, Falzarano D, Feldmann H, Seebach J, Schnittler H. Viral haemorrhagic fever and vascular alterations. Hämostaseologie. 2008;28(1):77-84.

16. Maiztegui JI. Clinical and epidemiological patterns of Argentine haemorrhagic fever. Bulletin of the World Health Organization. 1975;52(4-6):567-75. PubMed PMID: 1085212; PubMed Central PMCID: PMC2366633.
17. Bangash SA, Khan EA. Treatment and prophylaxis with ribavirin for Crimean-Congo Hemorrhagic Fever--is it effective? JPMA The Journal of the Pakistan Medical Association. 2003;53(1):39-41. PubMed PMID: 12666854.
18. McCormick JB, King IJ, Webb PA, Scribner CL, Craven RB, Johnson KM, Elliott LH, Belmont-Williams R. Lassa Fever. New England Journal of Medicine. 1986;314(1):20-6. doi: doi:10.1056/NEJM198601023140104. PubMed PMID: 3940312.
19. Rusnak JM, Byrne WR, Chung KN, Gibbs PH, Kim TT, Boudreau EF, Cosgriff T, Pittman P, Kim KY, Erlichman MS, Rezvani DF, Huggins JW. Experience with intravenous ribavirin in the treatment of hemorrhagic fever with renal syndrome in Korea. Antiviral Research. 2009;81(1):68-76. doi: http://dx.doi.org/10.1016/j.antiviral.2008.09.007.
20. Treatment of Viral Hemorrhagic Fever (Crimean-Congo Hemorrhagic Fever or Lassa Fever) With Intravenous Ribavirin in Department of Defense (DOD) Associated Medical Treatment Facilities: A Phase 2 Study 2009-2014 [updated June24, 2013; cited 2013 August, 30]. Available from: http://clinicaltrials.gov/show/NCT00992693.
21. A Phase 2 Treatment Protocol of Intravenous Ribavirin in Adult Subjects With Hemorrhagic Fever With Renal Syndrome (HFRS) in Landstuhl Regional Medical Center (Landstuhl, Germany) IND 16,666 2009-2014 [updated February 1, 2013; cited 2013 August 30]. Available from: http://clinicaltrials.gov/show/NCT00868946.
22. Maiztegui JI, Fernandez NJ, de Damilano AJ. Efficacy of immune plasma in treatment of Argentine haemorrhagic fever and association between treatment and a late neurological syndrome. Lancet. 1979;2(8154):1216-7. PubMed PMID: 92624.
23. Ambrosio A, Saavedra M, Mariani M, Gamboa G, Maiza A. Argentine hemorrhagic fever vaccines. Human Vaccines. 2011;7(6):694-700.
24. Monath TP. Yellow fever vaccine. Expert Review of Vaccines. 2005;4(4):553-74. doi: 10.1586/14760584.4.4.553.
25. Gubler DJ. Resurgent vector-borne diseases as a global health problem. Emerging infectious diseases. 1998;4(3):442-50. doi: 10.3201/eid0403.980326. PubMed PMID: 9716967; PubMed Central PMCID: PMC2640300.
26. Monath TP. Lassa fever: review of epidemiology and epizootiology. Bulletin of the World Health Organization. 1975;52(4-6):577-92. PubMed PMID: 782738; PubMed Central PMCID: PMC2366662.
27. PETERS CJ, KUEHNE RW, MERCADO RR, LE BOW RH, SPERTZEL RO, WEBB PA. HEMORRHAGIC FEVER IN COCHABAMBA, BOLIVIA, 1971. American Journal of Epidemiology. 1974;99(6):425-33.
28. Nabeth P, Cheikh DO, Lo B, Faye O, Vall IO, Niang M, Wague B, Diop D, Diallo M, Diallo B, Diop OM, Simon F. Crimean-Congo hemorrhagic fever, Mauritania. Emerging infectious diseases. 2004;10(12):2143-9. doi: 10.3201/eid1012.040535. PubMed PMID: 15663851; PubMed Central PMCID: PMC3323392.
29. Munyua P, Murithi RM, Wainwright S, Githinji J, Hightower A, Mutonga D, Macharia J, Ithondeka PM, Musaa J, Breiman RF, Bloland P, Njenga MK. Rift Valley Fever Outbreak in Livestock in Kenya, 2006–2007. The American Journal of Tropical Medicine and Hygiene. 2010;83(2 Suppl):58-64. doi: 10.4269/ajtmh.2010.09-0292.

30. Appannanavar SB, Mishra B. An update on crimean congo hemorrhagic Fever. Journal of global infectious diseases. 2011;3(3):285-92. doi: 10.4103/0974-777X.83537. PubMed PMID: 21887063; PubMed Central PMCID: PMC3162818.
31. Klempa B, Radosa L, Kruger DH. The broad spectrum of hantaviruses and their hosts in Central Europe. Acta virologica. 2013;57(2):130-7. PubMed PMID: 23600871.
32. MacNeil A, Rollin PE. Ebola and Marburg hemorrhagic fevers: neglected tropical diseases? PLoS neglected tropical diseases. 2012;6(6):e1546. doi: 10.1371/journal.pntd.0001546. PubMed PMID: 22761967; PubMed Central PMCID: PMC3385614.
33. Weingartl HM, Nfon C, Kobinger G. Review of ebola virus infections in domestic animals. Developments in biologicals. 2013;135:211-8. doi: 10.1159/000178495. PubMed PMID: 23689899.
34. Dash AP, Bhatia R, Sunyoto T, Mourya DT. Emerging and re-emerging arboviral diseases in Southeast Asia. Journal of vector borne diseases. 2013;50(2):77-84. PubMed PMID: 23995308.
35. Enria D, Bowen, M.D., Mills, J.N., Shieh, W.J., Bausch, D., Peters, C.J. Arenavirus infections. In: Guerrant RL, Walker, D. H., Weller, P.F., Saunders, W.B. , editor. Tropical Infectious Diseases: Principles, Pathogens, and Practice: Elsevier Churchill Livingstone; 2004. p. 1191–212
36. Muckenfuss RS, Armstrong, Charles, and McCordock, H. A. Public Health Report. 1933;48.
37. Armstrong C, Lillie RD. Experimental Lymphocytic Choriomeningitis of Monkeys and Mice Produced by a Virus Encountered in Studies of the 1933 St. Louis Encephalitis Epidemic. Public Health Reports (1896-1970). 1934;49(35):1019-27. doi: 10.2307/4581290.
38. Gonzalez JP, Emonet S, Lamballerie Xd, Charrel R. Arenaviruses. In: Childs J, Mackenzie J, Richt J, editors. Wildlife and Emerging Zoonotic Diseases: The Biology, Circumstances and Consequences of Cross-Species Transmission: Springer Berlin Heidelberg; 2007. p. 253-88.
39. Peters CJ. Human Infection with Arenaviruses in the Americas. In: Oldstone MA, editor. Arenaviruses I: Springer Berlin Heidelberg; 2002. p. 65-74.
40. Paweska JT, Sewlall NH, Ksiazek TG, Blumberg LH, Hale MJ, Lipkin WI, Weyer J, Nichol ST, Rollin PE, McMullan LK, Paddock CD, Briese T, Mnyaluza J, Dinh TH, Mukonka V, Ching P, Duse A, Richards G, de Jong G, Cohen C, Ikalafeng B, Mugero C, Asomugha C, Malotle MM, Nteo DM, Misiani E, Swanepoel R, Zaki SR, Outbreak C, Investigation T. Nosocomial outbreak of novel arenavirus infection, southern Africa. Emerging infectious diseases. 2009;15(10):1598-602. doi: 10.3201/eid1510.090211. PubMed PMID: 19861052; PubMed Central PMCID: PMC2866397.
41. Delgado S, Erickson BR, Agudo R, Blair PJ, Vallejo E, Albarino CG, Vargas J, Comer JA, Rollin PE, Ksiazek TG, Olson JG, Nichol ST. Chapare virus, a newly discovered arenavirus isolated from a fatal hemorrhagic fever case in Bolivia. PLoS pathogens. 2008;4(4):e1000047. doi: 10.1371/journal.ppat.1000047. PubMed PMID: 18421377; PubMed Central PMCID: PMC2277458.
42. Charrel RN, de Lamballerie X, Emonet S. Phylogeny of the genus Arenavirus. Current Opinion in Microbiology. 2008;11(4):362-8. doi: http://dx.doi.org/10.1016/j.mib.2008.06.001.
43. Cajimat MNB, Milazzo ML, Haynie ML, Hanson JD, Bradley RD, Fulhorst CF. Diversity and phylogenetic relationships among the North American Tacaribe serocomplex viruses (Family Arenaviridae). Virology. 2011;421(2):87-95. doi: http://dx.doi.org/10.1016/j.virol.2011.09.013.
44. Ishii A, Thomas Y, Moonga L, Nakamura I, Ohnuma A, Hang'ombe BM, Takada A, Mweene AS, Sawa H. Molecular surveillance and phylogenetic analysis of Old World arenaviruses in Zambia. Journal of General Virology. 2012;93(Pt 10):2247-51. doi: 10.1099/vir.0.044099-0.
45. Ehichioya DU, Hass M, Becker-Ziaja B, Ehimuan J, Asogun DA, Fichet-Calvet E, Kleinsteuber K, Lelke M, ter Meulen J, Akpede GO, Omilabu SA, Günther S, Ölschläger S. Current Molecular

Epidemiology of Lassa Virus in Nigeria. Journal of clinical microbiology. 2011;49(3):1157-61. doi: 10.1128/jcm.01891-10.
46. Takagi T, Ohsawa M, Morita C, Sato H, Ohsawa K. Genomic Analysis and Pathogenic Characteristics of Lymphocytic Choriomeningitis Virus Strains Isolated in Japan. Comparative Medicine. 2012;62(3):185-92.
47. Charrel RN, de Lamballerie X. Zoonotic aspects of arenavirus infections. Veterinary Microbiology. 2010;140(3–4):213-20. doi: http://dx.doi.org/10.1016/j.vetmic.2009.08.027.
48. Meyer BJ, Torre JC, Southern PJ. Arenaviruses: Genomic RNAs, Transcription, and Replication. In: Oldstone MA, editor. Arenaviruses I: Springer Berlin Heidelberg; 2002. p. 139-57.
49. Bishop DHL. Arenaviruses have ambisense S RNA. Med Microbiol Immunol. 1986;175(2-3):61-2. doi: 10.1007/BF02122415.
50. Bishop DHL, Auperin DD. Arenavirus Gene Structure and Organization. In: Oldstone MA, editor. Arenaviruses: Springer Berlin Heidelberg; 1987. p. 5-17.
51. Southern PJ. Arenaviridae: The viruses and their replication. In: Fields BN KD, Howley PM, editor. Fields Virology. Philadelphia: Lippincott-Raven 1996. p. 1505–19.
52. Auperin DD, Compans RW, Bishop DHL. Nucleotide sequence conservation at the 3′ termini of the virion RNA species of new World and Old World arenaviruses. Virology. 1982;121(1):200-3. doi: http://dx.doi.org/10.1016/0042-6822(82)90130-1.
53. Auperin DD, Romanowski V, Galinski M, Bishop DH. Sequencing studies of pichinde arenavirus S RNA indicate a novel coding strategy, an ambisense viral S RNA. Journal of Virology. 1984;52(3):897-904.
54. Auperin DD, Sasso DR, McCormick JB. Nucleotide sequence of the glycoprotein gene and intergenic region of the Lassa virus S genome RNA. Virology. 1986;154(1):155-67. doi: http://dx.doi.org/10.1016/0042-6822(86)90438-1.
55. Zhang L, Marriott K, Aronson JF. Sequence analysis of the small RNA segment of guinea pig-passaged Pichinde virus variants. The American Journal of Tropical Medicine and Hygiene. 1999;61(2):220-5.
56. Perez M, de la Torre JC. Characterization of the Genomic Promoter of the Prototypic Arenavirus Lymphocytic Choriomeningitis Virus. Journal of Virology. 2003;77(2):1184-94. doi: 10.1128/jvi.77.2.1184-1194.2003.
57. Southern PJ, Singh MK, Riviere Y, Jacoby DR, Buchmeier MJ, Oldstone MBA. Molecular characterization of the genomic S RNA segment from lymphocytic choriomeningitis virus. Virology. 1987;157(1):145-55. doi: http://dx.doi.org/10.1016/0042-6822(87)90323-0.
58. Salvato MS, Shimomaye EM. The completed sequence of lymphocytic choriomeningitis virus reveals a unique RNA structure and a gene for a zinc finger protein. Virology. 1989;173(1):1-10. doi: http://dx.doi.org/10.1016/0042-6822(89)90216-X.
59. Burri DJ, Palma JR, Kunz S, Pasquato A. Envelope Glycoprotein of Arenaviruses. Viruses. 2012;4(10):2162-81. PubMed PMID: doi:10.3390/v4102162.
60. Clegg JCS, Wilson SM, Oram JD. Nucleotide sequence of the S RNA of Lassa virus (Nigerian strain) and comparative analysis of arenavirus gene products. Virus Research. 1991;18(2–3):151-64. doi: http://dx.doi.org/10.1016/0168-1702(91)90015-N.
61. Lukashevich IS, Djavani M, Shapiro K, Sanchez A, Ravkov E, Nichol ST, Salvato MS. The Lassa fever virus L gene: nucleotide sequence, comparison, and precipitation of a predicted 250 kDa protein with monospecific antiserum. Journal of General Virology. 1997;78(3):547-51.
62. Burns JW, Buchmeier MJ. Protein-protein interactions in lymphocytic choriomeningitis virus. Virology. 1991;183(2):620-9. doi: http://dx.doi.org/10.1016/0042-6822(91)90991-J.

63. Ortiz-Riaño E, Cheng BYH, de la Torre JC, Martínez-Sobrido L. Self-Association of Lymphocytic Choriomeningitis Virus Nucleoprotein Is Mediated by Its N-Terminal Region and Is Not Required for Its Anti-Interferon Function. Journal of Virology. 2012;86(6):3307-17. doi: 10.1128/jvi.05503-11.
64. Rodrigo WWSI, Ortiz-Riaño E, Pythoud C, Kunz S, de la Torre JC, Martínez-Sobrido L. Arenavirus Nucleoproteins Prevent Activation of Nuclear Factor Kappa B. Journal of Virology. 2012;86(15):8185-97. doi: 10.1128/jvi.07240-11.
65. Kranzusch PJ, Schenk AD, Rahmeh AA, Radoshitzky SR, Bavari S, Walz T, Whelan SPJ. Assembly of a functional Machupo virus polymerase complex. Proceedings of the National Academy of Sciences. 2010;107(46):20069-74. doi: 10.1073/pnas.1007152107.
66. Kranzusch PJ, Whelan SPJ. Arenavirus Z protein controls viral RNA synthesis by locking a polymerase–promoter complex. Proceedings of the National Academy of Sciences. 2011;108(49):19743-8. doi: 10.1073/pnas.1112742108.
67. Cao W, Henry MD, Borrow P, Yamada H, Elder JH, Ravkov EV, Nichol ST, Compans RW, Campbell KP, Oldstone MB. Identification of alpha-dystroglycan as a receptor for lymphocytic choriomeningitis virus and Lassa fever virus. Science. 1998;282(5396):2079-81. PubMed PMID: 9851928.
68. Radoshitzky SR, Abraham J, Spiropoulou CF, Kuhn JH, Nguyen D, Li W, Nagel J, Schmidt PJ, Nunberg JH, Andrews NC, Farzan M, Choe H. Transferrin receptor 1 is a cellular receptor for New World haemorrhagic fever arenaviruses. Nature. 2007;446(7131):92-6. doi: 10.1038/nature05539. PubMed PMID: 17287727; PubMed Central PMCID: PMC3197705.
69. Glushakova SE, Lukashevich IS. Early events in arenavirus replication are sensitive to lysosomotropic compounds. Archives of virology. 1989;104(1-2):157-61. PubMed PMID: 2923547.
70. Di Simone C, Zandonatti MA, Buchmeier MJ. Acidic pH Triggers LCMV Membrane Fusion Activity and Conformational Change in the Glycoprotein Spike. Virology. 1994;198(2):455-65. doi: http://dx.doi.org/10.1006/viro.1994.1057.
71. Di Simone C, Buchmeier MJ. Kinetics and pH Dependence of Acid-Induced Structural Changes in the Lymphocytic Choriomeningitis Virus Glycoprotein Complex. Virology. 1995;209(1):3-9. doi: http://dx.doi.org/10.1006/viro.1995.1225.
72. Kunz S, Borrow P, Oldstone MB. Receptor structure, binding, and cell entry of arenaviruses. Current topics in microbiology and immunology. 2002;262:111-37. PubMed PMID: 11987803.
73. Kunz S, Edelmann KH, de la Torre JC, Gorney R, Oldstone MB. Mechanisms for lymphocytic choriomeningitis virus glycoprotein cleavage, transport, and incorporation into virions. Virology. 2003;314(1):168-78. PubMed PMID: 14517070.
74. Cordo SM, Valko A, Martinez GM, Candurra NA. Membrane localization of Junín virus glycoproteins requires cholesterol and cholesterol rich membranes. Biochemical and Biophysical Research Communications. 2013;430(3):912-7. doi: http://dx.doi.org/10.1016/j.bbrc.2012.12.053.
75. Buchmeier MJ dlTJ, Peters CJ. Arenaviridae: the viruses and their replication. In: Knipe DM HP, editor. Fields virology, 5th ed. Philadelphia, PA: Lippincott Williams & Wilkins; 2007. p. 1791–828.
76. Lee KJ, Novella IS, Teng MN, Oldstone MBA, de la Torre JC. NP and L Proteins of Lymphocytic Choriomeningitis Virus (LCMV) Are Sufficient for Efficient Transcription and Replication of LCMV Genomic RNA Analogs. Journal of Virology. 2000;74(8):3470-7. doi: 10.1128/jvi.74.8.3470-3477.2000.

77. Garcin D, Kolakofsky D. A novel mechanism for the initiation of Tacaribe arenavirus genome replication. Journal of Virology. 1990;64(12):6196-203.
78. Iapalucci S, López N, Franze-Fernández MT. The 3′ end termini of the tacaribe arenavirus subgenomic RNAs. Virology. 1991;182(1):269-78. doi: http://dx.doi.org/10.1016/0042-6822(91)90670-7.
79. Baird NL, York J, Nunberg JH. Arenavirus Infection Induces Discrete Cytosolic Structures for RNA Replication. Journal of Virology. 2012;86(20):11301-10. doi: 10.1128/jvi.01635-12.
80. Loureiro ME, D'Antuono A, Levingston Macleod JM, López N. Uncovering Viral Protein-Protein Interactions and their Role in Arenavirus Life Cycle. Viruses. 2012;4(9):1651-67. PubMed PMID: doi:10.3390/v4091651.
81. Urata S, Yasuda J. Molecular Mechanism of Arenavirus Assembly and Budding. Viruses. 2012;4(10):2049-79. PubMed PMID: doi:10.3390/v4102049.
82. Schley D, Whittaker RJ, Neuman BW. Arenavirus budding resulting from viral-protein-associated cell membrane curvature. Journal of The Royal Society Interface. 2013;10(86). doi: 10.1098/rsif.2013.0403.
83. Paessler S, Walker DH. Pathogenesis of the Viral Hemorrhagic Fevers. Annual Review of Pathology: Mechanisms of Disease. 2013;8(1):411-40. doi: doi:10.1146/annurev-pathol-020712-164041. PubMed PMID: 23121052.
84. Gonzalez PH, Cossio PM, Arana R, Maiztegui JI, Laguens RP. Lymphatic tissue in Argentine hemorrhagic fever. Pathologic features. Archives of pathology & laboratory medicine. 1980;104(5):250-4. PubMed PMID: 6154445.
85. Kenyon RH, McKee KT, Jr., Zack PM, Rippy MK, Vogel AP, York C, Meegan J, Crabbs C, Peters CJ. Aerosol infection of rhesus macaques with Junin virus. Intervirology. 1992;33(1):23-31. PubMed PMID: 1371270.
86. Geisbert TW, Jahrling PB. Exotic emerging viral diseases: progress and challenges. Nature medicine. 2004;10(12 Suppl):S110-21. doi: 10.1038/nm1142. PubMed PMID: 15577929.
87. Gomez RM, Pozner RG, Lazzari MA, D'Atri LP, Negrotto S, Chudzinski-Tavassi AM, Berria MI, Schattner M. Endothelial cell function alteration after Junin virus infection. Thrombosis and haemostasis. 2003;90(2):326-33. doi: 10.1267/THRO03020326. PubMed PMID: 12888881.
88. Lukashevich IS, Maryankova R, Vladyko AS, Nashkevich N, Koleda S, Djavani M, Horejsh D, Voitenok NN, Salvato MS. Lassa and mopeia virus replication in human monocytes/macrophages and in endothelial cells: Different effects on IL-8 and TNF-α gene expression. Journal of Medical Virology. 1999;59(4):552-60. doi: 10.1002/(SICI)1096-9071(199912)59:4<552::AID-JMV21>3.0.CO;2-A.
89. Oldstone MB, Sinha YN, Blount P, Tishon A, Rodriguez M, von Wedel R, Lampert PW. Virus-induced alterations in homeostasis: alteration in differentiated functions of infected cells in vivo. Science. 1982;218(4577):1125-7. PubMed PMID: 7146898.
90. de la Torre JC, Oldstone MB. Selective disruption of growth hormone transcription machinery by viral infection. Proceedings of the National Academy of Sciences. 1992;89(20):9939-43. doi: 10.1073/pnas.89.20.9939.
91. Yun NE, Linde NS, Dziuba N, Zacks MA, Smith JN, Smith JK, Aronson JF, Chumakova OV, Lander HM, Peters CJ, Paessler S. Pathogenesis of XJ and Romero Strains of Junin Virus in Two Strains of Guinea Pigs. The American Journal of Tropical Medicine and Hygiene. 2008;79(2):275-82.

92. Mahanty S, Hutchinson K, Agarwal S, Mcrae M, Rollin PE, Pulendran B. Cutting Edge: Impairment of Dendritic Cells and Adaptive Immunity by Ebola and Lassa Viruses. The Journal of Immunology. 2003;170(6):2797-801.
93. Ahmed R, Jamieson BD, Porter DD. Immune therapy of a persistent and disseminated viral infection. J Virol. 1987;61(12):3920-9. PubMed PMID: 3682061; PubMed Central PMCID: PMC256011.
94. Enria DA, Briggiler AM, Sanchez Z. Treatment of Argentine hemorrhagic fever. Antiviral Res. 2008;78(1):132-9. doi: 10.1016/j.antiviral.2007.10.010. PubMed PMID: 18054395.
95. Maiztegui JI, Fernandez NJ, de Damilano AJ. [Reduction in the mortality of American hemorrhagic fever (AHF) during treatment with immune serums]. Medicina. 1978;38(6 Pt 1):743. PubMed PMID: 750869.
96. Kenyon RH, Peters CJ. Actions of complement on Junin virus. Rev Infect Dis. 1989;11 Suppl 4:S771-6. PubMed PMID: 2546249.
97. Peters CJ. Lymphocytic Choriomeningitis Virus — An Old Enemy up to New Tricks. New England Journal of Medicine. 2006;354(21):2208-11. doi: doi:10.1056/NEJMp068021. PubMed PMID: 16723613.
98. Peters CJ. Lymphocytic choriomeningitis virus, Lassa Virus, and the South American Hemorrhagic Fevers. In: Mandell D, Bennett, editor. Principles and Practice of Infectious Diseases 6th ed. New York, NY: Churchill Livingstone; 2005. p. 2090-6.
99. Cunha B. Meningitis. In: Schlossberg D, editor. Central Nervous System Infections. New York, NY: Springer-Verlag; 1990.
100. Jr MK. Hemorrhagic fever virus. Infectious Diseases 2nd ed. Philadelphia, Pa: Saunders Co; 1998. p. 2249-65.
101. Bausch DG, Demby AH, Coulibaly M, Kanu J, Goba A, Bah A, Conde N, Wurtzel HL, Cavallaro KF, Lloyd E, Baldet FB, Cisse SD, Fofona D, Savane IK, Tolno RT, Mahy B, Wagoner KD, Ksiazek TG, Peters CJ, Rollin PE. Lassa fever in Guinea: I. Epidemiology of human disease and clinical observations. Vector borne and zoonotic diseases. 2001;1(4):269-81. PubMed PMID: 12653127.
102. Macher AM, Wolfe MS. Historical Lassa fever reports and 30-year clinical update. Emerging infectious diseases. 2006;12(5):835-7. doi: 10.3201/eid1205.050052. PubMed PMID: 16704848; PubMed Central PMCID: PMC3374442.
103. Sefing EJ, Wong MH, Larson DP, Hurst BL, Van Wettere AJ, Schneller SW, Gowen BB. Vascular leak ensues a vigorous proinflammatory cytokine response to Tacaribe arenavirus infection in AG129 mice. Virology journal. 2013;10:221. doi: 10.1186/1743-422X-10-221. PubMed PMID: 23816343; PubMed Central PMCID: PMC3707785.
104. Kunz S. The role of the vascular endothelium in arenavirus haemorrhagic fevers. Thrombosis and haemostasis. 2009;102(6):1024-9. doi: 10.1160/TH09-06-0357. PubMed PMID: 19967131.
105. Gómez RM, Jaquenod de Giusti C, Sanchez Vallduvi MM, Frik J, Ferrer MF, Schattner M. Junín virus. A XXI century update. Microbes and Infection. 2011;13(4):303-11. doi: http://dx.doi.org/10.1016/j.micinf.2010.12.006.
106. Maiztegui J, Feuillade M, Briggiler A. Progressive extension of the endemic area and changing incidence of Argentine Hemorrhagic Fever. Med Microbiol Immunol. 1986;175(2-3):149-52. PubMed PMID: 3014288.
107. Carballal G, Videla CM, Merani MS. Epidemiology of Argentine Hemorrhagic Fever. European Journal of Epidemiology. 1988;4(2):259-74. doi: 10.2307/3520710.

108. Lozano ME, Enria D, Maiztegui JI, Grau O, Romanowski V. Rapid diagnosis of Argentine hemorrhagic fever by reverse transcriptase PCR-based assay. Journal of clinical microbiology. 1995;33(5):1327-32. PubMed PMID: 7542268; PubMed Central PMCID: PMC228155.
109. Paris-Robidas S, Emond V, Tremblay C, Soulet D, Calon F. In Vivo Labeling of Brain Capillary Endothelial Cells after Intravenous Injection of Monoclonal Antibodies Targeting the Transferrin Receptor. Molecular Pharmacology. 2011;80(1):32-9. doi: 10.1124/mol.111.071027.
110. Andrews BS, Theofilopoulos AN, Peters CJ, Loskutoff DJ, Brandt WE, Dixon FJ. Replication of dengue and junin viruses in cultured rabbit and human endothelial cells. Infection and Immunity. 1978;20(3):776-81.
111. Ruggiero HA, Perez Isquierdo F, Milani HA, Barri A, Val A, Maglio F, Astarloa L, Gonzalez Cambaceres C, Milani HL, Tallone JC. [Treatment of Argentine hemorrhagic fever with convalescent's plasma. 4433 cases]. Presse medicale. 1986;15(45):2239-42. PubMed PMID: 2949253.
112. Moreno H, Grande-Pérez A, Domingo E, Martín V. Arenaviruses and Lethal Mutagenesis. Prospects for New Ribavirin-based Interventions. Viruses. 2012;4(11):2786-805. PubMed PMID: doi:10.3390/v4112786.
113. Salazar M, Yun NE, Poussard AL, Smith JN, Smith JK, Kolokoltsova OA, Patterson MJ, Linde J, Paessler S. Effect of Ribavirin on Junin Virus Infection in Guinea Pigs. Zoonoses and Public Health. 2012;59(4):278-85. doi: 10.1111/j.1863-2378.2011.01447.x.
114. Maiztegui JI, McKee KT, Oro JGB, Harrison LH, Gibbs PH, Feuillade MR, Enria DA, Briggiler AM, Levis SC, Ambrosio AM, Halsey NA, Peters CJ, Group tAS. Protective Efficacy of a Live Attenuated Vaccine against Argentine Hemorrhagic Fever. Journal of Infectious Diseases. 1998;177(2):277-83. doi: 10.1086/514211.
115. Enria DA, Oro JGB. Junin Virus Vaccines. In: Oldstone MA, editor. Arenaviruses II: Springer Berlin Heidelberg; 2002. p. 239-61.
116. Barrera Oro JG, McKee KT, Jr. Toward a vaccine against Argentine hemorrhagic fever. Bulletin of the Pan American Health Organization. 1991;25(2):118-26. PubMed PMID: 1654168.
117. Candurra NA, Damonte EB, Coto CE. Antigenic relationships between attenuated and pathogenic strains of Junin virus. J Med Virol. 1989;27(2):145-50. PubMed PMID: 2466103.
118. Ruggiero HA, Magnoni C, de Guerrero LB, Milani HA, Izquierdo FP, Milani HL, Weber EL. Immunogenicity of A/USSR (H1N1) subunit vaccine in unprimed young adults. J Med Virol. 1981;7(3):227-32. PubMed PMID: 6270279.
119. de Guerrero LB, Boxaca MC, Malumbres E, Dejean C, Caruso E. Early protection to Junin virus of guinea pig with an attenuated Junin virus strain. Acta virologica. 1985;29(4):334-7. PubMed PMID: 2413752.
120. Albarino CG, Ghiringhelli PD, Posik DM, Lozano ME, Ambrosio AM, Sanchez A, Romanowski V. Molecular characterization of attenuated Junin virus strains. The Journal of general virology. 1997;78 (Pt 7):1605-10. PubMed PMID: 9225036.
121. Enria DA, Ambrosio AM, Briggiler AM, Feuillade MR, Crivelli E, Study Group on Argentine Hemorrhagic Fever V. [Candid#1 vaccine against Argentine hemorrhagic fever produced in Argentina. Immunogenicity and safety]. Medicina. 2010;70(3):215-22. PubMed PMID: 20529769.
122. Enria DA, Barrera Oro JG. Junin virus vaccines. Current topics in microbiology and immunology. 2002;263:239-61. PubMed PMID: 11987817.
123. Gamboa GS, Ambrosio AM, Maiza AS, Mariani M, Rodrigues Garcia Armoa G, Saavedra Mdel C. [Phenotypic markers of attenuation in Junin virus strains recently isolated from

individuals vaccinated with Junin Candid#1 strain]. Medicina. 2013;73(4):303-9. PubMed PMID: 23924527.
124. Droniou-Bonzom ME, Reignier T, Oldenburg JE, Cox AU, Exline CM, Rathbun JY, Cannon PM. Substitutions in the Glycoprotein (GP) of the Candid#1 Vaccine Strain of Junin Virus Increase Dependence on Human Transferrin Receptor 1 for Entry and Destabilize the Metastable Conformation of GP. Journal of Virology. 2011;85(24):13457-62. doi: 10.1128/jvi.05616-11.
125. Ambrosio AM, Riera LM, Saavedra Mdel C, Sabattini MS. Immune response to vaccination against Argentine hemorrhagic Fever in an area where different arenaviruses coexist. Viral immunology. 2006;19(2):196-201. doi: 10.1089/vim.2006.19.196. PubMed PMID: 16817762.
126. Peters C.J. BM, Rollin Pierre E., Ksiazek Thomas G. Arenaviruses. In: Fields Bernard N. KDM, Howley Peter M, editor. Field's Virology Third Edition1996. p. 1521 - 51.
127. Kilgore PE, Peters CJ, Mills JN, Rollin PE, Armstrong L, Khan AS, Ksiazek TG. Prospects for the control of Bolivian hemorrhagic fever. Emerging infectious diseases. 1995;1(3):97-100. doi: 10.3201/eid0103.950308. PubMed PMID: 8903174; PubMed Central PMCID: PMC2626873.
128. Vieth S, Torda AE, Asper M, Schmitz H, Günther S. Sequence analysis of L RNA of Lassa virus. Virology. 2004;318(1):153-68. doi: http://dx.doi.org/10.1016/j.virol.2003.09.009.
129. Goñi S, Iserte J, Stephan B, Borio C, Ghiringhelli P, Lozano M. Molecular analysis of the virulence attenuation process in Junín virus vaccine genealogy. Virus Genes. 2010;40(3):320-8. doi: 10.1007/s11262-010-0450-2.
130. Chiu J-J, Chien S. Effects of Disturbed Flow on Vascular Endothelium: Pathophysiological Basis and Clinical Perspectives. Physiological Reviews. 2011;91(1):327-87. doi: 10.1152/physrev.00047.2009.
131. Vita JA. Endothelial Function. Circulation. 2011;124(25):e906-e12. doi: 10.1161/circulationaha.111.078824.
132. Deanfield JE, Halcox JP, Rabelink TJ. Endothelial Function and Dysfunction: Testing and Clinical Relevance. Circulation. 2007;115(10):1285-95. doi: 10.1161/circulationaha.106.652859.
133. Rubin LL, Staddon JM. The cell biology of the blood-brain barrier. Annual review of neuroscience. 1999;22:11-28. doi: 10.1146/annurev.neuro.22.1.11. PubMed PMID: 10202530.
134. Smith Q. A Review of Blood-Brain Barrier Transport Techniques. In: Nag S, editor. The Blood-Brain Barrier: Humana Press; 2003. p. 193-208.
135. Malik AB, Lynch JJ, Cooper JA. Endothelial barrier function. The Journal of investigative dermatology. 1989;93(2 Suppl):62S-7S. PubMed PMID: 2546995.
136. Folkman J. Angiogenesis. Annual review of medicine. 2006;57:1-18. doi: 10.1146/annurev.med.57.121304.131306. PubMed PMID: 16409133.
137. Risau W, Flamme I. Vasculogenesis. Annual review of cell and developmental biology. 1995;11:73-91. doi: 10.1146/annurev.cb.11.110195.000445. PubMed PMID: 8689573.
138. Chung AS, Ferrara N. Developmental and pathological angiogenesis. Annual review of cell and developmental biology. 2011;27:563-84. doi: 10.1146/annurev-cellbio-092910-154002. PubMed PMID: 21756109.
139. Folkman J. Angiogenesis in cancer, vascular, rheumatoid and other disease. Nature medicine. 1995;1(1):27-31. PubMed PMID: 7584949.
140. Folkman J. The influence of angiogenesis research on management of patients with breast cancer. Breast cancer research and treatment. 1995;36(2):109-18. PubMed PMID: 8534860.
141. Kerbel R, Folkman J. Clinical translation of angiogenesis inhibitors. Nature reviews Cancer. 2002;2(10):727-39. doi: 10.1038/nrc905. PubMed PMID: 12360276.

142. Rajkumar SV, Witzig TE. A review of angiogenesis and antiangiogenic therapy with thalidomide in multiple myeloma. Cancer Treatment Reviews. 2000;26(5):351-62. doi: http://dx.doi.org/10.1053/ctrv.2000.0188.
143. Burri PH, Hlushchuk R, Djonov V. Intussusceptive angiogenesis: Its emergence, its characteristics, and its significance. Developmental Dynamics. 2004;231(3):474-88. doi: 10.1002/dvdy.20184.
144. Xie Z, Ghosh CC, Patel R, Iwaki S, Gaskins D, Nelson C, Jones N, Greipp PR, Parikh SM, Druey KM. Vascular endothelial hyperpermeability induces the clinical symptoms of Clarkson disease (the systemic capillary leak syndrome). Blood. 2012;119(18):4321-32. doi: 10.1182/blood-2011-08-375816.
145. Lee WL, Slutsky AS. Sepsis and endothelial permeability. The New England journal of medicine. 2010;363(7):689-91. doi: 10.1056/NEJMcibr1007320. PubMed PMID: 20818861.
146. Weis S, Shintani S, Weber A, Kirchmair R, Wood M, Cravens A, McSharry H, Iwakura A, Yoon Y-s, Himes N, Burstein D, Doukas J, Soll R, Losordo D, Cheresh D. Src blockade stabilizes a Flk/cadherin complex, reducing edema and tissue injury following myocardial infarction. The Journal of Clinical Investigation. 2004;113(6):885-94. doi: 10.1172/JCI20702.
147. Weis SM, Cheresh DA. Pathophysiological consequences of VEGF-induced vascular permeability. Nature. 2005;437(7058):497-504. doi: 10.1038/nature03987. PubMed PMID: 16177780.
148. Dejana E, Orsenigo F. Endothelial adherens junctions at a glance. Journal of Cell Science. 2013;126(12):2545-9. doi: 10.1242/jcs.124529.
149. Dejana E. Endothelial cell-cell junctions: happy together. Nature reviews Molecular cell biology. 2004;5(4):261-70. doi: 10.1038/nrm1357. PubMed PMID: 15071551.
150. Harris TJ, Tepass U. Adherens junctions: from molecules to morphogenesis. Nature reviews Molecular cell biology. 2010;11(7):502-14. doi: 10.1038/nrm2927. PubMed PMID: 20571587.
151. Dejana E, Giampietro C. Vascular endothelial-cadherin and vascular stability. Current opinion in hematology. 2012;19(3):218-23. doi: 10.1097/MOH.0b013e3283523e1c. PubMed PMID: 22395663.
152. Vestweber D. Relevance of endothelial junctions in leukocyte extravasation and vascular permeability. Annals of the New York Academy of Sciences. 2012;1257(1):184-92. doi: 10.1111/j.1749-6632.2012.06558.x.
153. Williams MR, Azcutia V, Newton G, Alcaide P, Luscinskas FW. Emerging mechanisms of neutrophil recruitment across endothelium. Trends in Immunology. 2011;32(10):461-9. doi: http://dx.doi.org/10.1016/j.it.2011.06.009.
154. Hebda JK, Leclair HM, Azzi S, Roussel C, Scott MG, Bidere N, Gavard J. The C-terminus region of beta-arrestin1 modulates VE-cadherin expression and endothelial cell permeability. Cell communication and signaling : CCS. 2013;11(1):37. doi: 10.1186/1478-811X-11-37. PubMed PMID: 23714586; PubMed Central PMCID: PMC3669046.
155. Mehta D, Malik AB. Signaling mechanisms regulating endothelial permeability. Physiol Rev. 2006;86(1):279-367. doi: 10.1152/physrev.00012.2005. PubMed PMID: 16371600.
156. Roberts WG, Palade GE. Increased microvascular permeability and endothelial fenestration induced by vascular endothelial growth factor. Journal of Cell Science. 1995;108(6):2369-79.

157. Dejana E, Orsenigo F, Lampugnani MG. The role of adherens junctions and VE-cadherin in the control of vascular permeability. Journal of Cell Science. 2008;121(13):2115-22. doi: 10.1242/jcs.017897.
158. Carman CV, Sage PT, Sciuto TE, de la Fuente MA, Geha RS, Ochs Hans D, Dvorak HF, Dvorak AM, Springer TA. Transcellular Diapedesis Is Initiated by Invasive Podosomes. Immunity. 2007;26(6):784-97. doi: http://dx.doi.org/10.1016/j.immuni.2007.04.015.
159. Engelhardt B, Wolburg H. Mini-review: Transendothelial migration of leukocytes: through the front door or around the side of the house? European Journal of Immunology. 2004;34(11):2955-63. doi: 10.1002/eji.200425327.
160. Millan J, Hewlett L, Glyn M, Toomre D, Clark P, Ridley AJ. Lymphocyte transcellular migration occurs through recruitment of endothelial ICAM-1 to caveola- and F-actin-rich domains. Nature cell biology. 2006;8(2):113-23. doi: 10.1038/ncb1356. PubMed PMID: 16429128.
161. Muller WA. Leukocyte–endothelial-cell interactions in leukocyte transmigration and the inflammatory response. Trends in Immunology. 2003;24(6):326-33. doi: http://dx.doi.org/10.1016/S1471-4906(03)00117-0.
162. Vestweber D. Adhesion and signaling molecules controlling the transmigration of leukocytes through endothelium. Immunological Reviews. 2007;218(1):178-96. doi: 10.1111/j.1600-065X.2007.00533.x.
163. Andriopoulou P, Navarro P, Zanetti A, Lampugnani MG, Dejana E. Histamine Induces Tyrosine Phosphorylation of Endothelial Cell-to-Cell Adherens Junctions. Arteriosclerosis, Thrombosis, and Vascular Biology. 1999;19(10):2286-97. doi: 10.1161/01.atv.19.10.2286.
164. Tolstanova G, Deng X, French SW, Lungo W, Paunovic B, Khomenko T, Ahluwalia A, Kaplan T, Dacosta-Iyer M, Tarnawski A, Szabo S, Sandor Z. Early endothelial damage and increased colonic vascular permeability in the development of experimental ulcerative colitis in rats and mice. Laboratory investigation; a journal of technical methods and pathology. 2012;92(1):9-21. doi: 10.1038/labinvest.2011.122. PubMed PMID: 21894149.
165. Bazzoni G, Dejana E. Endothelial Cell-to-Cell Junctions: Molecular Organization and Role in Vascular Homeostasis. Physiological Reviews. 2004;84(3):869-901. doi: 10.1152/physrev.00035.2003.
166. Wallez Y, Huber P. Endothelial adherens and tight junctions in vascular homeostasis, inflammation and angiogenesis. Biochimica et Biophysica Acta (BBA) - Biomembranes. 2008;1778(3):794-809. doi: http://dx.doi.org/10.1016/j.bbamem.2007.09.003.
167. Ivanov D, Philippova M, Antropova J, Gubaeva F, Iljinskaya O, Tararak E, Bochkov V, Erne P, Resink T, Tkachuk V. Expression of cell adhesion molecule T-cadherin in the human vasculature. Histochemistry and cell biology. 2001;115(3):231-42. PubMed PMID: 11326751.
168. Weis WI, Nelson WJ. Re-solving the Cadherin-Catenin-Actin Conundrum. Journal of Biological Chemistry. 2006;281(47):35593-7. doi: 10.1074/jbc.R600027200.
169. Navarro P, Caveda L, Breviario F, Mândoteanu I, Lampugnani M-G, Dejana E. Catenin-dependent and -independent Functions of Vascular Endothelial Cadherin. Journal of Biological Chemistry. 1995;270(52):30965-72. doi: 10.1074/jbc.270.52.30965.
170. Carmeliet P, Lampugnani M-G, Moons L, Breviario F, Compernolle V, Bono F, Balconi G, Spagnuolo R, Oosthuyse B, Dewerchin M, Zanetti A, Angellilo A, Mattot V, Nuyens D, Lutgens E, Clotman F, de Ruiter MC, Gittenberger-de Groot A, Poelmann R, Lupu F, Herbert J-M, Collen D, Dejana E. Targeted Deficiency or Cytosolic Truncation of the VE-cadherin Gene in Mice Impairs VEGF-Mediated Endothelial Survival and Angiogenesis. Cell. 1999;98(2):147-57. doi: http://dx.doi.org/10.1016/S0092-8674(00)81010-7.

171. Corada M, Mariotti M, Thurston G, Smith K, Kunkel R, Brockhaus M, Lampugnani MG, Martin-Padura I, Stoppacciaro A, Ruco L, McDonald DM, Ward PA, Dejana E. Vascular endothelial–cadherin is an important determinant of microvascular integrity in vivo. Proceedings of the National Academy of Sciences. 1999;96(17):9815-20. doi: 10.1073/pnas.96.17.9815.
172. Navarro P, Ruco L, Dejana E. Differential Localization of VE- and N-Cadherins in Human Endothelial Cells: VE-Cadherin Competes with N-Cadherin for Junctional Localization. The Journal of Cell Biology. 1998;140(6):1475-84. doi: 10.1083/jcb.140.6.1475.
173. Gerhardt H, Wolburg H, Redies C. N-cadherin mediates pericytic-endothelial interaction during brain angiogenesis in the chicken. Developmental Dynamics. 2000;218(3):472-9. doi: 10.1002/1097-0177(200007)218:3<472::AID-DVDY1008>3.0.CO;2-#.
174. Paik J-H, Skoura A, Chae S-S, Cowan AE, Han DK, Proia RL, Hla T. Sphingosine 1-phosphate receptor regulation of N-cadherin mediates vascular stabilization. Genes & Development. 2004;18(19):2392-403. doi: 10.1101/gad.1227804.
175. Luo Y, Radice GL. N-cadherin acts upstream of VE-cadherin in controlling vascular morphogenesis. J Cell Biol. 2005;169(1):29-34. doi: 10.1083/jcb.200411127. PubMed PMID: 15809310; PubMed Central PMCID: PMC2171890.
176. Cattelino A, Liebner S, Gallini R, Zanetti A, Balconi G, Corsi A, Bianco P, Wolburg H, Moore R, Oreda B, Kemler R, Dejana E. The conditional inactivation of the β-catenin gene in endothelial cells causes a defective vascular pattern and increased vascular fragility. The Journal of Cell Biology. 2003;162(6):1111-22. doi: 10.1083/jcb.200212157.
177. Shasby DM, Ries DR, Shasby SS, Winter MC. Histamine stimulates phosphorylation of adherens junction proteins and alters their link to vimentin. American Journal of Physiology - Lung Cellular and Molecular Physiology. 2002;282(6):L1330-L8. doi: 10.1152/ajplung.00329.2001.
178. Angelini DJ, Hyun S-W, Grigoryev DN, Garg P, Gong P, Singh IS, Passaniti A, Hasday JD, Goldblum SE. TNF-α increases tyrosine phosphorylation of vascular endothelial cadherin and opens the paracellular pathway through fyn activation in human lung endothelia. American Journal of Physiology - Lung Cellular and Molecular Physiology. 2006;291(6):L1232-L45. doi: 10.1152/ajplung.00109.2006.
179. Hudry-Clergeon H, Stengel D, Ninio E, Vilgrain I. Platelet-activating factor increases VE-cadherin tyrosine phosphorylation in mouse endothelial cells and its association with the PtdIns3′-kinase. The FASEB Journal. 2005;19(6):512-20. doi: 10.1096/fj.04-2202com.
180. Esser S, Lampugnani MG, Corada M, Dejana E, Risau W. Vascular endothelial growth factor induces VE-cadherin tyrosine phosphorylation in endothelial cells. Journal of Cell Science. 1998;111(13):1853-65.
181. Lampugnani MG, Corada M, Andriopoulou P, Esser S, Risau W, Dejana E. Cell confluence regulates tyrosine phosphorylation of adherens junction components in endothelial cells. Journal of Cell Science. 1997;110(17):2065-77.
182. Allingham MJ, van Buul JD, Burridge K. ICAM-1-Mediated, Src- and Pyk2-Dependent Vascular Endothelial Cadherin Tyrosine Phosphorylation Is Required for Leukocyte Transendothelial Migration. The Journal of Immunology. 2007;179(6):4053-64.
183. Turowski P, Martinelli R, Crawford R, Wateridge D, Papageorgiou A-P, Lampugnani MG, Gamp AC, Vestweber D, Adamson P, Dejana E, Greenwood J. Phosphorylation of vascular endothelial cadherin controls lymphocyte emigration. Journal of Cell Science. 2008;121(1):29-37. doi: 10.1242/jcs.022681.
184. Orsenigo F, Giampietro C, Ferrari A, Corada M, Galaup A, Sigismund S, Ristagno G, Maddaluno L, Koh GY, Franco D, Kurtcuoglu V, Poulikakos D, Baluk P, McDonald D, Grazia

Lampugnani M, Dejana E. Phosphorylation of VE-cadherin is modulated by haemodynamic forces and contributes to the regulation of vascular permeability in vivo. Nature communications. 2012;3:1208. doi: 10.1038/ncomms2199. PubMed PMID: 23169049; PubMed Central PMCID: PMC3514492.
185. Baumeister U, Funke R, Ebnet K, Vorschmitt H, Koch S, Vestweber D. Association of Csk to VE-cadherin and inhibition of cell proliferation. The EMBO journal. 2005;24(9):1686-95. doi: 10.1038/sj.emboj.7600647. PubMed PMID: 15861137; PubMed Central PMCID: PMC1142580.
186. Nawroth R, Poell G, Ranft A, Kloep S, Samulowitz U, Fachinger G, Golding M, Shima DT, Deutsch U, Vestweber D. VE-PTP and VE-cadherin ectodomains interact to facilitate regulation of phosphorylation and cell contacts. The EMBO journal. 2002;21(18):4885-95. PubMed PMID: 12234928; PubMed Central PMCID: PMC126293.
187. Bäumer S, Keller L, Holtmann A, Funke R, August B, Gamp A, Wolburg H, Wolburg-Buchholz K, Deutsch U, Vestweber D. Vascular endothelial cell–specific phosphotyrosine phosphatase (VE-PTP) activity is required for blood vessel development. Blood. 2006;107(12):4754-62. doi: 10.1182/blood-2006-01-0141.
188. Lampugnani MG, Zanetti A, Corada M, Takahashi T, Balconi G, Breviario F, Orsenigo F, Cattelino A, Kemler R, Daniel TO, Dejana E. Contact inhibition of VEGF-induced proliferation requires vascular endothelial cadherin, β-catenin, and the phosphatase DEP-1/CD148. The Journal of Cell Biology. 2003;161(4):793-804. doi: 10.1083/jcb.200209019.
189. Sui XF, Kiser TD, Hyun SW, Angelini DJ, Del Vecchio RL, Young BA, Hasday JD, Romer LH, Passaniti A, Tonks NK, Goldblum SE. Receptor Protein Tyrosine Phosphatase μ Regulates the Paracellular Pathway in Human Lung Microvascular Endothelia. The American Journal of Pathology. 2005;166(4):1247-58. doi: http://dx.doi.org/10.1016/S0002-9440(10)62343-7.
190. Ukropec JA, Hollinger MK, Salva SM, Woolkalis MJ. SHP2 Association with VE-Cadherin Complexes in Human Endothelial Cells Is Regulated by Thrombin. Journal of Biological Chemistry. 2000;275(8):5983-6. doi: 10.1074/jbc.275.8.5983.
191. Potter MD, Barbero S, Cheresh DA. Tyrosine Phosphorylation of VE-cadherin Prevents Binding of p120- and β-Catenin and Maintains the Cellular Mesenchymal State. Journal of Biological Chemistry. 2005;280(36):31906-12. doi: 10.1074/jbc.M505568200.
192. Wallez Y, Cand F, Cruzalegui F, Wernstedt C, Souchelnytskyi S, Vilgrain I, Huber P. Src kinase phosphorylates vascular endothelial-cadherin in response to vascular endothelial growth factor: identification of tyrosine 685 as the unique target site. Oncogene. 2007;26(7):1067-77. doi: 10.1038/sj.onc.1209855. PubMed PMID: 16909109.
193. Huber AH, Weis WI. The Structure of the β-Catenin/E-Cadherin Complex and the Molecular Basis of Diverse Ligand Recognition by β-Catenin. Cell. 2001;105(3):391-402. doi: http://dx.doi.org/10.1016/S0092-8674(01)00330-0.
194. Lilien J, Balsamo J. The regulation of cadherin-mediated adhesion by tyrosine phosphorylation/dephosphorylation of β-catenin. Current Opinion in Cell Biology. 2005;17(5):459-65. doi: http://dx.doi.org/10.1016/j.ceb.2005.08.009.
195. Xiao K, Garner J, Buckley KM, Vincent PA, Chiasson CM, Dejana E, Faundez V, Kowalczyk AP. p120-Catenin Regulates Clathrin-dependent Endocytosis of VE-Cadherin. Molecular Biology of the Cell. 2005;16(11):5141-51. doi: 10.1091/mbc.E05-05-0440.
196. Alcaide P, Martinelli R, Newton G, Williams MR, Adam A, Vincent PA, Luscinskas FW. p120-Catenin prevents neutrophil transmigration independently of RhoA inhibition by impairing Src dependent VE-cadherin phosphorylation. American Journal of Physiology - Cell Physiolog. 2012;303(4):C385-C95. doi: 10.1152/ajpcell.00126.2012.

197. Gavard J, Gutkind JS. VEGF controls endothelial-cell permeability by promoting the beta-arrestin-dependent endocytosis of VE-cadherin. Nature cell biology. 2006;8(11):1223-34. doi: 10.1038/ncb1486. PubMed PMID: 17060906.
198. Herren B, Levkau B, Raines EW, Ross R. Cleavage of β-Catenin and Plakoglobin and Shedding of VE-Cadherin during Endothelial Apoptosis: Evidence for a Role for Caspases and Metalloproteinases. Molecular Biology of the Cell. 1998;9(6):1589-601. doi: 10.1091/mbc.9.6.1589.
199. Luplertlop N, Misse D, Bray D, Deleuze V, Gonzalez JP, Leardkamolkarn V, Yssel H, Veas F. Dengue-virus-infected dendritic cells trigger vascular leakage through metalloproteinase overproduction. EMBO reports. 2006;7(11):1176-81. doi: 10.1038/sj.embor.7400814. PubMed PMID: 17028575; PubMed Central PMCID: PMC1679776.
200. Lampugnani MG, Resnati M, Raiteri M, Pigott R, Pisacane A, Houen G, Ruco LP, Dejana E. A novel endothelial-specific membrane protein is a marker of cell-cell contacts. The Journal of Cell Biology. 1992;118(6):1511-22. doi: 10.1083/jcb.118.6.1511.
201. Xiao K, Allison DF, Kottke MD, Summers S, Sorescu GP, Faundez V, Kowalczyk AP. Mechanisms of VE-cadherin Processing and Degradation in Microvascular Endothelial Cells. Journal of Biological Chemistry. 2003;278(21):19199-208. doi: 10.1074/jbc.M211746200.
202. Miaczynska M, Pelkmans L, Zerial M. Not just a sink: endosomes in control of signal transduction. Current Opinion in Cell Biology. 2004;16(4):400-6. doi: http://dx.doi.org/10.1016/j.ceb.2004.06.005.
203. Lampugnani MG, Orsenigo F, Gagliani MC, Tacchetti C, Dejana E. Vascular endothelial cadherin controls VEGFR-2 internalization and signaling from intracellular compartments. The Journal of Cell Biology. 2006;174(4):593-604. doi: 10.1083/jcb.200602080.
204. Eliceiri BP, Paul R, Schwartzberg PL, Hood JD, Leng J, Cheresh DA. Selective Requirement for Src Kinases during VEGF-Induced Angiogenesis and Vascular Permeability. Molecular Cell. 1999;4(6):915-24. doi: http://dx.doi.org/10.1016/S1097-2765(00)80221-X.
205. Allport JR, Ding H, Collins T, Gerritsen ME, Luscinskas FW. Endothelial-dependent Mechanisms Regulate Leukocyte Transmigration: A Process Involving the Proteasome and Disruption of the Vascular Endothelial–Cadherin Complex at Endothelial Cell-to-Cell Junctions. The Journal of Experimental Medicine. 1997;186(4):517-27. doi: 10.1084/jem.186.4.517.
206. Newman PJ. The biology of PECAM-1. J Clin Invest. 1997;100(11 Suppl):S25-9. PubMed PMID: 9413397.
207. Klavinskis LS, Oldstone MB. Lymphocytic choriomeningitis virus selectively alters differentiated but not housekeeping functions: block in expression of growth hormone gene is at the level of transcriptional initiation. Virology. 1989;168(2):232-5. PubMed PMID: 2916325.
208. Bureau JF, Le Goff S, Thomas D, Parlow AF, de la Torre JC, Homann D, Brahic M, Oldstone MB. Disruption of differentiated functions during viral infection in vivo. V. Mapping of a locus involved in susceptibility of mice to growth hormone deficiency due to persistent lymphocytic choriomeningitis virus infection. Virology. 2001;281(1):61-6. doi: 10.1006/viro.2000.0800. PubMed PMID: 11222096.
209. Candurra NA, Lago MJ, Maskin L, Damonte EB. Involvement of the cytoskeleton in Junin virus multiplication. The Journal of general virology. 1999;80 (Pt 1):147-56. PubMed PMID: 9934697.
210. Martinez MG, Cordo SM, Candurra NA. Involvement of cytoskeleton in Junin virus entry. Virus Res. 2008;138(1-2):17-25. doi: 10.1016/j.virusres.2008.08.004. PubMed PMID: 18789362.

211. Stairs DB, Bayne LJ, Rhoades B, Vega ME, Waldron TJ, Kalabis J, Klein-Szanto A, Lee JS, Katz JP, Diehl JA, Reynolds AB, Vonderheide RH, Rustgi AK. Deletion of p120-catenin results in a tumor microenvironment with inflammation and cancer that establishes it as a tumor suppressor gene. Cancer Cell.19(4):470-83. Epub 2011/04/13. doi: S1535-6108(11)00083-3 [pii]

10.1016/j.ccr.2011.02.007. PubMed PMID: 21481789; PubMed Central PMCID: PMC3077713.
212. Herron CR, Lowery AM, Hollister PR, Reynolds AB, Vincent PA. p120 regulates endothelial permeability independently of its NH2 terminus and Rho binding. American journal of physiology Heart and circulatory physiology.300(1):H36-48. Epub 2010/10/26. doi: ajpheart.00812.2010 [pii]

10.1152/ajpheart.00812.2010. PubMed PMID: 20971762; PubMed Central PMCID: PMC3023255.
213. Wright TJ, Leach L, Shaw PE, Jones P. Dynamics of vascular endothelial-cadherin and beta-catenin localization by vascular endothelial growth factor-induced angiogenesis in human umbilical vein cells. Exp Cell Res. 2002;280(2):159-68. Epub 2002/11/05. doi: S0014482702956363 [pii]. PubMed PMID: 12413882.
214. Dejana E, Lampugnani MG, Martinez-Estrada O, Bazzoni G. The molecular organization of endothelial junctions and their functional role in vascular morphogenesis and permeability. Int J Dev Biol. 2000;44(6):743-8. Epub 2000/11/04. PubMed PMID: 11061439.
215. Hossain MA, Russell JC, Miknyoczki S, Ruggeri B, Lal B, Laterra J. Vascular endothelial growth factor mediates vasogenic edema in acute lead encephalopathy. Annals of neurology. 2004;55(5):660-7. doi: 10.1002/ana.20065. PubMed PMID: 15122706.
216. Angelini DJ, Hyun SW, Grigoryev DN, Garg P, Gong P, Singh IS, Passaniti A, Hasday JD, Goldblum SE. TNF-alpha increases tyrosine phosphorylation of vascular endothelial cadherin and opens the paracellular pathway through fyn activation in human lung endothelia. American journal of physiology Lung cellular and molecular physiology. 2006;291(6):L1232-45. doi: 10.1152/ajplung.00109.2006. PubMed PMID: 16891393.
217. Cheung LW, Leung PC, Wong AS. Cadherin switching and activation of p120 catenin signaling are mediators of gonadotropin-releasing hormone to promote tumor cell migration and invasion in ovarian cancer. Oncogene. 2010;29(16):2427-40. doi: 10.1038/onc.2009.523. PubMed PMID: 20118984.
218. Gorbunova E, Gavrilovskaya IN, Mackow ER. Pathogenic hantaviruses Andes virus and Hantaan virus induce adherens junction disassembly by directing vascular endothelial cadherin internalization in human endothelial cells. J Virol. 2010;84(14):7405-11. doi: 10.1128/JVI.00576-10. PubMed PMID: 20463083; PubMed Central PMCID: PMC2898267.
219. Shrivastava-Ranjan P, Rollin PE, Spiropoulou CF. Andes virus disrupts the endothelial cell barrier by induction of vascular endothelial growth factor and downregulation of VE-cadherin. J Virol. 2010;84(21):11227-34. doi: 10.1128/JVI.01405-10. PubMed PMID: 20810734; PubMed Central PMCID: PMC2953207.
220. Ferrara N. Vascular Endothelial Growth Factor: Basic Science and Clinical Progress. Endocrine Reviews. 2004;25(4):581-611. doi: 10.1210/er.2003-0027.
221. Hoeben A, Landuyt B, Highley MS, Wildiers H, Van Oosterom AT, De Bruijn EA. Vascular Endothelial Growth Factor and Angiogenesis. Pharmacological Reviews. 2004;56(4):549-80. doi: 10.1124/pr.56.4.3.
222. Bunn Jr PA, Shepherd FA, Sandler A, Le Chevalier T, Belani CP, Kosmidis PA, Scagliotti GV, Giaccone G. Ongoing and future trials of biologic therapies in lung cancer. Lung Cancer. 2003;41, Supplement 1(0):175-86. doi: http://dx.doi.org/10.1016/S0169-5002(03)00161-2.

223. Kuenen BC, Levi M, Meijers JC, Kakkar AK, van Hinsbergh VW, Kostense PJ, Pinedo HM, Hoekman K. Analysis of coagulation cascade and endothelial cell activation during inhibition of vascular endothelial growth factor/vascular endothelial growth factor receptor pathway in cancer patients. Arterioscler Thromb Vasc Biol. 2002;22(9):1500-5. PubMed PMID: 12231573.
224. Oosthuyse B, Moons L, Storkebaum E, Beck H, Nuyens D, Brusselmans K, Van Dorpe J, Hellings P, Gorselink M, Heymans S, Theilmeier G, Dewerchin M, Laudenbach V, Vermylen P, Raat H, Acker T, Vleminckx V, Van Den Bosch L, Cashman N, Fujisawa H, Drost MR, Sciot R, Bruyninckx F, Hicklin DJ, Ince C, Gressens P, Lupu F, Plate KH, Robberecht W, Herbert JM, Collen D, Carmeliet P. Deletion of the hypoxia-response element in the vascular endothelial growth factor promoter causes motor neuron degeneration. Nature genetics. 2001;28(2):131-8. doi: 10.1038/88842. PubMed PMID: 11381259.
225. Alcaide P, Newton G, Auerbach S, Sehrawat S, Mayadas TN, Golan DE, Yacono P, Vincent P, Kowalczyk A, Luscinskas FW. p120-Catenin regulates leukocyte transmigration through an effect on VE-cadherin phosphorylation. Blood. 2008;112(7):2770-9. doi: 10.1182/blood-2008-03-147181.
226. Pieters T, van Roy F, van Hengel J. Functions of p120ctn isoforms in cell-cell adhesion and intracellular signaling. Frontiers in bioscience. 2012;17:1669-94. PubMed PMID: 22201829.
227. Reynolds AB, Roczniak-Ferguson A. Emerging roles for p120-catenin in cell adhesion and cancer. Oncogene. 2004;23(48):7947-56. doi: 10.1038/sj.onc.1208161. PubMed PMID: 15489912.
228. Türler A, Schwarz NT, Türler E, Kalff JC, Bauer AJ. MCP-1 causes leukocyte recruitment and subsequently endotoxemic ileus in rat. American Journal of Physiology - Gastrointestinal and Liver Physiology. 2002;282(1):G145-G55. doi: 10.1152/ajpgi.00263.2001.
229. ter Meulen J, Sakho M, Koulemou K, Magassouba NF, Bah A, Preiser W, Daffis S, Klewitz C, Bae H-G, Niedrig M, Zeller H, Heinzel-Gutenbrunner M, Koivogui L, Kaufmann A. Activation of the Cytokine Network and Unfavorable Outcome in Patients with Yellow Fever. Journal of Infectious Diseases. 2004;190(10):1821-7. doi: 10.1086/425016.
230. Nakajima K, Matsuda T, Fujitani Y, Kojima H, Yamanaka Y, Nakae K, Takeda T, Hirano T. Signal transduction through IL-6 receptor: involvement of multiple protein kinases, stat factors, and a novel H7-sensitive pathway. Ann N Y Acad Sci. 1995;762:55-70. PubMed PMID: 7545378.
231. Bihl MP, Heinimann K, Rüdiger JJ, Eickelberg O, Perruchoud AP, Tamm M, Roth M. Identification of a Novel IL-6 Isoform Binding to the Endogenous IL-6 Receptor. American Journal of Respiratory Cell and Molecular Biology. 2002;27(1):48-56. doi: 10.1165/ajrcmb.27.1.4637.
232. Maruo N, Morita I, Shirao M, Murota S. IL-6 increases endothelial permeability in vitro. Endocrinology. 1992;131(2):710-4. PubMed PMID: 1639018.
233. Biswas P, Delfanti F, Bernasconi S, Mengozzi M, Cota M, Polentarutti N, Mantovani A, Lazzarin A, Sozzani S, Poli G. Interleukin-6 induces monocyte chemotactic protein-1 in peripheral blood mononuclear cells and in the U937 cell line. Blood. 1998;91(1):258-65. PubMed PMID: 9414293.
234. Arendt BK, Velazquez-Dones A, Tschumper RC, Howell KG, Ansell SM, Witzig TE, Jelinek DF. Interleukin 6 induces monocyte chemoattractant protein-1 expression in myeloma cells. Leukemia. 2002;16(10):2142-7. doi: 10.1038/sj.leu.2402714. PubMed PMID: 12357369.
235. Clifton DR, Rydkina E, Huyck H, Pryhuber G, Freeman RS, Silverman DJ, Sahni SK. Expression and secretion of chemotactic cytokines IL-8 and MCP-1 by human endothelial cells after Rickettsia rickettsii infection: regulation by nuclear transcription factor NF-kappaB. International journal of medical microbiology : IJMM. 2005;295(4):267-78. PubMed PMID: 16128401.

236. Lee YR, Liu MT, Lei HY, Liu CC, Wu JM, Tung YC, Lin YS, Yeh TM, Chen SH, Liu HS. MCP-1, a highly expressed chemokine in dengue haemorrhagic fever/dengue shock syndrome patients, may cause permeability change, possibly through reduced tight junctions of vascular endothelium cells. The Journal of general virology. 2006;87(Pt 12):3623-30. doi: 10.1099/vir.0.82093-0. PubMed PMID: 17098977.
237. Volk T, Hensel M, Schuster H, Kox WJ. Secretion of MCP-1 and IL-6 by cytokine stimulated production of reactive oxygen species in endothelial cells. Molecular and cellular biochemistry. 2000;206(1-2):105-12. PubMed PMID: 10839200.
238. Hebda PA, Piltcher OB, Swarts JD, Alper CM, Zeevi A, Doyle WJ. Cytokine Profiles in a Rat Model of Otitis Media With Effusion Caused by Eustachian Tube Obstruction With and Without Streptococcus pneumoniae Infection. The Laryngoscope. 2002;112(9):1657-62. doi: 10.1097/00005537-200209000-00024.
239. Rübe C, Wilfert F, Palm J, König J, Burdak-Rothkamm S, Liu L, Schuck A, Willich N, Rübe C. Irradiation Induces a Biphasic Expression of Pro-Inflammatory Cytokines in the Lung. Strahlenther Onkol. 2004;180(7):442-8. doi: 10.1007/s00066-004-1265-7.
240. Tieu BC, Lee C, Sun H, LeJeune W, Recinos A, 3rd, Ju X, Spratt H, Guo D-C, Milewicz D, Tilton RG, Brasier AR. An adventitial IL-6/MCP1 amplification loop accelerates macrophage-mediated vascular inflammation leading to aortic dissection in mice. The Journal of Clinical Investigation. 2009;119(12):3637-51. doi: 10.1172/JCI38308.
241. Elsner B, Schwarz E, Mando OG, Maiztegui J, Vilches A. Pathology of 12 fatal cases of Argentine hemorrhagic fever. Am J Trop Med Hyg. 1973;22(2):229-36. PubMed PMID: 4688419.
242. Levis SC, Saavedra MC, Ceccoli C, Falcoff E, Feuillade MR, Enria DA, Maiztegui JI, Falcoff R. Endogenous interferon in Argentine hemorrhagic fever. The Journal of infectious diseases. 1984;149(3):428-33. PubMed PMID: 6232326.
243. Riviere Y, Bandu MT. [Induction of interferon by lymphocytic choriomeningitis virus in mice (author's transl)]. Annales de microbiologie. 1977;128A(3):323-9. PubMed PMID: 921139.
244. Riviere Y, Gresser I, Guillon JC, Tovey MG. Inhibition by anti-interferon serum of lymphocytic choriomeningitis virus disease in suckling mice. Proceedings of the National Academy of Sciences of the United States of America. 1977;74(5):2135-9. PubMed PMID: 266735; PubMed Central PMCID: PMC431090.
245. Cuevas CD, Lavanya M, Wang E, Ross SR. Junin virus infects mouse cells and induces innate immune responses. J Virol. 2011;85(21):11058-68. doi: 10.1128/JVI.05304-11. PubMed PMID: 21880772; PubMed Central PMCID: PMC3194972.
246. Faure E, Equils O, Sieling PA, Thomas L, Zhang FX, Kirschning CJ, Polentarutti N, Muzio M, Arditi M. Bacterial lipopolysaccharide activates NF-kappaB through toll-like receptor 4 (TLR-4) in cultured human dermal endothelial cells. Differential expression of TLR-4 and TLR-2 in endothelial cells. The Journal of biological chemistry. 2000;275(15):11058-63. PubMed PMID: 10753909.
247. Hippenstiel S, Soeth S, Kellas B, Fuhrmann O, Seybold J, Krull M, Eichel-Streiber C, Goebeler M, Ludwig S, Suttorp N. Rho proteins and the p38-MAPK pathway are important mediators for LPS-induced interleukin-8 expression in human endothelial cells. Blood. 2000;95(10):3044-51. PubMed PMID: 10807767.
248. Manukyan M, Nalbant P, Luxen S, Hahn KM, Knaus UG. RhoA GTPase activation by TLR2 and TLR3 ligands: connecting via Src to NF-kappa B. Journal of immunology. 2009;182(6):3522-9. doi: 10.4049/jimmunol.0802280. PubMed PMID: 19265130; PubMed Central PMCID: PMC2684960.

249. Emonet SF, Seregin AV, Yun NE, Poussard AL, Walker AG, de la Torre JC, Paessler S. Rescue from cloned cDNAs and in vivo characterization of recombinant pathogenic Romero and live-attenuated Candid #1 strains of Junin virus, the causative agent of Argentine hemorrhagic fever disease. J Virol. 2011;85(4):1473-83. doi: 10.1128/JVI.02102-10. PubMed PMID: 21123388; PubMed Central PMCID: PMC3028888.

BIOGRAPHICAL SKETCH

Heather McSharry Lander was born February 9, 1972 in Kittitas, Washington. She received her Bachelor of Science in Molecular Cell Biology from California State University San Marcos in 1999. Prior to her doctoral studies at UTMB, she worked with Dr. David Cheresh at The Scripps Research Institute studying angiogenesis in the context of tumor growth and metastasis. While attending UTMB Heather worked in a high containment BSL4 laboratory studying the hemorrhagic fever virus Junín, and became the first pregnant woman ever allowed to work in a BSL4 laboratory in the U.S. She also received recognition for her graduate work: ASM/NAS IUMS Travel Grant, NIH Predoctoral T32 Biodefense Training Grant and the Edward S. Reynolds Award- UTMB Pathology Research Day.

In August 2004 Heather married Todd Lander. They live in Galveston Texas with their son, Colten.